Studying the Post-translational regulation of Enhancer of Zeste Homolog 2 on its function as Histone Methyltransferase of the Polycomb Repressive Complex 2

Thesis

Submitted in partial fulfilment

of the requirements for the degree of

DOCTOR OF PHILOSOPHY

by

Ashima Sakhuja

2019PHXF0007P

Under the Supervision of

Prof. Syamantak Majumder

and

Co-supervision of

Prof. Shibasish Chowdhury

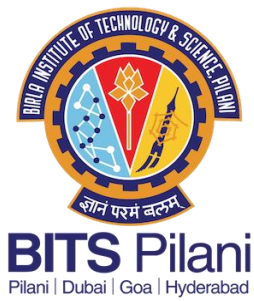

BIRLA INSTITUTE OF TECHNOLOGY & SCIENCE, PILANI
2024

Table of Contents

BIRLA INSTITUTE OF TECHNOLOGY AND SCIENCE,

PILANI

CERTIFICATE

This is to certify that the thesis titled **"Studying the Post-translational regulation of Enhancer of Zeste Homolog 2 on its function as Histone Methyltransferase of the Polycomb Repressive Complex 2"** submitted by **Ms. Ashima Sakhuja** ID No **2019PHXF0007P** for award of Ph.D. of the Institute embodies original work done by her under my supervision.

Signature of the Supervisor:

Name: Syamantak Majumder

Designation: Associate Professor,
Department of Biological Sciences
BITS Pilani, Rajasthan

Date:

Signature of the Co-Supervisor:

Name: Shibasish Chowdhury

Designation: Professor,
Department of Biological Sciences
BITS Pilani, Rajasthan

Date:

Acknowledgement

I would like to express my humble and deepest regards to my Ph.D. research supervisor Prof. Syamantak Majumder, Department of Biological Sciences for providing me an excellent platform to pursue my passion for science and research. I am obliged to have a got an opportunity to work under his skilled guidance, I am also grateful for the constant guidance and express my deepest gratitude for his unmatched support.

I would like to thank my Co-supervisor Prof. Shibasish Chowdhury for his constructive evaluation. I would also like to thank and acknowledge Prof. Sandeep Sundriyal and Shailesh Mani Tripathi for helping me with the bioinformatics work and performing all the molecular simulation studies for the same.

This work would not have been possible without the infrastructural and administrative support from the institute for which I thank Prof. Ramgopal Rao, Vice Chancellor, BITS Pilani and Prof. Sudhir Kumar Barai, Director, BITS Pilani, Pilani Campus. I also thank Prof. SK Verma, Dean Administration; Prof. Shamik Chakraborty, Associate Dean, AGSRD; Prof. Rajdeep Chowdhury, Head of the Department, Department of Biological Sciences and Prof. Prabhat Nath Jha, BITS Pilani, Convener, Departmental Research Committee, for their timely guidance and support regarding the academic formalities throughout the thesis work. I acknowledge CSIR and BITS Pilani for helping me with the financial assistance. This research work would not have been the same without constructive evaluation of my DAC members – Prof. Rajdeep Chowdhury and Prof. Sandhya Marathe, Department of Biological Sciences.

I would also like to extend my heartful gratitude to my seniors Dr. Leena, Dr. Heena, Dr. Swati, Dr. Swetha, Dr. Neelam, Dr. Abhilasha, Dr. Aastha, Dr. Nidhi, Dr. Vivek, Ankita Daiya, Ankita Sharma and Aniruddha for answering all my queries and questions patiently.

Special thanks to my co-worker Yash for always helping me and providing timely help and guidance. I also extend thanks to my lab mates Ritobrata, Sumukh, Ramakrishnan, Srinjoy, Niyati and Hariharan for their contributions.

I would like to specially thank my friends and colleagues Mahima and Swarnima for their selfless love and support and motivation in every situation.

I would like to extend my heartfelt thanks to all the faculty members and research scholars, department of Biological Sciences for extending their help and support during my research and teaching practices. I owe a special thanks to the non-teaching staff especially Suman ji, Mukesh Ji, Ajay Ji and Naresh Ji and Dr. Iti for providing me with the pre-requisites for my experiments and support in coursework.

I am indebted to my Mummy and Papa for always having faith in me and always standing by my side in every situation and making me what I am today. I owe all my success to them. A very special and heartfelt thanks to my husband Namit for being a constant friend, critic and biggest supporter throughout this journey.

I would especially like to thank my brother Tushar and sister-in-law Neha for their selfless love, admiration and support both personally and professionally. I would also like to extend my thanks to my father and mother-in-law for keeping me motivated and helping me in whichever way possible.

This work is dedicated to my son Nivaan who has inspired me to become a better version of myself and has made me stronger, better and more fulfilled than I could ever imagine. Thank you for coming into our lives and making it complete. I love you to the moon and back.

Abstract

PRC2 (Polycomb repressive complex-2), is a well-studied chromatin modulator which is associated with the methylation of histone H3 lysine 27 (H3K27). PRC2 is formed by three major classes of proteins; the functional enzymatic component of the PRC2, Enhancer of Zeste Homolog-2 (EZH2); SUZ12, a PRC2 subunit and a scaffolding protein, EED which assembles and stabilizes the PRC2 complex. The major subunit EZH2 is responsible for regulating the epigenetic process through the catalysis of repressive H3K27me3 marks in endothelial cells (EC) and its importance in different disease outcomes including its role in chronic diseases is well studied.

NO, a versatile bio-active molecule modulates cellular function through diverse mechanisms including S-nitrosylation of proteins. However, the role of this post-translational modification in regulating epigenetic pathways is not explored. Herein, we report that NO causes S-nitrosylation of selected cysteine residues of EZH2 in EC resulting in diminished nuclear localization, disassembly of PRC2 complex, and interplaying with EZH2 protein stability. We detected a significant reduction in H3K27me3 upon exposure to NO as contributed by early dissociation of SUZ12 from the PRC2 complex. Longer exposure to NO donors caused EZH2 ubiquitination and its degradation primarily through autophagosome-lysosome pathway. Moreover, endogenous induction of NO production through agonist bradykinin in EC also manifested the same effect as observed with NO donor while quenching NO in such a setting reversed its effect on EZH2 and H3K27me3. Through in silico S-nitrosylation prediction analysis, we identified three cysteine residues namely at locations 260, 329, and 700 in EZH2 that exhibited the highest probability of being S-nitrosylated. We next generated mutants through site-directed mutagenesis of these residues by converting the codon to code for cysteine to serine.

Overexpression of these mutants in HEK-293 cells followed by NO exposure revealed that cysteine residue at locations 329 and 700 played the most critical role in the NO-dependent effect on EZH2's stability and catalytic activity respectively. Furthermore, by reinforcing H3K27me3 in NO-exposed EC through the use of an inhibitor of H3K27me3 demethylase, we confirmed a significant contribution of the EZH2-H3K27me3 axis in defining NO-mediated regulation of endothelial gene expression and migration. A molecular dynamics simulation study revealed SUZ12's inability to efficiently bind to the SAL domain of EZH2 upon S-nitrosylation of C329 and C700. Taken together, our study for the first-time reports that S-nitrosylation-dependent regulation of EZH2 and its associated PRC2 complex influences endothelial homeostasis and identifies new mechanisms targeting the role of EZH2 in endothelial dysfunction for better therapeutic outcome.

List of Figures

List of Tables

List of Abbreviations

Abbreviation	Meaning
EZH2	Enhancer of Zeste homolog 2
PRC2	Polycomb repressive complex 2
EED	Embryonic Ectoderm Development
SUZ 12	Suppressor of Zeste 12
JARID2	Jumonji and AT rich interaction domain 2
AEBP2	Adipocyte Enhancer Binding Protein 2
RbAp 46/48	Retinoblastoma Binding protein
H3K27me3	Trimethylation of histone H3 at lysine 27
NO	Nitric Oxide
EC	Endothelial cells
HUVEC	Human umbilical vein endothelial cells
HEK-293	Human Embryonic Kidney 293

Chapter 1:
Introduction and Review

1. INTRODUCTION:

Chromatin regulation is a complex and dynamic process essential for the control of gene expression and various chromatin-associated functions such as gene regulation, DNA repair, and the maintenance of genome stability. The chromatin structure governs the alteration in gene expression both in lineage specification during development as well as during the onset and progression of diseases. Chromatin structure can be altered by covalent modifications made to DNA or histone proteins which are attributed by diverse families of DNA- and chromatin-modifying complexes, including enzymes. For eg. - DNA modifications can occur through DNA methylation which occurs at CpG dinucleotides that can regulate chromatin structure as well as the recruitment of transcriptional regulators[1]. Histone modifications occur through processes such as acetylation, methylation, phosphorylation, ubiquitination, SUMOylation etc, which can influence chromatin structure and gene expression changes[2]. Apart from the above-mentioned examples, various classes of non-coding RNAs, like microRNAs (miRNAs) and long non-coding RNAs (lncRNAs), work through mechanisms like RNA interference and chromatin remodeling at the transcriptional and post-transcriptional levels and are involved in chromatin regulation by modulating gene expression[3]. The understanding of the mechanisms involved in chromatin regulation is important for the unwinding of fundamental biological processes and in the development of novel therapeutic interventions for diseases associated with chromatin dysregulation.

1.1 Chromatin Regulation via Polycomb group (PcG) of proteins

Polycomb group (PcG) of proteins is one family of chromatin-modifying enzymes that work as repressors of gene expression. PcG proteins are components of multiprotein complexes that can be categorized into PRC 1 and 2[4].

PcG-driven gene silencing is thought to rely mostly on the regulation of chromatin structure, in part through post-translational modification (PTM) of histones. Hence, the PRC2 complex is responsible for the methylation (di- and tri-) of Lys 27 of histone H3 (H3K27me2/3)[5,6], thereby causing repression of gene expression through its enzymatic subunits EZH1 and EZH2. PRC1 is chromatin modifier with histone H2A E3 ligase activity where PRC1 complex monoubiquitylates Lys 119 of histone H2A (H2AK119ub) via the ubiquitin ligases RING1A and RING1B. In addition, some PRC1 complexes can regulate gene expression by compacting chromatin in a manner independent of enzymatic activity[7]. The PRC1 component Pc (known as CBX in mammals) binds specifically to the product of PRC2 catalysis, H3K27me3, leading to the hypothesis that PRC1 functions downstream of PRC2. Although this premise is still cited in the literature, its operational status is equivocal as there are genes targeted by PRC2 that lack H2AK119ub8 and genes targeted by PRC1 in the absence of PRC2[8,9]. Nonetheless, PRC2 and PRC1 are often required to maintain gene repression[10].

1.2 Structure and functions of Polycomb Repressive Complex-2

1.2.1 Functional Components of PRC2; role of EZH2

The core of PRC2, which is conserved from Drosophila to mammals, comprises four components: EZH1/2, SUZ12, EED and additional subunit RbAp46/48 (also known as RBBP7/4). The presence of PRC2 in various unicellular eukaryotes led to the suggestion

that it existed in the last common unicellular ancestor, but it was lost at times during evolution as exemplified by the cases of *Schizosaccharomyces pombe* and *Saccharomyces cerevisiae*, in which PRC2 is absent [11] Notably, the PRC2 components underwent little duplication in mammals, with vertebrates containing two copies of Enhancer of Zeste homolog, EZH1 and EZH2[11]. EZH1 is present in both dividing and differentiated cells, whereas EZH2 is found only in actively dividing cells. Also, PRC2 complexes containing EZH1 (PRC2–EZH1) instead of EZH2 have low methyltransferase activity compared with PRC2–EZH2[12]. This indicates that PRC2–EZH2 establishes cellular H3K27me2/3 levels through its EZH2-mediated methyltransferase activity and that PRC2–EZH1 restores H3K27me2/3 that could have been lost after histone exchange or through demethylase activity. Moreover, PRC2–EZH1 and PRC2–EZH2 have distinct chromatin-binding properties, as illustrated by the specific chromatin-compaction property of PRC2-EZH1[10].

The human PRC2 is formed by three major classes of proteins; the functional enzymatic component of the PRC2, EZH2; SUZ12, a PRC2 subunit and a scaffolding protein, EED which assembles and stabilizes the PRC2 complex. Along with that it also comprises of the subunit RbAp46/48 and cofactors such as AeBP2 and JARID2[13,14].

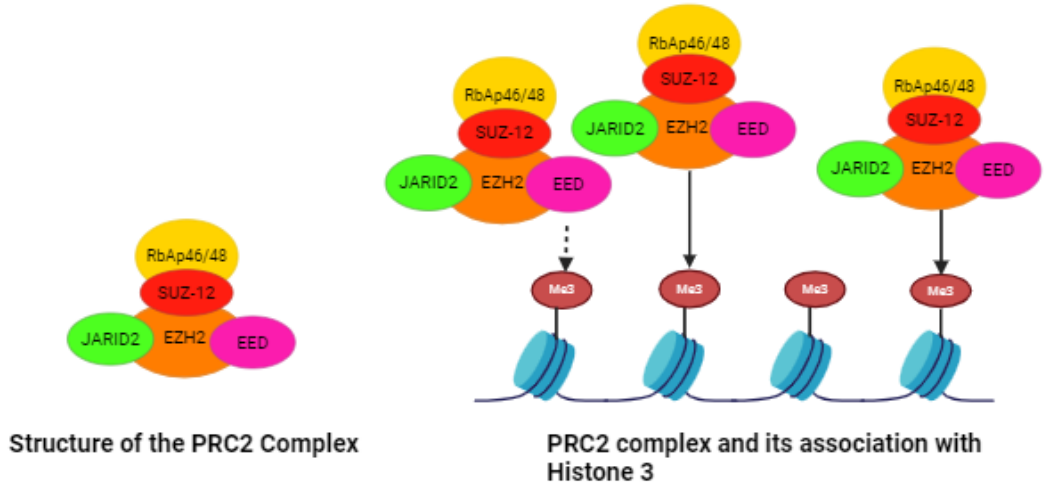

Figure 1.2.1.1- PRC2 complex and its association with Histone 3

The subunit EZH2 is divided into several domains such as CXC, MCSS, SANT2, SANT1, SRM, SAL, BAM, EBD, and SBD, etc. which are responsible for performing different roles. For e.g.-CXC domain of EZH2 is the region where the unmodified nucleosome attaches to EZH2 to undergo modifications[14,15]. The nucleosome that has H3K27me3 marks interacts with the SBD domain as it acts as the primary binding site for the nucleosome along with the subunit EED. The SET domain is the region where the catalytic activity of PRC2 complex resides which catalyzes the deposition of methylation marks on H3K27 along with the subunits EED which stimulates the methyltransferase activity of PRC2 along with SUZ12[13].

SUZ12 helps in the integration of the PRC2 complex and also acts as a docking platform for binding AEBP2 and JARID2 as AEBP2 sits on RBAP48 and SUZ12. Along with this, the VEFS domain of SUZ12 participates in the functional regulation of the PRC2 complex.

The subunit RBAP48 is responsible for maintaing the stability of the PRC2 complex and enhancing its methyltransferase activity. It is also responsible for the interaction between the subunits of PRC2 and chromosomes[14]. The subunit RBAP48 interacts with the cofactor AEBP2, which in turn stimulates the HMT activity of the PRC2 complex. The cofactor Jarid2, is trimethylated at K116 by PRC2, which results in further stimulating the methyltransferase activity of the complex. Basically, the cofactors AEBP2 and JARID2 are capable of mimicking role of histone H3 which can contribute to the deposition of methylation marks on H3K27 at specific gene loci[14,16].

1.3 Role of EZH2 in Cytosol

Although EZH2, through forming the PRC2 complex, is well known for its role in regulating epigenetic processes through histone methylation, EZH2 also mediates cytosolic function by driving methylation of actin cytoskeleton remodeling proteins. A pioneering study indicated that cytosolic EZH2 works via the regulation of methylation of proteins such as small GTPase[17] and Talin[18] that essentially controls actin cytoskeleton remodeling. The majority of these studies indicated that even in the cytosol, EZH2 still forms an active PRC2 complex, which essentially works as methyltransferase of non-histone protein[18,19], thereby regulating their downstream function. However, how EZH2 changes its location and catalytic substrate based on the location is remained to be elusive. There are limited studies describing such regulation of EZH2 through post-translational modification, especially in the context of its methyltransferase activity and localization.

Till now, the main role of EZH2 was thought to be intranuclear, but recent studies have identified its cytosolic localization pertaining to various types of cancer cells such as in fibroblasts, T lymphocytes, breast cancer[20], and prostate cancer cells[21,22]. Recent

research has also concluded the non-canonical methyltransferase-independent role of EZH2[23,24].

Cytosolic EZH2 is associated with repression of transcriptional genes linked to tumor suppression[25], cell cycle inhibition, cell differentiation and antigen processing and presentation pathways or with the activation of the oncogenes[26,27]. The importance of EZH2 in regulating glucose, lipid[28], and amino acid metabolism and in turn affecting the development and progression of various types of tumours has also been identified[29].

1.4 Importance of EZH2 in Development and Diseases

EZH2, a SET-domain-containing protein is closely associated with several other subunits and is key for the catalytic function of the PRC2 complex. Genetic ablation of EZH2, is shown to result in lethality at the early stages of mouse development[30]. EZH2 mutant mice either cease developing after implantation or initiate but fail to complete gastrulation. Moreover, EZH2-deficient blastocysts display an impaired potential for outgrowth, preventing the establishment of EZH2-null embryonic stem cells. In contrast, EZH2 has been shown to be responsible for cancer progression and metastasis, as well as the pathogenesis of different other diseases[31,32]. Many studies have been published depicting the importance of EZH2 in different disease outcomes, including its role in chronic kidney diseases. The same studies indicated that EZH2 and its associated H3K27me3 mark are essential for the physiological functioning of specific kidney cells and any loss in EZH2 and H3K27me3 level is responsible for onset and progression of chronic kidney disease[33,34]. These reported studies highlighted the importance of EZH2 as a key mediator of cellular differentiation during both development and diseases[35]. In contrast, studies have also shown the importance of EZH2 in different disease outcomes[36].

1.5 Association of Cancer progression with EZH2

The PRC2 dependent and independent roles of EZH2 in regulating tumorigenesis and cancer are well studied. Impaired EZH2 regulation results in altered gene expression and functions leading to cancer development and progression[37].

EZH2 has a known role in promoting cancer onset and progression via canonical pathway[38]. It occurs either by the activation of several oncogenes or inactivation of certain tumour suppressor genes via deposition of repressive trimethylation marks on lysine 27 of histone H3 (H3K27me3)[39].

The non-canonical and histone methyltransferase independent role of EZH2 has been found to be associated with the onset and progression of various kinds of cancers. It acts as a transcriptional activator/coactivator via non-canonical pathway. It also has a GTP-dependent function in the tumorigenesis and metastasis of melanoma cancer[40]. Mutations leading to overexpression of EZH2 has been observed in various cancer types such as prostrate, breast, melanoma, colon, lung, liver, endometrial cancer etc[41]. Overexpressed EZH2 is associated with disturbed migration, invasion, cell proliferation and apoptosis. Mutations leading to loss of function of EZH2 acts as tumor suppressor genes in various cancer types such as human T-cell acute lymphoblastic leukaemia (T-ALL)[42–44] and myeloproliferative neoplasms (MPN)[45] etc.

1.6 Regulation of EZH2 via different PTMs

Post-translational modifications (PTMs) of EZH2 contribute to its functional diversity and epigenetic regulatory mechanisms. Some of the known post-translational modifications on

EZH2 include Phosphorylation, Acetylation, methylation, Ubiquitination, SUMOylation and O-Glc NAcylation etc.-

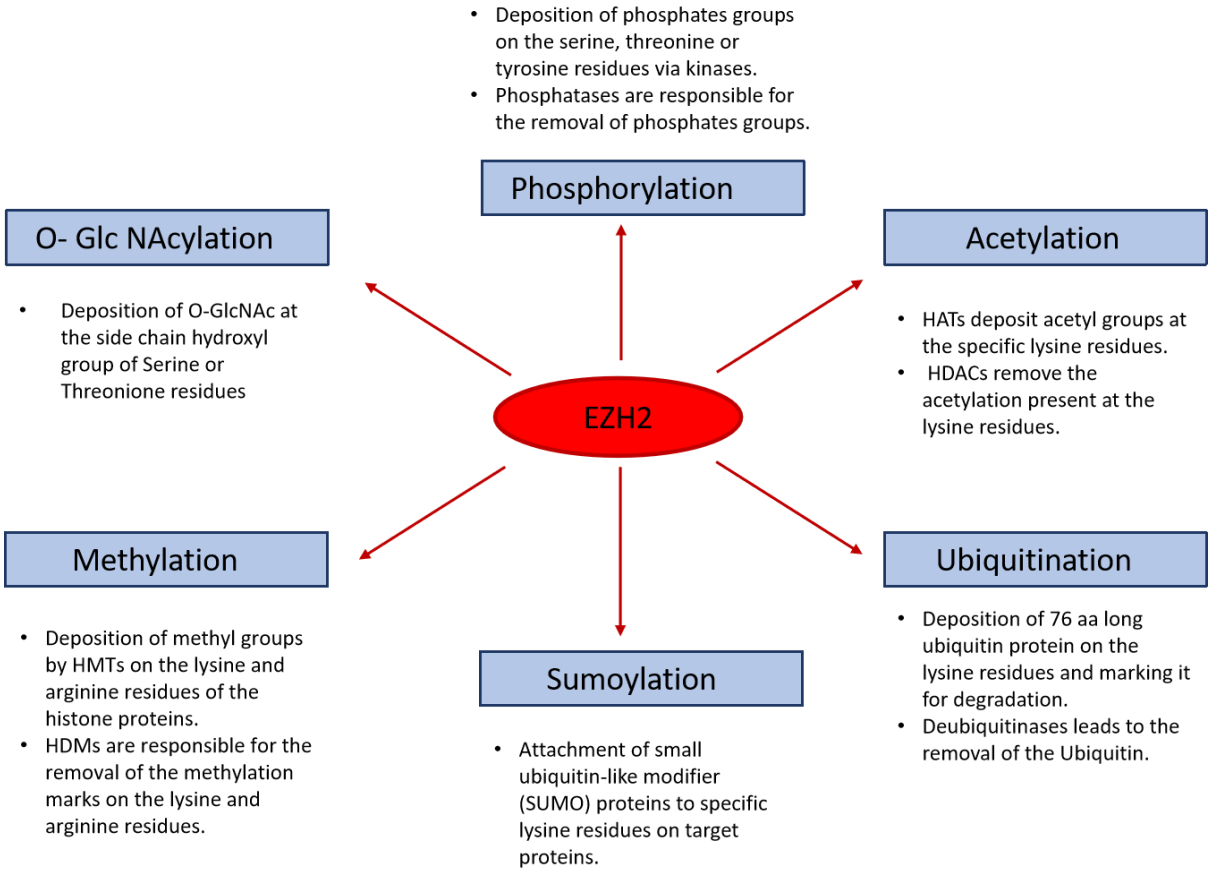

Different PTMs affecting EZH2

Figure 1.6.1- Role of different post-translational modifications on EZH2

1.6.1 Phosphorylation

Phosphorylation is a critical post-translational modification (PTM) occurring at serine (S)/threonine (T) sites on EZH2 which regulates its function as an epigenetic regulator. EZH2 has been shown to be phosphorylated by Akt[46] and AMPK[47], which leads to

suppression of its methyltransferase activity. Phosphorylation of EZH2 at Thr311 occurs by AMPK which affect its interaction with SUZ12 thereby abrogating its enzymatic activity that is related to increased activation of the TSGs and in turn hampering its oncogenic function[47]. Phosphorylation at serine21 of EZH2 by AKT accompanies with tumor recurrence and poor survival[48]. P38 mediated phosphorylation of EZH2 at T367 is also associated with its increased cytosolic translocation and further promoting metastasis during breast cancer [20].

It is reported that phosphorylation of EZH2 at threonine residues 345[49,50] and 487[50] by CDK1 is associated with ubiquitination followed by proteasome pathway degradation of the EZH2, that has an important role in regulating cell proliferation in several cancer types such as cervical and prostate cancer. Phosphorylation at these residues is responsible for maintaining different functions in different cell types. Apart from these residues phosphorylation at threonine positions T350, T372, T419, and T492 help in the association of the EZH2 with E3 ligase smurf2 marking it for its degradation[48].

It is also known that this post-translational modification on serine, threonine hampers the assembly of PRC2, suggesting that EZH2 along with Suz12 and EED mediated assembling of PRC2 is affected and ultimately causing the methyltransferase activity of EZH2 for histone to be completely altered.

1.6.2 Ubiquitination

Ubiquitination is a type of PTM that occurs through a protein known as Ubiquitin (Ub). Ub is a highly conserved protein consisting of 76 amino acid residues, crucial for marking target proteins for post-translational degradation. Ubiquitination, plays a pivotal role in regulating the stability, functions, and localization of modified proteins[48]. Ubiquitination is implicated in various functions and diseases, particularly in tumorigenesis and cancer

metastasis[51]. It involves a well-orchestrated cascade of enzymatic reactions dependent on three essential enzymes: an E1 ubiquitin activating enzyme, an E2 ubiquitin-conjugating enzyme, and an E3 ubiquitin-ligating enzyme[52].

Ubiquitination of EZH2 leading to its degradation via proteasomal pathway is well known[48]. Praja1 and Smurf2, c-Cbl etc. act as certain kinds of E3 ligases responsible for the ubiquitination of EZH2 and ultimately marking it for its degradation. For eg-Praja1 facilitates EZH2 protein degradation through the ubiquitination-proteasome pathway in breast cancer cell line suggesting that Praja1 promotes EZH2 degradation via K48-linkage polyubiquitination, thereby suppressing cell growth and migration in breast cancer. FOXP3 is also associated with the acceleration of the transcriptional expression of Praja1, thereby promoting the degradation of EZH2[53,54].

Smurf2 has also been shown to interact with EZH2 and mediate its ubiquitination-proteasome degradation, with lysine 421 of EZH2 playing a crucial role in this process. Furthermore, the E3 ligase c-Cbl has been implicated in EZH2 ubiquitination and proteasomal degradation in breast cancer. β-TrCP, is linked to reduced EZH2 stability and H3K27me3 deposition in breast cancer cells through mediating EZH2 ubiquitination-proteasome degradation[55,56].

Similarly, TRAF6 catalyzes the K63-linked polyubiquitination of EZH2, leading to decreased EZH2 and H3K27me3 levels in prostate cancer cells and patients[56].

A recent study also indicates that EZH2 degradation is governed by Hsp70-interacting protein (CHIP)-mediated ubiquitination[57]. Such ubiquitination of EZH2 essentially could regulate the degradation pathways that essentially can control the final protein expression level of EZH2 in head and neck cancer cells[58].

Deubiquitination is also a type of PTM but unlike ubiquitination, it facilitates targeted protein degradation with the help of Deubiquitinases (DUBs), also known as

deubiquitylases. They counterbalance this process by removing ubiquitin molecules from ubiquitin-labelled proteins or polyubiquitin chains, thereby enhancing the stability of targeted proteins[56]. DUBs play pivotal roles in cancer metastasis and tumorigenesis. For eg. - studies have reported ZRANB1 (also known as Trabid) a DUB which binds to EZH2, deubiquitinates it and maintains its stability, thereby promoting breast cancer tumorigenesis and metastasis[59]. Additionally, ubiquitin-specific protease 7 (USP7), also referred to as herpesvirus-associated ubiquitin-specific protease, has been shown to deubiquitinate EZH2, leading to its stabilization. Similarly, other studies have demonstrated that USP7-mediated EZH2 deubiquitination enhances the growth, motility, tumorigenesis, and metastatic invasive potential of prostate cancer cells[60].

It has also been demonstrated that ubiquitin-specific protease 36 (USP36) deubiquitinates EZH2 at the K222 site, thereby enhancing EZH2 stability in natural killer/T-cell lymphoma (NKTL)[61].

1.6.3 Acetylation

Acetylation is one kind of a reversible PTM which is responsible for catalyzing a number of cellular processes like cell cycle, splicing, chromatin remodeling, actin nucleation and nuclear transport. Histone acetyltransferases (HATs) deposits acetyl groups at the specific lysine residues whereas histone deacetylases (HDACs) are responsible for the removal of the acetylation at the lysine residues. Acetylation of EZH2 at lysine residues can affect its stability and activity. For eg- P300/CBP-associated factor (PCAF) an HAT acetylates EZH2 at lysine 348 (K348) leading to an increase in the stability of EZH2 without affecting the PRC2 assembly[62]. This acetylation is linked to increased suppression of the target genes and as a result increased invasion and cell migration in the lung cancer. SIRT1, an NAD-dependent protein deacetylase, when inhibited is associated with elevated EZH2

protein stability[62,63]. Cross talk between the two types of PTMs phosphorylation and acetylation are important for the regulation of a number of important TFs such as p53, FOXO1 and STAT1[48].

1.6.4 SUMOylation

Analogous to ubiquitination, there exists a PTM called SUMOylation, which involves the attachment of small ubiquitin-like modifier (SUMO) proteins to specific lysine residues on target proteins. SUMOylation works via a highly conserved enzymatic cascade akin to ubiquitination[64]. SUMO modifications are associated with adding a new docking site to target molecules, allowing them for novel protein-protein interactions via the SUMO interacting motif during signaling pathways. Although the SUMOylation of EZH2 has been associated with its activity in osteosarcoma cancer cell line, the specific SUMOylation residue on EZH2 and the molecular mechanisms underlying its involvement in SUMOylation remain elusive.

The significance of SUMOylation in regulating the stability and function of EZH2 has been explored recently. Recent studies show that SUMOylation is associated with EZH2 function through its expression but it do not alter its enzymatic functions. EZH2 regulation via SUMOylation involves SUMO modification of the transcription factor E2F1. Inhibiting SUMOylation reduces E2F1 binding to the EZH2 promoter, decreasing EZH2 expression. E2F transcriptional activators, are associated with cell cycle progression, and are negatively regulated by the tumor suppressor Rb protein. SUMOylation at certain EZH2 lysine residues are associated with enhanced EZH2 stability and promotes EZH2-mediated gene silencing[65,66]. Moreover, disruption of EZH2 SUMOylation impairs its oncogenic activity, highlighting its importance in modulating EZH2 function in cancer cells[66].

While the precise mechanisms and functional consequences of EZH2 SUMOylation are still being elucidated, emerging evidence suggests that SUMOylation plays a crucial role in modulating EZH2 stability, activity, and transcriptional regulation, particularly in the context of cancer.

1.6.5 Methylation

It is also an important type of PTM that acts by depositing the methyl groups on the lysine and arginine residues of the histone and non- histone proteins. For eg- A study in 2019, unveiled that SMYD2-mediated EZH2 di-methylation at lysine 307 (K307) heightens its stability within breast cancer cells. This methylation process can be reversed by the histone H3K4 demethylase LSD1[67]. EZH2-K307 di-methylation was observed to spur the proliferation and invasion of breast cancer cells by streamlining EZH2 recruitment to chromatin and subsequent transcriptional repression of target genes[62,67]. Also, SETD2 methylates EZH2 at K735, thereby triggering EZH2 degradation and impeding prostate cancer metastasis. It illustrated that SETD2-mediated EZH2-K735me1 fosters the binding of the E3 ligase Smurf to EZH2, culminating in its degradation[68]. Furthermore, recent research unearthed that PRMT1-mediated R342-EZH2 asymmetric di-methylation (ADMA) bolsters EZH2 stability and fuels breast cancer metastasis[69].

1.6.6 O-Glc NAcylation

O-GlcNAcylation is a dynamic and reversible PTM, that is regulated by the enzyme *O*-linked *N*-acetylglucosamine transferase (OGT) which deposits O-linked N-acetylglucosamine (O-GlcNAc) at the side chain hydroxyl group of serine or threonine residues[62] . O-GlcNAcylation of EZH2 has been implicated in regulating its stability and function, although the exact mechanisms remain to be fully elucidated. For eg- Recent

studies showed that OGT-mediated *O*-GlcNAcylation at serine 75 on EZH2 aids in the stability of the EZH2, and the PRC2 complex in turn formulates the deposition of H3K27me3 marks on PRC2 target TSGs in breast carcinoma[70]. *O*-GlcNAcylation of EZH2 on serine residues 73, 84, 87, 313, and 729 aid in maintaing the stability of EZH2 and maintaing its association with the PRC2 complex. Also, the *O*-GlcNAcylation at S729, which resides in the SET domain of EZH2 increases the methyltransferase activity and facilitates the deposition of theH3K27me2/3 marks on the target gene[71].

These PTMs collectively regulate the activity, stability, and subcellular localization of EZH2, thereby influencing its function in epigenetic regulation. Further studies are required to fully understand the dynamics and functional consequences of these PTMs in the context of EZH2-mediated gene regulation and their relevance in health and disease. As despite the identification of few of these post-translational modifications of EZH2, it's regulation of methyltransferase activity, localization and degradation through unique PTMs still remain elusive.

1.7 Role of Nitric Oxide

NO is a versatile free radical that mediates numerous biological functions by selective modification of protein at cysteine residues. NO is an important signalling molecule responsible for many different cellular and organ functions. It has a widespread role due to its high ability to diffuse across membranes and its specific interactions with target cell-response proteins as well as the metalloproteins[72]. There are many ways by which NO regulates the physiology and pathophysiology of our body like through protein kinase activity or redox interactions with thiols, or its interactions with metal centre containing proteins[7374].

NO is a highly labile molecule with a short half-life of less than 1 sec[75] thereby making its direct measurement a difficult task. It is rapidly oxidized by oxyhaemoglobin to nitrate and nitrite in the blood. Hence, NO produced in vivo is measured by the concentration of its metabolites[76].

Nitrosylation is a crucial post-translational modification mediated by NO which impacts various physiological and pathological processes. It operates through either the canonical or the non-canonical pathways, each influencing protein function in distinct ways.

1.7.1 Canonical Pathway

In the canonical pathway, NO directly interacts with target proteins, forming S-nitrosothiol bonds (S-nitrosylation). This reversible post-translational modification modulates protein activity, localization, and stability. Enzymatic/Canonical NO production occurs via NO Synthase (NOS) that leads to the conversion of L-arginine to L-citrulline and NO, where oxygen and NADPH act as cofactors[77]. NO synthesis, catalysed by this NO synthases (NOS) from L-arginine, precedes target protein interaction. It also regulates diverse cellular processes by modifying protein conformation and function. For eg- Enzymes like S-nitrosoglutathione reductase (GSNOR) and thioredoxin regulate S-nitrosylation dynamics by catalysing denitrosylation and restoring the original protein structure and function[78] .In our body NO production occurs majorly through the enzymatic and minorly through non-enzymatic/ non-canonical pathway.

NOS has three isoforms- endothelial NOS (eNOS or NOS3), neuronal NOS (nNOS or NOS1) and inducible NOS (iNOS or NOS2). Out of these 3 isoforms, NOS1 and NOS3 are regulated by intracellular Ca^{2+}/calmodulin and is constitutively expressed whereas NOS2 which is Ca^{2+} independent is an inducible isoform. NOS2 is expressed during stress/inflammatory conditions by macrophages and other tissues[72,74].

The cofactors present for NOS include essentially Tetrahydrobiopterin (BH4) and others include flavin adenine dinucleotide (FAD), flavin mononucleotide (FMN) and heme.NO once produced from NOS reacts with various cofactors BH4, FAD, FMN and heme which leads to the formation of compounds with increased stability like tetrahydrobiopterin (THB), S-nitrosothiols, peroxynitrites and metal adducts etc. which have important roles to play in the physiological functions in our body[74,79]. For e.g. THB is required for the biosynthesis of key aromatic amino acid hydroxylase enzyme precursors which are a prerequisite for the production of important neurotransmitters for signalling like epinephrine, dopamine, serotonin, and melatonin[77].

1.7.2 Functions of Isoforms of NOS

1.7.2.1 NOS 1& NOS 3

Mitochondrial oxygen consumption, leucocyte adhesion and platelet aggregation, are few important roles played by NOS 1& 3. NOS 1 i.e. nNOS is involved in neural transmission. NOS3 i.e. eNOS which is also constitutively expressed is found in normal vascular endothelium[74,75]. In the vascular smooth muscles, they are responsible for maintaing vascular tone as well as blood flow. Irregularities as well as abnormalities leading to NO production and transport results in cardiovascular disorders such as atherosclerosis, angiogenesis related disorders and hypertension as well as endothelial dysfunction[79,80]. Conditions such as like diabetes, hypercholesterolaemia and hypertension result in uncoupling of NOS3 which responds to low L-arginine or BH4 concentrations by forming superoxides[81,82]. NO is responsible in regulating many processes in brain such as cellular redox state, neuronal survival, angiogenesis and blood flow etc[83]. Additionally, NO is also responsible in regulating numerous physiological roles in brain affecting behaviour and cognitive functions[84].

1.7.2.2 NOS2

NOS2 production of NO occurs in many inflammatory and degenerative conditions[85] such as metabolic hypoxia, atherosclerosis, oxidative stress or during vasodilation or septic shock in cells[75] etc. NOS2 is responsible in promoting atherosclerosis either directly or indirectly through NO adducts formation, eg. peroxynitrite. It is also associated with the activation of macrophages leading to the production of NO in these cells and ultimately helping in the cytotoxic functions performed by these cells[75,86].

1.7.3 Non- Canonical Pathway

In addition to the canonical pathway, there are non-canonical mechanisms of nitrosylation, wherein NO can indirectly influence protein nitrosylation through intermediary molecules or processes. The Non-enzymatic NO production occurs mainly through nitrite formation via various different pathways to produce NO under ischemic conditions where normal NO production from NOS is affected[75]. These include-

1. **Metal-Catalyzed Nitrosylation**: NO can interact with transition metal ions, such as iron (Fe) or copper (Cu), leading to the formation of metal-nitrosyl complexes. These complexes can subsequently transfer the NO group to nearby cysteine residues on proteins, resulting in S-nitrosylation[78,87].
2. **Transnitrosylation**: In transnitrosylation, NO is transferred from a donor SNO to a recipient protein cysteine residue, mediated by transnitrosylase enzymes or through protein-protein interactions. This process allows for the propagation of S-nitrosylation signals across different proteins[78].
3. **Heterogeneous Nitrosylation**: Heterogeneous nitrosylation involves the formation of SNOs on proteins indirectly via reaction with nitrosylating agents or reactive nitrogen

species (RNS), such as peroxynitrite (ONOO-) or nitrous acid (HNO2). These RNS can nitrosylate proteins by mechanisms independent of direct NO interaction[78].

1.8 Role of NO in Disease and Development

Deprivation of NO is a main contributor to endothelial dysfunction which leads to diabetes-associated diseases and disorders like cardiovascular disease[88], myocardial infarction, atherosclerosis etc[79]. Extreme low or high concentrations of NO are both associated with malfunctions of different physiology in our body.

In low concentrations, NO is responsible for the regulation and maintenance of normal mammalian and human physiology. Elevated NO levels are associated with damage and dysfunction of the normal physiological processes occurring in our body. Regulating the amount of NO is a therapeutic target for maintaining the active physiology of the body[89].

Maintaining the amount of NO production and avoiding low NO levels is important for maintaining the vasculature and protection against vascular diseases. Regulation of the excessive increase in inducible NO production is also important and can act as an important factor. Dietary factors also have the potential to modulate NO production, with substrate bioavailability playing a crucial role. While arginine is a primary precursor for NO synthesis, citrulline supplementation presents itself as a promising alternative[89,90]. Future research aimed at expanding our understanding of NO production regulation by different nitric oxide synthase (NOS) isoforms and its accurate measurement at the organ level is essential for developing effective therapies. Additionally, investigating the interrelation between arginine, citrulline, and glutamine in NO production regulation, as well as exploring the interaction and potential synergy among various dietary factors affecting NO production, requires further study. Such efforts will contribute to the optimization of dietary strategies aimed at enhancing NO levels and promoting overall health[89,90].

The optimum level of NO at a particular location depends on the physiological system in which it is found or the impact made by NO molecules in a particular mechanism and biochemical environment. For eg, Higher levels of NO concentrations are related to Akt phosphorylation, and ranges between 300 to 800 nM of NO are related to the stabilization of p53 and HIF-1 α. NO• concentrations of (<100 nM), lead to the activation of cGMP-dependent protein kinase (PKG) and extracellular signal-regulated kinase (ERK). Higher levels of NO apart from these ranges result in the activation of the nitrosylation and oxidative processes which in turn start stressful cellular events. This also leads us to conclude the importance of the biochemical content of the microenvironment in which NO occurs, depending on which the role of NO can be varied, it can either have a protective or toxic role[91].

1.9 NO and Cardiovascular Diseases

NO is an important molecule for the cardiovascular system which acts as a key determinant of basal vascular tone. Cardiovascular disease encompasses various disorders such as hypercholesterolemia, hypertension, and diabetes. Atherosclerosis, a common underlying pathology in many cardiovascular conditions, is closely linked to endothelial dysfunction[77,80].

NO is also known to exert various cardioprotective functions, such as the regulation of the blood pressure and vascular tone, prevention of platelet activation and aggregation. It also limits leukocyte adhesion to the endothelium, and regulates the myocardial contractility[92]. However, the role of NO extends beyond maintaining physiological functions, as it also contributes to the pathogenesis of common cardiovascular disorders such as hypertension, reperfusion injury, atherosclerosis, and myocardial depression associated

with septic shock[93]. Any alterations in NO levels or activity can contribute to the development and progression of cardiovascular related dysfunction and pathology[81,82].

In essential hypertension, dysregulation of NO production can lead to impaired vasodilation and increased vascular resistance, contributing to elevated blood pressure levels. Similarly, in reperfusion injury, inadequate NO production or bioavailability during the restoration of blood flow to ischemic tissues can worsen the tissue damage through oxidative stress and inflammation[93,94].

During myocardial depression associated with septic shock, dysregulated NO production contributes to cardiovascular collapse and myocardial dysfunction. Excessive NO production, often induced by inflammatory mediators, can lead to vasodilation, hypotension, and impaired myocardial contractility, contributing to the development of shock and organ dysfunction in sepsis[94].The condition atherosclerosis is characterized by the buildup of plaque in arterial walls, which is influenced by NO dysregulation[93].

NO has a known role in maintaining endothelial function and preventing endothelial dysfunction. Decreased NO availability is associated with impaired endothelial function which occurs during the early stages of atherosclerosis development and progression[77].

Overall, dysregulation of NO production represents a common pathological mechanism underlying various cardiovascular disorders. Understanding the intricate balance of NO signaling in health and disease is crucial for developing targeted therapeutic interventions to mitigate the adverse effects of NO dysregulation and improve cardiovascular outcomes[89].

1.10 Role of NO in the Tumour Growth

The role of NO in the growth and development of tumors is well studied. NO has emerged as a molecule with multifaceted and often contradictory roles in tumor biology and growth. Higher levels of NO production are a culprit in maintaining the vascular tone of the blood vessel system of the tumors and promoting neoplastic transformation as well as tumor angiogenesis[95], Long term exposure to higher concentrations of NO also regulates inflammation along with tumor growth and metastatic behaviour[96].

Many studies involving cancer patients have shown that NO is associated with decreasing the NO synthesis, leading to vasoconstriction as well as increasing the blood flow to the tumours leading to an increase in blood pressure[97].

Exogenously produced NO such as from smoking forms N-nitrosamines and N-nitrosamides and is a contributor to head and neck cancers by causing subcellular damage[98]. Depending on the microenvironment ROS can play a dual role of either being a protector through eliminating microorganisms and malignant cells or a pathological contributor of NO reactions with oxygen. Elevated levels of ROS are linked to ROS and NOS which are associated with abrogating normal cellular physiology of cells by affecting transcription and translational processes, inhibiting antioxidants levels or by causing DNA damage[96]. DNA damage is associated with the activation of defensive apoptotic systems such as the increase in p53 or inhibiting caspase activation leading to the induction of the normal apoptosis of the cell. It is also associated with forbidding apoptosis in various cell types as well as in tumour cells[95].

1.11 Role of NO in regulating other Disorders

NO also has a role in regulating diseases such as sepsis, trauma, nutrition deficiency etc.

1.11.1 Sepsis and Trauma: In patients with sepsis or traumatic injuries, there's a noticeable decrease in the levels of stable isotopes of NO, such as arginine and citrulline. This decline is attributed to reduced arginine production and lower citrulline levels. To maintain adequate NO production, supplementation with arginine and citrulline becomes imperative. Research conducted on macrophages indicates that while NO production is limited by arginine availability, citrulline supplementation effectively restores NO levels in environments lacking arginine. Interestingly, glutamine has been found to impede citrulline-mediated NO production. Thus, citrulline supplementation emerges as a potential therapeutic strategy to replenish NO levels in conditions characterized by arginine deficiency, such as trauma or surgery. Although plasma levels of the endogenous NOS inhibitor NG-methyl-L-arginine (ADMA) exhibit wide variations in sepsis patients, they do not directly correlate with NO production. However, higher ADMA levels are associated with increased mortality in sepsis[93,99].

1.11.2 Undernutrition in Children and Neonates: Children suffering from severe undernutrition display comparable NO production to that observed during recovery, despite experiencing lower plasma arginine levels and reduced arginine flux. Studies conducted on neonatal pigs fed an arginine-deficient diet suggest that NO production is influenced by arginine availability[99].

1.11.3 Vascular diseases: Arginase could act as a potential therapy to modify arterial response to injury and may offer promising interventions in the treatment of vascular diseases. Pharmacological inhibition of arginase activity has shown potential benefits in increasing NO production and improving vascular function in animal models of spontaneous hypertension, thereby suggesting potential therapeutic avenues. Moreover, L-arginine therapy has been proposed as a means to disrupt the cycle of low NO observed

in hypertension. Elevated levels of homocysteine have been found to exhibit a strong inverse correlation with NO production, particularly mediated by NOS3. Additionally, reduced NO production due to BH4 deficiency contributes to impaired insulin action in the vasculature of obese and diabetic individuals[93,99].

1.12 Importance of Nitrosylation in Endothelial Cells

eNOS in EC is responsible in regulating endothelial homeostasis. Endothelial homeostasis is a complex process that encompasses both acute responses and more sustained reactions to various stimuli. Acute responses involve the adaptation of blood flow to meet the demands of the surrounding tissues. Meanwhile, more sustained responses occur in the context of injury, such as re-endothelialisation and the sprouting of EC, as well as the attraction of circulating angiogenic cells (CAC). These sustained responses are crucial for the repair and restoration of damaged endothelium, thereby maintaining vascular integrity and function[99].

In EC, cellular NO signalling is essential for endothelial survival and migration. NO is known to be an important constituent of endothelium-derived relaxing factor EDRF. It does so by either conventionally regulating the canonical pathway or the non-canonical pathways or both. In canonical pathways, NO activity occurs via the regulation of soluble guanylyl cyclase, which in downstream governs the level of cGMP, thereby regulating further downstream signalling[100].

NO works via nitrosylation of different proteins at different residues (majorly through nitrosylation of cysteine, methionine and tyrosine residues), through the non-canonical pathway, thereby determining the important role and functions of these proteins[101,102]

Though it is well entrenched that NO treatment alters endothelial gene expression, NO is yet to be established as a direct regulator of epigenetic processes. There are a few studies which have shown that either through the regulation of the cGMP-Protein kinase G (PKG) axis or coordinating nitrosylation of the transcription factor, NO can alter gene expression[103].

1.13 Role of NO as a PTM

The discovery of over 200 reversible protein post-translational modifications (PTMs) has significantly enriched our understanding of the proteome, allowing proteins to fulfil a diverse array of functions beyond their genetic coding. PTMs are known to typically target specific amino acid residues within conserved motifs. Different types of PTMs target different amino acid residues residing at specific locations within the conserved domains leading to an aid or prevention of the protein functions. In this regard, redox signaling has rapidly emerged as a pivotal regulator of protein functionality which is responsible in influencing various physiological roles and processes[104].

NO, is a small gaseous molecule, that serves as a central mediator in redox signalling. NO has the ability to directly alter target proteins through post-translational modifications (i.e. through non-canonical pathway), with three of these modifications being particularly significant[87,104]. The first involves the interaction of the NO moiety with metalloproteins, known as metal nitrosylation. The second modification involves the alteration of tyrosine residues within proteins by NO, leading to the formation of 3-nitrotyrosine. Lastly, NO can induce the formation of nitrosothiol groups on cysteine residues of target proteins, a process referred to as S-nitrosylation. NO primarily exerts its effects through S-nitrosylation i.e. the addition of a NO moiety to mostly cysteine (Cys) sydryl/thiol groups,

forming S-nitrosothiols (SNO)[78,87]. Recent findings have also proved that NO plays a pivotal role as a PTM in coordinating the physiological processes[105].

Like many other PTMs, S-nitrosylation of cysteine residues of different proteins impacts their function, stability, and cellular localization[106]. However, whether EZH2 is regulated by S-nitrosylation has never been explored previously. Although NO signalling is well known to alter gene expression changes, which is partly responsible for its downstream functioning of different cells is yet to be established as a direct regulator of epigenetic processes such as histone methyltransferase EZH2.

1.14 Gaps and Objectives

EZH2 is responsible for regulating the epigenetic process through the catalysis of repressive H3K27me3 marks in EC and its importance in different disease outcomes including its role in chronic diseases is well studied. NO, a versatile bio-active molecule that is also endogenously produced by EC through endothelial nitric oxide synthase modulates cellular function through diverse mechanisms including S-nitrosylation of proteins. However, the role of this post-translational modification in regulating epigenetic pathways specifically in EZH2 and the PRC2 complex was never explored. Through, the proposed study, we expect to establish the role of S-nitrosylation of cysteine residue(s) of EZH2 protein in regulating its function as an epigenetic modulator, thereby proving the role of NO as a direct modulator of epigenetic processes. Indeed, we believe that this study will open up a new area of research to understand how NO release through eNOS/nNOS/iNOS in different and versatile cell types could modulate epigenetic processes thereby altering the epigenetic landscape of a cell when the level of NO is changed in these cells. Furthermore, the proposed study will open up new areas of

research to understand how globally NO could possibly regulate other histone-modifying enzymes, including HDACs, HATs, HMTs, KDMs and other epigenetic modulators to directly interplay with the epigenetic landscape of a cell.

However, if such NO-dependent gene expression changes are the cause of NO's direct effect on the epigenomic landscape of the cells is needed to be confirmed. In the present proposal, we proposed experiments, that essentially will address whether NO-mediated post-translational modification of histone methyltransferase EZH2 could control EZH2 catalytic activity, localization, and stability.

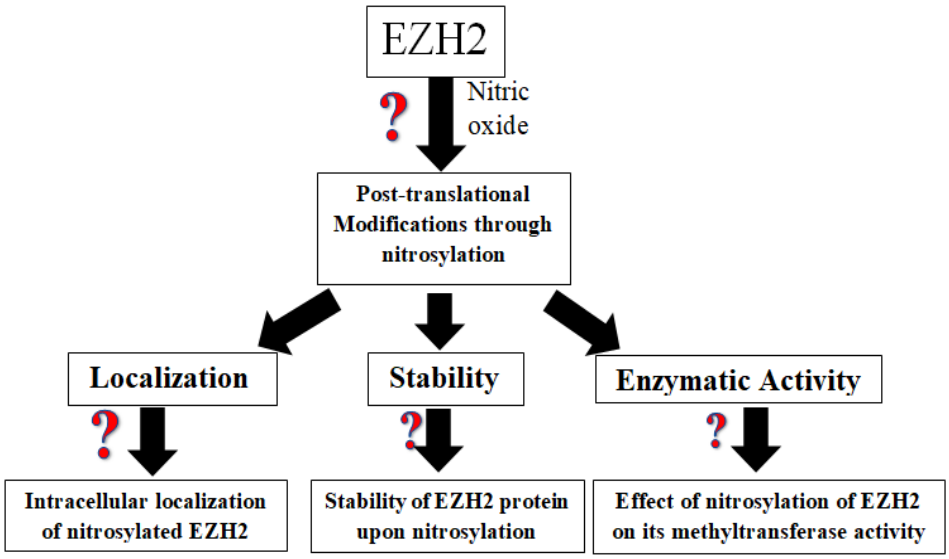

Figure 1.14.1- Flow diagram showing the gaps in the research.

Objective 1: Identifying and validating new post-translational modification of Enhancer of Zeste Homolog 2 through in silico and experimental analysis.

Objective 2: Understanding the effect of the post-translational modification on EZH2 stability and localization.

Objective 3: Exploring the effect of nitrosylation of EZH2 on its catalytic activity and epigenetic regulation.

Chapter 2:
Materials and Methods

2. MATERIALS AND METHODS:

2.1 Cell culture

Experiments were done primarily in EA. hy926 (immortalized human umbilical vein endothelial cell), purchased from ATCC, Manassas, USA (#CRL-2922). The cells were cultured in Dulbecco's modified Eagle's medium (DMEM) (#AL006A; HiMedia Laboratories) supplemented with 10% fetal bovine serum (#RM1112, FBS; HiMedia Laboratories) and 1% penicillin/streptomycin (#10378, PS; Gibco). The cells were passaged every 2-3 days. Human umbilical vein EC (HUVEC) (#CL002-2XT25, Hi Media Laboratories) were cultured and passaged using HiEndoXL™ EC Expansion medium (#AL517, HiMedia Laboratories) along with 4%growth factor, 5% fetal bovine serum and 1% penicillin/streptomycin antibiotic. Human Embryonic Kidney (HEK-293) cell line was a kind gift from Prof. Uma Dubey (Department of Biological Sciences, Birla Institute of Technology and Science Pilani, Pilani Campus, India) was maintained in Minimum Essential Media Eagle (MEM) (#AT154; HiMedia Laboratories). All the cells were maintained at 37 ° C with 5% CO2 in a humidified incubator.

2.2 Inducers and Inhibitors

Sodium Nitroprusside dihydrate (SNP, 500 µM) (#71778, Sigma 514 Aldrich) was used as an exogenous donor of NO in our experiments. Natural induction of NO was activated using 10 µM of Bradykinin (BK) (#B3259; Sigma Aldrich). Inhibition of NO in cell system was achieved by treating the cells with *N*ω-Nitro-L-arginine methyl ester hydrochloride (L-NAME, (1 mM) (#N5751; Sigma Aldrich) which is an analog of arginine. Bafilomycin A1 (100 nM) (#11038; Cayman Chemicals) was used as an

autophagy Inhibitor. MG132 (1 µM) (#M7449), a proteasomal inhibitor was from Sigma Aldrich. GSK J4 (5 µM) (#SML-0701), a H3K27me3 demethylase inhibitor was from Sigma Aldrich.

2.3 Griess Assay

Cells grown to 85% confluency in the 96 well plate, were provided treatment conditions, following which the cells were washed with sterile1xPBS. This was followed by addition of 50 ul of Sulfanilamide Solution (prepared by diluting 1% sulfanilamide in 5% phosphoric acid) to all the samples. This sample was then incubated for 10 mins in dark at RT. 50 ul of NED solution(prepared by diluting 0.1% N-1-napthylethylenediamine dihydrochloride in water) was then added to each well followed by incubating again in dark conditions for 10- 15 mins. The absorbance was measured at 540nm.

2.4 Immunoblotting

Cells grown to 80% confluency were provided treatment conditions followed by washing with sterile1xPBS. They were then incubated in RIPA buffer (#9806; Cell Signaling Technology) containing protease inhibitor for lysis after washing with sterile 1X PBS. After scraping, the cells were subjected to repeated cycles of sonication for 10 s (×2). This was followed by a centrifugation step at 10,000 g for 10 min to pellet down the cell debris and collect the supernatant. Protein 550 quantification was done by Bradford assay. After this, the protein samples were mixed with 5× laemmli buffer and heated at 100°C for 10 mins. They were then processed for SDS polyacrylamide gel electrophoresis with 10–250 kDa prestained protein ladder (#PG-PMT2922;

Genetix) used for molecular weight reference. Proteins were transferred onto a nitrocellulose membrane (Bio-Rad) at 15 V, 2.5 A for 35 min. The membrane was blocked with 5% skimmed milk for 1 h. The membrane was incubated overnight at 4°C with the primary antibodies: EZH2 mAb (1:1000; #5246), JARID2 Rabbit mAb (1:1000; #13594), SUZ12 Rabbit mAb (1:1000; #3737), EZH1 Rabbit mAb (1:1000; #42088), EED Rabbit mAb (1:1000; #51673), AEBP2 Rabbit mAb (1:1000; #14129). H3K27me3 (1:1000), UTX (1:1000), JMJD3 (1:1000), HA-Tag Rabbit mAb (1:500; #3724), GAPDH Rabbit mAb (1:2000; #5174), β-actin (1:2000; #3700), H3 Rabbit mAb(1:2000, #4499) (Cell Signaling Technology), S-Nitrocysteine mAb (1:500; #94930) Ubiquitin mAb(1:1000;#3933). Afterward, the blots were washed with TBS-T(x3) and incubated with a secondary peroxidase-conjugated antirabbit or mouse IgG antibody (1:2000) (#7074 or #7076, Cell Signaling Technology) overnight. These conjugation reactions were detected using the Clarity™ (#1705061) or Clarity™ Max Western ECL Substrates (#1705062) (Bio-Rad).

2.5 Cyclohexamide Chase Assay

Cyclohexamide chase experiment was performed to block cellular translation in order to inhibit the synthesis of any new proteins. For this, EAhy926 cells, grown to 80% confluency were pre-treated with 100µg/ml cycloheximide(#239764, Merck) for 4 hours, this was followed by GSNO exposure for 2 hours and the cells were then harvested for immunoblot studies.

2.6 Subcellular fractionation

Following the treatment with SNP for the given time point conditions, EA. hy926 cells were washed with phosphate-buffered saline (PBS) followed by scraping. The cell pellet was resuspended in ice-cold PBS containing 0.1% Nonidet P-40 (NP-40) and 1% protease inhibitor (#P8340; Sigma Aldrich) following centrifugation. After 10 mins of centrifugation, the supernatant was collected as the cellular and cytoplasmic fraction, and the nuclear fraction was further pelleted down. The cellular and nuclear lysate obtained was sonicated for 10 s (×2) followed by Immunoblotting experiments.

2.7 Coimmunoprecipitation Experiments

Protein extraction was carried out using 1x RIPA buffer. After washing the Dynabeads (SureBeads™ Protein A Magnetic Beads, #1614013, BioRad) in PBS-T(x3), they were preincubated with the EZH2 mAb, Ha Tagged mAb, ubiquitin mAb or S-Nitrocysteine mAb (1:50) for 2hrs. The beads were then washed and incubated overnight with a protein cell lysate containing 1000 µg of total protein for pulldown of the desired protein from the cell lysate. The cell lysate was then heated at 70° C for 10 mins and magnetized to be separated from the beads. This was then 585 processed for immunoblotting experiments.

2.8 RNA Isolation, cDNA Synthesis and qPCR

Reverse transcriptase-quantitative polymerase chain reaction (RT-qPCR) was performed to measure different gene expressions at the transcription level. Upon reaching 80% confluency EA. hy926 cells underwent GSK-J4 treatment for 4 hr

followed by SNP exposure for 2hrs. After that, RNA was isolated from the cells using Trizol Reagent (#15596, TRIzol™ Reagent; Life Technologies, Thermo Fisher Scientific). RNA isolation was succeeded by cDNA preparation from 1µg of total RNA using iScript™ cDNA Synthesis Kit (#1708891; Bio-Rad Laboratories, Hercules, CA, United States). The quality and quantity of the RNA was measured using a Nano-Drop spectrophotometer (SimpliNano; GE Lifesciences). Before cDNA synthesis, DNA contamination was removed by pre-treating isolated RNAs with the DNase. This was followed by Real-time PCR where iTaq™ Universal SYBR® Green Supermix (#1725124; Bio-Rad Laboratories) was used with a total master mix volume of 10 µl and GAPDH was taken as the housekeeping gene. Data analysis was done by calculating delta-delta Ct. Details of the primers are as given in **Table 2.6.1**.

Details of the primers for qPCR analysis are as follows-

Primer Name	**Sequence (5'->3')**
KDR Forward	CCTCCTTCTCTAGACAGGCG
KDR Reverse	CCTCTGTCCCCTGCAAGTAA
TBX20 Forward	ACAGCCTCATTGCTCAACCT
TBX20 Reverse	GCTCTCCACACTTTCCCTCT
VEGFAa Forward	GGCCAGCACATAGGAGAGA T
VEGFAa Reverse	ACGCTCCAGGACTTATACCG
MMP2 Forward	CTACTGAGTGGCCGTGTTTG
MMP2 Reverse	TCCCTGAGGTTCTCTTGCTG
TIE 1 Forward	CAGCCTCTACCCTTAGCTCC
TIE 1 Reverse	AAAGGCCGAAGTCTGCAATC
TEK Forward	TGGACAAGAGGGATGCAAGT
TEK Reverse	TGCCTTCTCTCTCACACTGG
FGF2 Forward	AGTCTTCGCCAGGTCATTGA
FGF2 Reverse	CCTGAGTATTCGGCAACAGC

Angiopoietin2 Forward	GTGTCCTCTTCCACCACAGA
Angiopoietin2 Reverse	TCAGCCTCGGGTTCATCTTT

Table2.6.1- List primers for qPCR analysis

2.9 Immunofluorescence and Confocal Microscopy

Following SNP treatment in EA. hy926 & transfected HEK-293 cells were fixed using 2% paraformaldehyde (10 mins). The coverslips were then treated with 0.1% Triton X-100 (5 min) for permeabilizing the cells. Blocking was done with 2% bovine serum albumin (BSA) for 60 mins at room temperature. Afterward, cells were incubated with primary antibodies EZH2 Rabbit mAb (1:1000) or HA-tag (Alexa Fluor™ mAb 647 Conjugate) (1:2000; #37297) overnight at 4°C. The cells were co stained with Alexa Fluor™ Plus 480 conjugated antirabbit IgG secondary antibody (1:4000; #A32732) (Thermo Fisher Scientific) for 1 h followed with phalloidin for staining F-actin (1:5000; #A22287 or #A12379, Thermo Fisher Scientific) for 30 min. At last, the cells were stained with 1 μM of DAPI (#D9542; Sigma-Aldrich) for 10 min for nuclear staining. Imaging was done using Zeiss Apotome 2.0 microscope (Carl Zeiss) and fully Spectral Confocal Laser Scanning Microscope (#LSM 880Carl Zeiss).

2.10 Ex vivo experiments using rat aortic tissues

The Institutional Animal Ethics Committee of BITS Pilani, Pilani Campus approved all experimental procedures for the rodent studies. Ex vivo experiments were done using Male Wistar rats aged 12–16 weeks. After giving anaesthesia, the rats were dissected from the ventral end. PBS was used to perfuse the heart and aorta, eliminating blood cells from the vessels. The primary aortas were then collected, and the fatty tissue

layers were removed carefully. For acquiring the aortic explants, the aorta was cut in a size of 4-5 mm cylindrical pieces. Following a PBS wash, the explants were cultured in HiEndoXL™ EC expansion medium and incubated in the complete growth medium for 12 hrs before initiating the treatment. Afterward, the tissue fractions were homogenized and subjected to sonication after suspending them in RIPA lysis buffer. The protein was estimated using Bradford assay followed by immunoblotting studies.

2.11 Biotin Switch Assay

EA. hy926 cells or EZH2 WT/mutant overexpressing HEK-293 treated with NO donor SNP (500 µM) for 2 hours were processed with the help of a Biotin Switch Assay kit (Abcam) using the standard manufacturer protocol. With this, all the "S-NO" (S-nitrosylated) groups were replaced with Biotin, forming an S-Biotin complex, which was detected by incubation with the streptavidin bound HRP reagent. After this, the samples were immunoprecipitated with EZH2 specific antibody using the above mentioned protocol. This was followed by dot blot and immunoblotting experiments for the detection of the S-nitrosylation of the EZH2 protein.

2.12 Scratch wound healing Assay

EA. hy926 cells were grown in a 24-well plate. They were pre-treated with GSK-J4 for 4 hrs following SNP treatment at regular intervals(0-24hrs) to measure the wound healing under different treatment conditions or in combination. Imaging was done at definite intervals to calculate the wound healed by cell migration. The wound was created in a straight line. Another perpendicular wound to the first one was drawn to create a cross-shaped wound using a 1mm microtip.

2.13 Detection of S-Nitrosylation using iodoTMT labelling ™ Reagent

EZH2 recombinant protein (#MBS2097714, MyBioSource) were treated with GSNO (100µM) for 30 mins. The samples were then processed for iodoTMT labelling with Pierce TM S-Nitrosylation Western Blot kit (#90105, Thermo Fisher Scientific™). A total of 5µg/ml of EZH2 recombinant protein sample was prepared for both control and GSNO treated conditions in 100µl of HENS Buffer. Next, MMTS was added to each, following vortexing for 1 min and incubating it at room temperature for 30 mins to block all free thiols. The protein was then precipitated by adding 600µl of pre-chilled (-20°C) acetone and freezing the samples at -20°C for 1 hr for MMTS removal. The samples were centrifuged at 4°C for 10 minutes (at 12000g). The tubes were inverted to decant the acetone and the white pellet was dried for 10-15 mins. The pellet was resuspended in 100µl of HENS Buffer 658 and 2µl of the iodoTMT zero labelling reagent was added followed by the addition of 4µl of 1M sodium ascorbate and vortexing briefly to mix and incubating it for 2 hrs at room temperature. The samples were then processed for immunoblotting experiments with anti-TMT antibody.

2.14 Sample Preparation for Mass Spectroscopy analysis

EA. hy926 cells were treated with GSNO (100µM) for 30 mins followed by lysis with RIPA buffer. Protein extraction was carried out using 1x RIPA buffer. After washing the Dynabeads (SureBeads™ Protein A Magnetic Beads, in PBS-T(x3), they were pre-incubated with the EZH2 mAb, (1:50) for 2hrs.The beads were then washed and incubated overnight with a protein cell lysate containing 1000ug of total protein for pulldown of EZH2 from the cell lysate. The cell lysate was then heated at 70° C for 10 mins and magnetized to be separated from the beads. Dynabead bound

immunoprecipitated proteins were eluted by heating the samples in 1X PBS. Eluted protein per sample was used for digestion and reduced with 5 mM TCEP and further alkylated with 50 mM iodoacetamide and then digested with Trypsin (1:50, Trypsin/lysate ratio) for 16 h at 37 °C. Digests were cleaned using a C18 silica cartridge to remove the salt**.** Protein per sample was used for digestion and reduced with 5 mM TCEP and further alkylated with 50 mM iodoacetamide and then digested with Trypsin (1:50, Trypsin/lysate ratio) for 16 h at 37 °C. Digests were cleaned using a C18 silica cartridge to remove the salt and dried using a speed vac. The dried pellet was resuspended in buffer A (2% acetonitrile, 0.1% formic acid).

2.15 Mass Spectrometric Analysis of Peptide Mixtures

Experiments were performed on an Easy-nlc-1000 system coupled with an Orbitrap Exploris mass spectrometer. 1µg of peptide sample were loaded on C18 column 15 cm, 3.0µm Acclaim PepMap (Thermo Fisher Scientific) and separated with a 0–40% gradient of buffer B (80% acetonitrile, 0.1% formic acid) at a flow rate of 500 nl/min) and injected for MS analysis. LC gradients were run for 110 minutes. MS1 spectra were acquired in the Orbitrap (Max IT = 60ms, AGQ target = 300%; RF Lens = 70%; R=60K, mass range = 375−1500; Profile data). Dynamic exclusion was employed for 30s excluding all charge states for a given precursor. MS2 spectra were collected for top 20 peptides. MS2 (Max IT= 60ms, R= 15K, AGC target 100%).

2.16 Data Processing

All samples were processed and RAW files generated were analysed with Proteome Discoverer (v2.5) against the Uniprot Human database. For dual Sequest and Amanda

search, the precursor and fragment mass tolerances were set at 10 ppm and 0.02 Da, respectively. The protease used to generate peptides, i.e. enzyme specificity was set for trypsin/P (cleavage at the C terminus of “K/R: unless followed by “P”). Carbamidomethyl on cysteine as fixed modification and oxidation of methionine and N-terminal acetylation were considered as variable modifications for database search. 694 Both peptide spectrum match and protein false discovery rate were set to 0.01 FDR.

2.17 Prediction of S-nitrosylation site in EZH2 protein using GPS-SNO prediction tools

To identify the cysteine residues that are likely to be S-nitrosylated in EZH2 protein, we performed an in-silico analysis of the same by using GPS-SNO prediction tools as available at http://sno.biocuckoo.org/. These tools have been developed by a group of scientists by manually collecting 467 experimentally verified S-nitrosylation sites in 302 unique proteins from scientific literature and can be used for the prediction of S-nitrosylation sites. The developer performed extensive leave-one-out validation and 4-, 6-, 8-, 10-fold cross-validation techniques to calculate the prediction performance and system robustness[107]. More than 250 publications have used these tools for the prediction of possible S-nitrosylation sites. We next used the human EZH2 primary protein sequence available in the addgene for hEZH2 plasmid (#24230, Addgene) and predicted the possible cysteine residues using the GPS-SNO prediction tools. EZH2 in total has 34 cysteine residues, and according to the partially resolved crystal structure of EZH2, none of these residues are involved in di-sulphide bonds and are likely to be cysteine residues with free –SH group. The analysis through the GPS-SNO

platform revealed three unique sites at cysteine 260, 329, and 700 which are likely to be S-nitrosylated.

2.18 Site-directed mutagenesis reaction

Phusion Site-Directed Mutagenesis Kit (#F541Thermo Fisher Scientific™) was used to insert point mutations at the specific positions in the pCMV-HA hEZH2 plasmid as mentioned in the manufacturer's protocol. Prior to this, the primers were phosphorylated using T4 Polynucleotide Kinase (#EK0031, Thermo Fisher Scientific™). After the ligation step, the mutated product was transformed in the competent Dh5-Alpha E. coli cells. The sequence of primers for inserting point mutations at the predicted sites to convert cysteine to serine are provided in **Table 2.16.1**(The point mutation inserted is marked in Red).

Primer Name	**Sequence (5'>3')**
EZH2 -260 Forward Reverse	TCCTCCTGAAAGTACCCCCAACATAGATG GAGTGCGCCTGGGAGCTGC
EZH2 329 Forward Reverse	TGGACCACAGAGTTACCAGCATT CAAGGTTTGTTGTCTAGAGC
EZH2 700 Forward Reverse	AAATCCAAACAGCTATGCAAAAG ACCGAATGATTTGCAAAAC

Table 2.16.1. List primers for inserting point mutation at specific locations

2.19 Transformation experiments and Plasmid Isolation

The ligation product from the SDM reaction was mixed with 100µl of competent DH5-Alpha cells and kept on ice for 25 mins. This was followed by heat shock at 42° C for 30 seconds. After adding 900 µl of SOC medium, the product was kept at 37° C for 1 hr. This was followed by centrifugation at 3000 rpm for 5 mins. 800 µl of supernatant was removed, and the pellet was resuspended in the remaining 100 µl media. The product was then spread on the LB Agar plate with the help of a spreader and kept overnight at 37° C. A single colony picked from the plate was used to inoculate 5 ml of Luria Broth (LB) containing ampicillin, which was kept overnight at 200 rpm and 37˚C. This was used for plasmid isolation, which was performed using the manufacturer's protocol (#12123, Qiagen Plasmid Minikit). Isolated plasmid was then sent for Sanger Sequencing to confirm the insertion of point mutations at the desired location and then used for further transfection experiments.

2.20 Plasmid and Transfection

Transfection experiments were done with human WT PCMVHA hEZH2 plasmid (#24230, Addgene), a kind gift from Dr. Kristian Helin (Biotech Research and Innovation Centre, University of Copenhagen, Copenhagen, Denmark). HEK-293 cells with 80% of confluency were transfected using 250ng/ml of pCMVHA hEZH2 and Lipofectamine 2000 (#11668030, Invitrogen, Thermo Fisher Scientific) for 4 hrs. After 48 hours of incubation, the cells were then used for immunoblotting and immunofluorescence experiments.

2.21 Model and Protein Preparation for *in silico* analysis

The crystal structure of the Human PRC2 (PDB ID: 5HYN) was acquired from the Protein Data Bank[108]. This complex exhibits multiple missing loops, particularly within the EZH2 residues at positions 1-9, 182-210, 249-256, and 345-421. To address these structural gaps, the EZH2 structure was downloaded from AlphaFold, assigned an AFDB accession code AF-Q15910-F1, and possessed an average pLDDT score of 76.25 (Uniport ID: Q15910)[109]. Subsequently, the EZH2 alphafold model was superposed to the original PDB file (5HYN) to obtain the PRC2 complex. Finally, EED, H3K79M, and JARID2 K116m3 proteins were deleted to keep only the EZH2-SUZ12 complex for further modelling studies. The EZH2-SUZ12 complex was pre-processed using Protein Preparation Workflow tool in Schrödinger suite 2022[110]. Hydrogens were added, charges were assigned, bond orders were refined, and all water molecules and non-standard residues were deleted before proceeding. The protein backbone was minimized by employing OPLS 2005 force field. Further residues Cys324 and Cys695 were S-nitrosylated by Vienna-PTM[111].

2.22 Molecular dynamics (MD) simulations

The charges of both wild-type and mutant complexes were neutralized by placing a total of 10 Na+ ions at positions with high electronegative potential. Both complex and counter ions were then placed in a pre-equilibrated cubic box of SPC/E water molecules. The periodic box of water was extended to a distance of 10 Å from the protein complex and counter ions. Another 442 NaCl molecules were added to the system to maintain a 150 mM salt concentration. The prepared systems were

subjected to 50,000 steps of steepest descent energy minimization. The structural fluctuations and stability of the relaxed protein complex were analyzed by time-dependent molecular dynamics (MD) simulation studies using GROMACS 5.1.5. The particle mesh Ewald method (PME) was used for the calculation of electrostatic interactions[112]. Periodic boundary conditions were imposed in all directions. The long-range electrostatic interactions have been calculated without any truncation, while a 10 Å cutoff was applied to Lennard– Jones interactions. The LINCS-like algorithm were employed to restrain hydrogen-containing bonds only and handle long-range electrostatic interactions. SHAKE algorithm was applied to constrain the bond involving hydrogens[113]. The temperature was controlled at 300 K using Langevin dynamics with the collision frequency 1. A time step of 2 fs was used and the structures were saved at every 10 ps interval for the entire duration of the MD run. Equilibrium phase was comprised of two short 1 ns simulations in NVT and NPT ensembles, utilizing a Berendsen thermostat and Parrinello-Rahman barostat respectively at 300K and 1 bar pressure. The unrestrained 1 μs simulation with NPT ensembles at 300 K was considered as production simulation.

2.23 Structure Analysis

Built-in features of GROMACS, such as gmx rms, rmsf, and hbond, were employed to assess the root mean-square deviation (RMSD), root-mean-square fluctuation (RMSF), and hydrogen bonds (Hbond), respectively, throughout the trajectory. Visualization of the structures was performed using PYMOL and VMD software[114,115].

2.24 Binding energy calculations using MM/PBSA

The MM-PBSA protocol was employed to determine the effect of PTMs addition on the binding of subunits within a chosen EZH2-SUZ12 complex. The free binding energies of each complex were computed utilizing the equations provided below. Briefly, the provided set of equations were applied to represent an imaginary AB dimer, where A corresponds to EZH2 and B to SUZ12.

$$\Delta Gbind = GAB - (GA + GB)$$

Where GAB is the binding free energy of the EZH2-SUZ12 complex, GA is the binding free energy of the EZH2, and GB is the binding free energy of the SUZ12.

$$\Delta\Delta G\_bind = \Delta G\_bindABnitrosylation - \Delta G\_bindABwildtype$$

To evaluate the impact of incorporating post-translational modifications (PTMs) into the complex on their binding, we compute the disparity in binding free energy (ΔΔGbind) between the S-nitrosylated and wildtype complexes using Equation 2. The binding free energy was determined by utilizing the 1μs trajectory obtained from molecular dynamics simulations, and calculations were performed on every 500 frames extracted from the last 500 ns of the trajectory using the g_mmpbsa tool integrated with GROMACS[116–118].

2.25 Statistics Analysis

All the values are expressed as the mean ± SD. An unpaired t-test was used to determine the statistical differences in comparisons between the two groups and one-

way ANOVA with a false discovery ratem(FDR) method was used for comparison between multiple groups. GraphPad Prism software (GraphPad Prism 9) was used to perform statistical analyses. A p-value (<0.05) was considered statistically significant.

Chapter 3:
Nitric Oxide caused S-Nitrosylation of EZH2 to induce PRC2 disassembly, EZH2 protein instability and loss of its catalytic activity

3.1 INTRODUCTION:

PRC2 works as chromatin-modifying group of proteins that act as repressors of gene expression. PRC2 is formed by three major classes of proteins; the functional enzymatic component of the PRC2, Enhancer of Zeste Homolog-2 (EZH2); suppressor of Zeste 12 (SUZ12), a PRC2 subunit and a scaffolding protein, and embryonic ectoderm development (EED) which assembles and stabilizes the PRC2 complex[119,120]. The importance of EED and SUZ12 in maintaining the Histone methyltransferase activity of EZH2 and in the stability of the PRC2 complex is well studied[121,122]. EZH2 is responsible for methylating the 27th lysine residue of histone H3 (H3K27) which results in the repression of gene expression[30,120]. Many studies have highlighted the importance of EZH2 as a crucial player in mediating cellular differentiation during development and also has a considerable role in various disease conditions[123]. Moreover, EZH2 mediates gene silencing in embryonic stem cells thereby promoting pluripotency, and in contrast also in the activation of differentiation[123,124]. The link between EZH2 regulation via deposition of the methylation marks and cancer progression is well reported describing its role in cancer progression and metastasis[31,32]. Indeed, EZH2 dependent suppression of the tumor suppressor genes during cancer progression promotes tumorigenesis[119,120].

The role of several post-translational modifications such as ubiquitination[57], phosphorylation[125], O-GlcNAcylation[70,71], SUMOylation[126], and methylation[127] in regulating EZH2 and its methyltransferase activity were previously reported. Ubiquitination is known to cause a decrease in the methyltransferase activity of EZH2 leading to its degradation. EZH2 has been shown to be phosphorylated by Akt[46] and AMPK[47], which leads to suppression of its methyltransferase activity[32].O-GlcNAcylation at serine in the SET domain of EZH2 is associated with increase in its methyltransferase activity[33]. Similarly, other mentioned PTMs at specific residues of EZH2, can regulate its stability

and catalytic activity. However, till date, no studies described how S-nitrosylation of EZH2 regulates its localization, degradation and catalytic activity. Nitrosylation by S-NO formation is one such PTM that has a potential in regulating protein function, stability, and cellular localization. It occurs through NO, a versatile free radical that forms SNO by selective modification of the protein at cysteine/methionine residues and mediate numerous biological functions[34]. Moreover, many cells harbor endogenous NO producing machinery including NO synthase class of enzymes. NO synthase (NOS) family of enzymes use L-arginine to endogenously produce NO which plays diverse roles in different cell types[17]. EC is one of such cell type that contain a very cell type specific NO producing machinery named as endothelial NOS (eNOS). eNOS dependent release of NO mediates various signaling cascade which are essential for endothelial migration, survival and growth. Indeed, eNOS driven release of NO uses S-nitrosylation dependent regulation of proteins to govern endothelial functions[18,19,57,128]. However, how eNOS dependent release of NO directs gene expression changes in EC through chromatin regulation remains elusive.

In this study, we addressed whether NO-mediated post-translational modification of histone methyltransferase EZH2 could influence its catalytic activity, localization, and stability. Through the present study, we established that S-nitrosylation of cysteine residue(s) in EZH2 protein amends its function as an epigenetic modulator, thereby proving the role of NO as a direct modulator of epigenetic processes and further regulating gene expression changes. This study for the first time connects the link between eNOS dependent NO release and its function as epigenetic modulator through regulation of EZH2 to alter chromatin structure and thereby dictate NO dependent gene expression changes.

3.2 RESULTS:

3.2.1 NO exposure interplayed with EZH2 including PCR2 assembly, its methyltransferase activity, subcellular localization, and stability.

NO is well-reported to regulate gene expression changes in EC[129]. However, whether such an effect is dependent on epigenetic processes specifically via regulation of EZH2 and PRC2 complex was never been reported. We therefore used sodium nitroprusside (SNP) as an external nitric oxide donor. We quantified cellular nitrite level using Griess assay which revealed significant increase in cellular nitrite level upon SNP challenge**(Fig. 3.2.1.1)**.

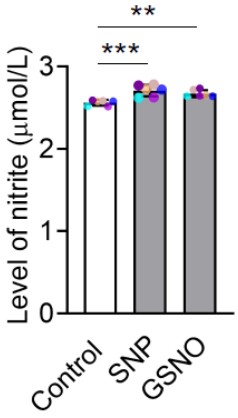

Figure 3.2.1.1- NO caused an increased in cellular Nitrite levels. *Griess Assay to analyze cellular Nitrite levels (n=6) upon SNP exposure.*

We also, assessed the effect of NO exposure on EZH2 protein and its catalytic product H3K27me3 level in EC. NO exposure time-dependently caused a reduction in the level of EZH2 protein specifically observing a significant reduction at 2 hours post-exposure to sodium nitroprusside (SNP), **(Figs. 3.2.1.2A, B)**. We also observed a significant reduction in the catalytic product H3K27me3, however, the reduction in H3K27me3 was detected

within 1 hour of SNP treatment, much earlier than the degradation of EZH2 **(Figs. 3.2.1.2C, D)**.

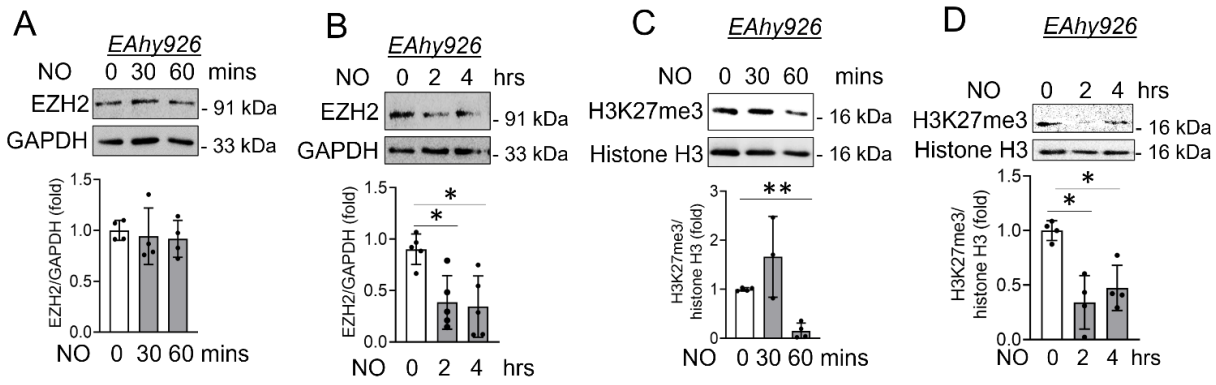

Figure 3.2.1.2- NO caused degradation of EZH2 protein accompanied with an early reduction in H3K27me3 levels. (A-D) *Immunoblots analysis of EZH2 (n=4) and H3K27me3 (n=5) proteins levels on exposure to SNP (500 µmol/L) in EA. hy926 cells for variable times.*

To confirm if such an effect of NO on EZH2 is exerted through transcriptional regulation, we performed qPCR analysis of EZH2 transcripts which revealed no alteration in EZH2 transcript level upon SNP exposure **(Fig-3.2.1.3).**

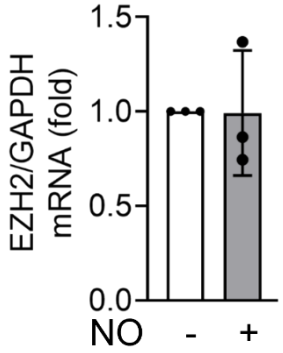

Figure 3.2.1.3 Unaltered EZH2 transcript levels on exposure to NO: *qPCR analysis to measure the transcript level of EZH2 in cultured EA. hy926 cells exposed to SNP (500 µmol/L) for 2 hours. (n=3)*

We next confirmed such changes in EZH2 and H3K27me3 levels *ex vivo* in rat aorta exposed to NO. Similar to *in vitro* findings, diminished EZH2 and H3K27me3 levels were detected in rat aorta exposed to SNP **(Figs..2.1.4 A-B).**

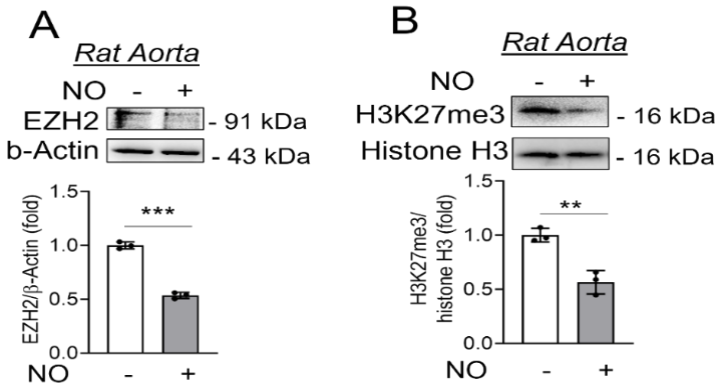

Figure 3.2.1.4 (A-B) Ex-vivo experiment to show the effect of NO on EZH2 & H3K27me3: *Immunoblot analysis using lysate of rat aortic explants exposed to SNP (500 µmol/L) for 2hrs. (n=3) showing EZH2**(A)** and H3K27me3 levels**(B)**.*

Because EC possesses endogenous NO-producing machinery namely eNOS, we next question whether activation of endogenous NO-production machinery shall also affect the levels of EZH2 and H3K27me3. Induction of EC by bradykinin dose- and time-dependently caused a reduction in EZH2 and H3K27me3 levels **(Figs.3.2.1.5 A-B).**

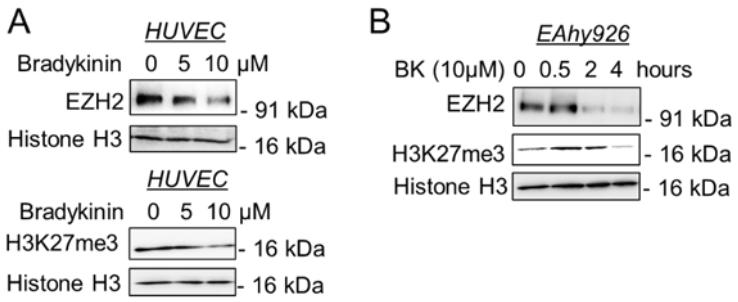

Figure 3.2.1.5 Induction of endogenous NO altered EZH2 and H3K27me3 levels (A-B) *Immunoblotting for EZH2 and H3K27me3 in HUVEC* ***(A)*** *and EA. hy926 cells* ***(B)*** *exposed to bradykinin (BK) (10 μmol/L). (n=3)*

To understand the cell-specific effect of NO on EZH2 and H3K27me3, we next exposed HEK-293, a non-EC type of human cells to NO donor and measured the level of EZH2 and H3K27me3. Through such an experiment, we established that NO exposure caused a reduction in EZH2 and associated H3K27me3 levels independent of the cell type under study suggesting such alteration on EZH2 and its downstream product could be sensitive to NO in many different cell types **(Fig-3.2.1.6 A).**

We next evaluated the effect of NO on EZH2 overexpressed through plasmid construct and confirmed that NO exposure also affects the level of overexpressed EZH2 as detected through HA tag or by detecting the total EZH2 **(Fig-3.2.1.6 B).**

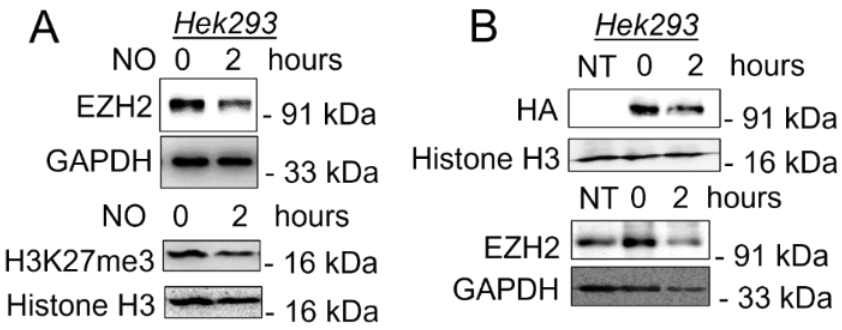

Figure 3.2.1.6 NO supplementation is associated with reduced EZH2 & H3K27me3 levels independent of cell types. (A) *Immunoblotting for EZH2 and H3K27me3 in HEK-293 cells on exposure to SNP (500 µmol/L) for 2 hrs. (n=3)* ***(B)*** *Immunoblotting experiment to show the HA-EZH2 and EZH2 levels in the lysates collected from HEK-293 cells transfected with plasmid containing HA tagged EZH2 followed by treatment with SNP (500 µmol/L) for 2 hrs. (n=3)*

Because we observed a reduction in H3K27me3 level much earlier than EZH2 degradation, we next urged whether NO exposure interplays with the assembly of the PRC2 complex which is essential for EZH2 catalytic activity to cause H3K27me3 deposition. We therefore performed a immunoprecipitation experiment using EZH2 antibody and detected dissociation of SUZ12 from EZH2 in EC exposed to SNP for only 30 minutes **(Fig.3.2.1.7).** All other components of the PRC2 complex remain associated with EZH2 at least until 30 minutes of NO exposure to EC**(Fig.3.2.1.7).**

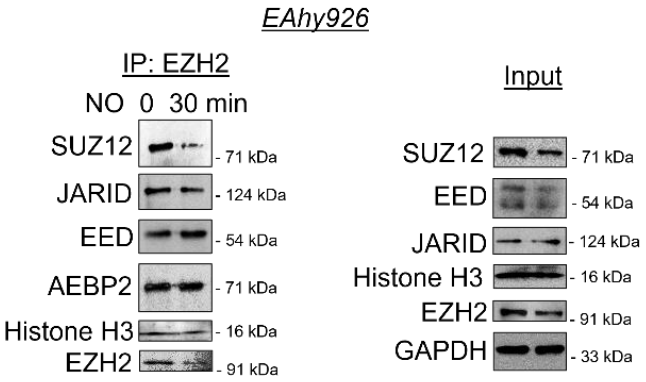

Figure 3.2.1.7 NO caused degradation of EZH2 protein due to dissociation of SUZ12 *EA. hy926 cells treated with SNP (500 µM) for 30 minutes were subjected to co-immunoprecipitation using EZH2 antibody followed by immunoblotting to show the association of EZH2 with other subunits of the PRC2 complex and histone H3. (n=3)*

Interestingly, the protein level of other components of PRC2 including SUZ12, AEBP2, EED, and JARID2 in total cell lysate remain unaltered upon NO exposure to EC. ***(Figure 3.2.1.8 A-B***)

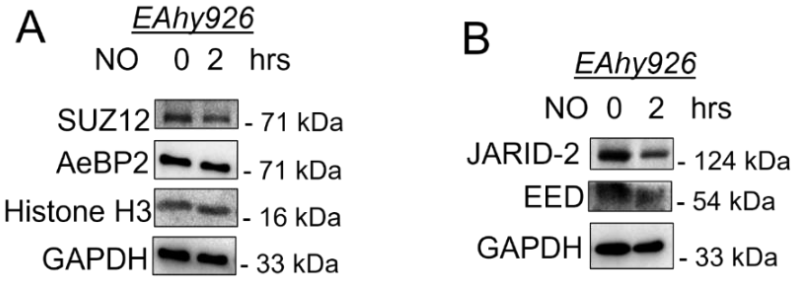

Figure 3.2.1.8 NO did not alter the levels of other PCR2 complex proteins. (A-B) *Immunoblotting for SUZ12, AEBP2, and histone H3* ***(A)*** *along with JARID2 and EED* ***(B)*** *after exposure of EA. hy926 cells to NO donor SNP (500 µmol/L) for 2 hrs. GAPDH was used as controls. (n=3)*

Being a histone-modifying enzyme and part of the PRC2 complex, EZH2 is primarily localized in the nucleus. However, cytosolic translocation of EZH2 was reported by many

earlier studies which also reported its cytosolic substrates including Talin[18] and small GTPases[17] to cause actin polymerization. We thus wanted to explore the effect of NO exposure on EZH2 localization. Subcellular fractionation and immunofluorescence **(Fig.3.2.1.9 A-B)** followed by confocal imaging strongly indicated cytosolic translocation of EZH2 in EC upon NO exposure. Moreover, confocal imaging also indicated recruitment of EZH2 protein to the filamentous actin **(Fig. 3.2.1.9 B)**.

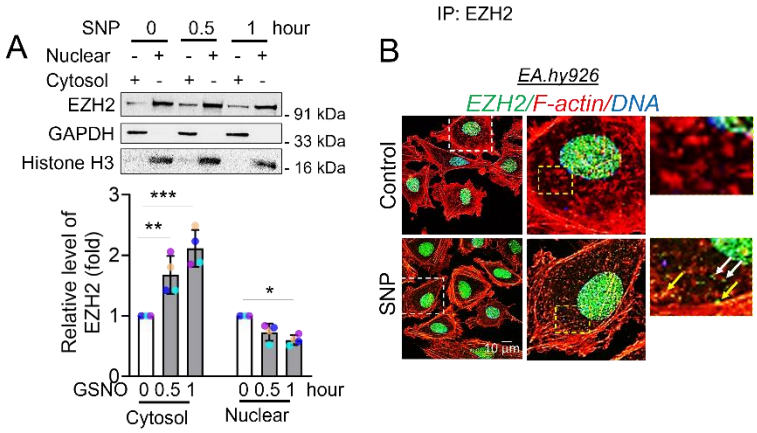

Figure 3.2.1.9 NO caused cytosolic localization and degradation of EZH2 protein with no effect on the localization of the other PRC2 subunits. (A) *Immunoblotting for EZH2 in nuclear and cytosolic fractions from EA. hy926 cells treated with SNP (500 µmol/L for 30 & 60 mins). GAPDH and histone H3 showed the purity of cytosolic and nuclear fractions respectively. (n=3)* ***(B)*** *Immunofluorescence followed by confocal imaging of EA. hy926 cells exposed to 1 hr of SNP to show cytosolic translocation of EZH2 (green). F-actin (red) is stained with phalloidin-Alexa Fluor 555. DAPI staining is shown in blue (Scale bar: 10 µm). (n=3) Values represent the mean ± SD. *p < 0.05, and **p < 0.01 by unpaired t-test for two groups.*

We next performed cycloheximide chase experiment in the presence of GSNO and detected the level of EZH2 when cellular translation was compromised. Absence of translation-dependent replenishment of EZH2 protein in GSNO treated cells revealed a significant reduction in EZH2 protein level within 0.5 and 1 hour which we failed to detect in translationally active normal cells**(Figure-3.2.1.10)**. Hence, this data confirmed the quick turnover of EZH2 protein through degradation pathways upon S- nitrosylation**.**

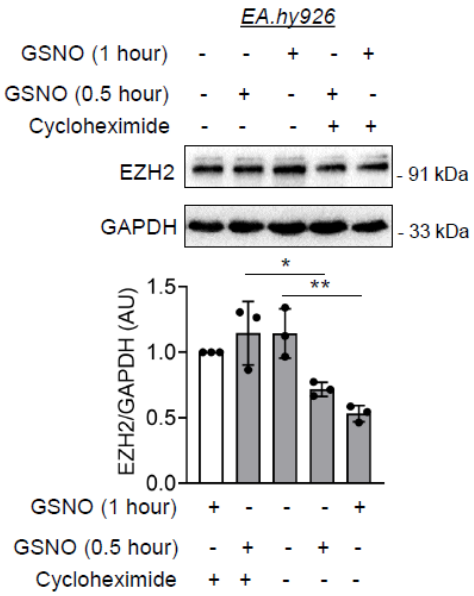

Figure 3.2.1.10 Cycloheximide chase experiment revealed early degradation of EZH2 when EZH2 protein turnover was blocked by inhibiting translation. *EZH2 was detected in EA.hy926 cells pretreated with cycloheximide(10mg/mL) for 4 hours followed by exposing to GSNO(100mmol/L)for different time points(0,0.5,and1hour).(n=3)*

No significant changes were detected in other components of the PRC2 including SUZ12, AEBP2, EED, and JARID2 which were primarily localized in the nucleus independent of NO treatment **(Figure 3.2.1.11).**

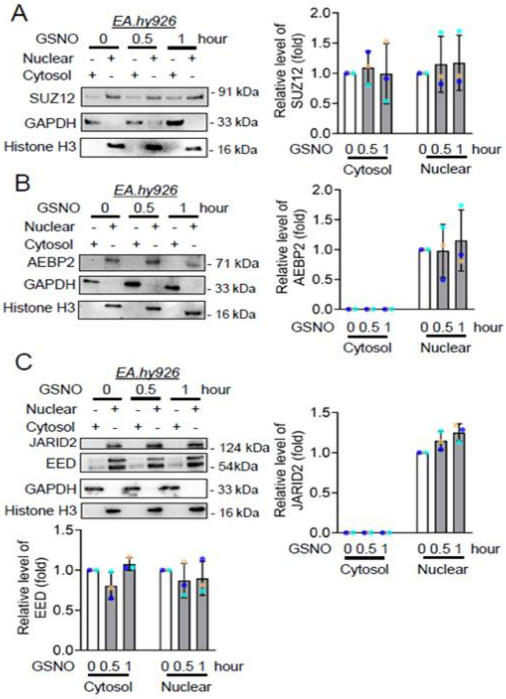

Figure 3.2.1.11 NO had no effect on the localization of the other subunits of PRC2 complex *Sub-cellular fractionation of cell lysates collected from EA. hy926 cells exposed to SNP (500 µmol/L) for 30 and 60 minutes followed by immunoblotting experiment for SUZ12, AEBP2, JARID2 and EED. Presence of GAPDH and histone H3 only in cytosolic and nuclear fractions respectively to indicate the purity of the cellular fractions. (n=3)*

Because the turnover of H3K27me3 is not only dependent on the methyl transferase EZH2 but also H3K27me3 specific demethylases UTX and JMJD3, we thus detected the quantity of UTX and JMJD3 protein in EC exposed to NO. UTX and JMJD3 protein levels remained unaltered in EC exposed to NO for 2 hours **(Figure 3.2.1.12)**.

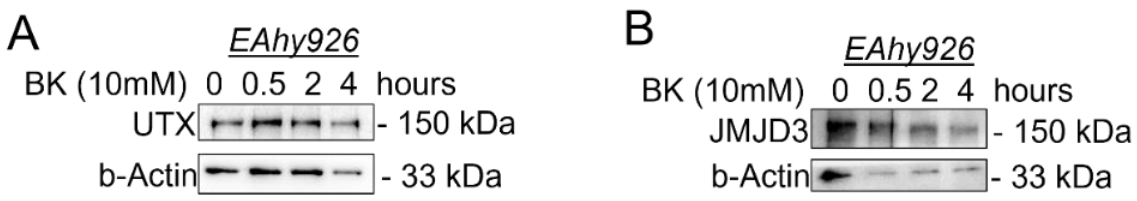

Figure 3.2.1.12 No changes were observed in the levels of H3K27me3 demethylases UTX and JMJD3 on NO exposure. A-B *Immunoblotting for UTX* ***(A)*** *and JMJD3* ***(B)*** *after exposing EA. hy926 cells to endogenous NOS machinery activator BK (10 µmol/L) for different time points. (n=3)*

3.2.2 NO exposure caused S-Nitrosylation of EZH2 leading to early SUZ12 dissociation and further altering its binding partners.

In the non-canonical NO signaling pathway, many proteins are post-translationally modified through nitrosylation of cysteine/methionine/tyrosine residue thereby regulating the function of such proteins. We, therefore, next questioned whether such could be the case with EZH2 as well. Thus, after establishing the effect of NO exposure on EZH2's methyltransferase activity, localization, and degradation, we next evaluated whether NO post-translationally modified EZH2 through S nitrosylation thereby regulating its function. Previous studies reported regulation of EZH2 localization and function via phosphorylation of distinct residues. S-nitrosylation of EZH2 protein has never been reported earlier and therefore we first assessed whether EZH2 is S-nitrosylated upon NO exposure.

Through the iodoTMT assay using truncated recombinant EZH2 protein (carrying residues from 429- 728 aa) in a cell-free system, we first confirmed that NO exposure caused S-nitrosylation of a truncated form of the EZH2 protein in a cell-free system **(Figure 3.2.2.1)**.

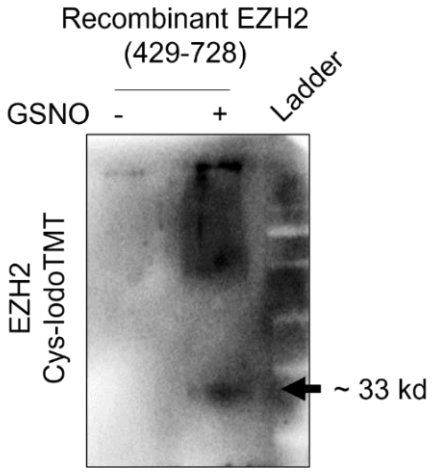

Figure 3.2.2.1 Confirming S-nitrosylation of recombinant human EZH2 (containing aa 429-728) using IodoTMT assay in a cell free system. *In a cell free system, a total of 1 µg recombinant human EZH2 (containing aa 429-728) protein was incubated with GSNO (100 µmol/L) for 30 minutes followed by processing through iodoTMT protocol. Samples were run through SDS-PAGE followed by transferring to nitrocellulose membrane and were incubated with anti-IodoTMT antibody. Blots were developed with chemiluminescence substrate for visualization*.

Further to confirm this in a cellular system, EC were exposed to SNP followed by Biotin Switch assay and immunoprecipitation using EZH2 antibody. Such an experiment also demonstrated S-nitrosylation of EZH2 protein in EC subjected to NO treatment **(Figure**

3.2.2.2 A-B). Further to ascertain the S-nitrosylation, we next used a pan S nitrosylated antibody and confirmed through an immunoprecipitation followed by an immunoblot experiment that EZH2 in EC was indeed S-nitrosylated upon NO exposure **(Figure 3.2.2.2 C)**.

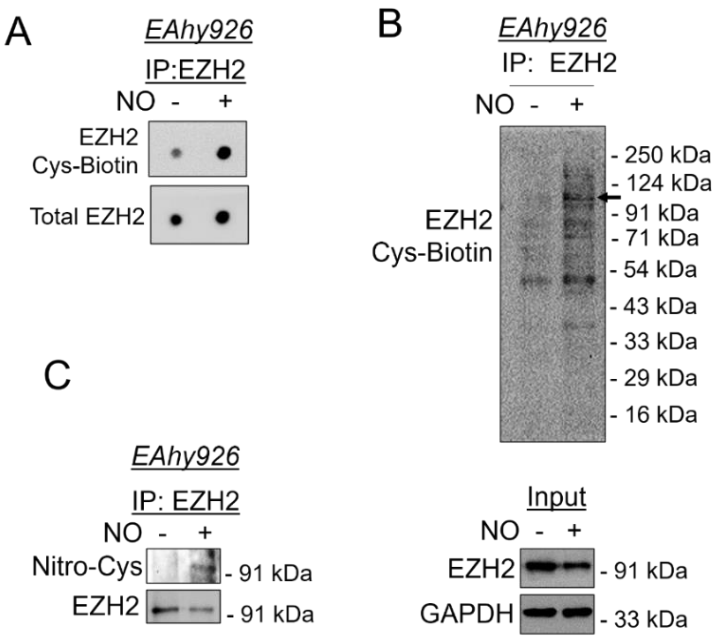

Figure 3.2.2.2 External NO supplementation was accompanied with S-nitrosylation of EZH2 (A) *Dot blot of protein lysates collected from EA. hy926 cells exposed to SNP (500 µmol/L) for 30 min and processed through biotin switch assay followed by immunoprecipitation with EZH2 antibody. Blots were incubated with Streptavidin-HRP followed by developing with chemiluminescence substrate for visualization. (n=3)* ***(B)*** *Same samples were run through SDS-PAGE followed by transfer to nitrocellulose membrane followed by incubation with Streptavidin-HRP and developing the blot with chemiluminescence substrate for visualization. (n=3)* ***(C)*** *EA. hy926 cells were exposed to either SNP (500 µmol/L) for 30 minutes followed by immunoprecipitation with EZH2 antibody and further immunoblotting to show the presence of S-nitrosylation of EZH2 using Nitro-Cysteine antibody. (n=3)*

We next performed a co-immunoprecipitation experiment using EC which was exposed to bradykinin, a natural inducer of endogenous NO production. In doing so, we detected a robust S-nitrosylation of EZH2 protein concurrent with the loss of EZH2 binding with SUZ12 of the PRC2 complex **(*Figure 3.2.2.3* A)**. Furthermore, to support this data, we also analyzed the S-nitrosylation of HA-tagged EZH2 protein in a HEK-293 overexpression system. Through a co-immunoprecipitation experiment using HA antibody, we again confirmed S-nitrosylation of overexpressed EZH2 protein upon exposure to NO **(*Figure 3.2.2.3* B)**.

Figure 3.2.2.3 Induction of endogenous NO producing machinery caused S-

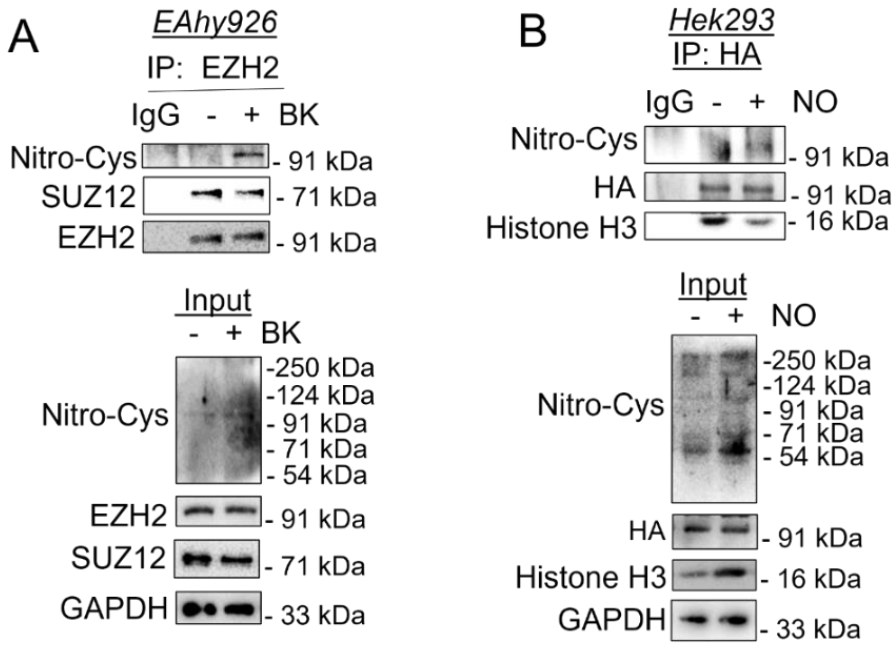

nitrosylation of EZH2 and dissociation of SUZ12 and histone H3*.(A) EA. hy926 cells were exposed to bradykinin (10 µmol/L, D) for 30 minutes followed by immunoprecipitation with EZH2 antibody and further immunoblotting to show the presence of S-nitrosylation of EZH2 using Nitro-Cysteine antibody. (n=3)* ***(B)*** *Plasmid containing HA tagged EZH2 were transfected in HEK-293 cells followed by exposing to SNP (500 µmol/L) for 30 minutes. Cell lysates were then immunoprecipitated using HA antibody followed by immunoblotting with respective antibodies. (n=3)*

To exclude the possibility of the effect of SNP on EZH2 as non-specific, we next used GSNO which is more well-accepted to impart S-nitrosylation of cellular proteins. In so doing, we found similar reduction in the level of EZH2 after 120 minutes of GSNO exposure (***Figure 3.2.2.4 A***). As similar to SNP treated EC, further analysis of H3K27me3 in the GSNO treated cells revealed time dependent depletion of H3K27me3 by 60 minutes which remained significantly low at least up to 120 minutes post-GSNO treatment (***Figure 3.2.2.4 B***).

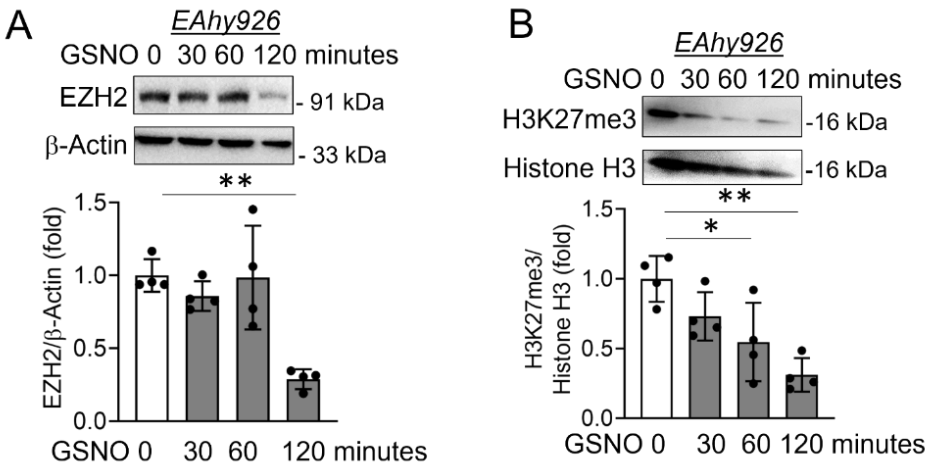

Figure 3.2.2.4 GSNO exposure also caused reduction in EZH2 and H3K27me3 level similar to the effects observed with SNP (A-B) *Immunoblotting for EZH2* ***(A)*** *and H3K27me3* ***(B)*** *in cultured EA. hy926 cells upon exposure to GSNO (100 µmol/L) for different time points (0, 30, 60, and 120 minutes). (n=4)*

We next wanted to explore the comprehensive interacting partners of EZH2 upon S-nitrosylation to understand the effect of such post-translational modifications on its methylation, translocation and degradation. Mass spectrometric analysis revealed the comprehensive association map of EZH2 in control and GSNO treated cells **(Figure 3.2.2.4 A)**. A total of 261 proteins were identified to be associated with EZH2 while 341

different proteins associated with EZH2 upon GSNO exposure **(Figure 3.2.2.5 B,C)**. Out of 261 proteins in control condition, 48 unique proteins were associated with EZH2 which completely dissociated upon GSNO exposure. In contrast, 128 (out of 341 in total) unique proteins were bound to EZH2 upon GSNO exposure which were not detected to be associated with EZH2 in untreated cells **(Figure 3.2.2.5 B, D) (Tables 3.2.2.1-3.2.2.2)**.

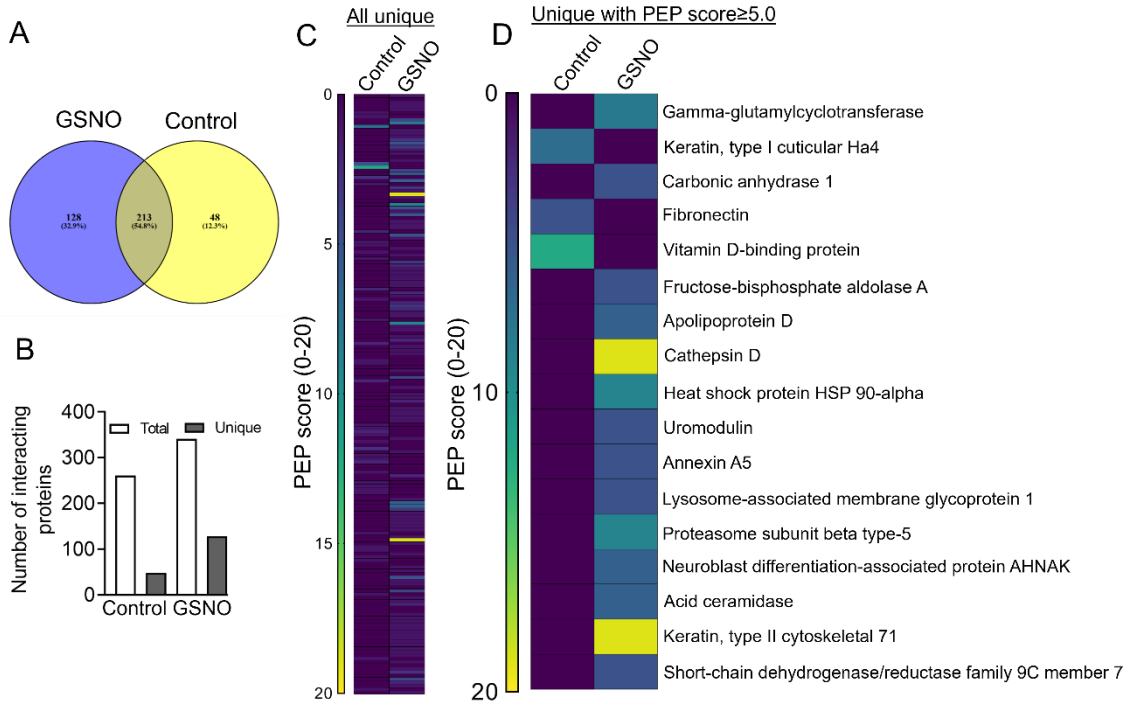

Figure 3.2.2.5 GSNO exposure was also accompanied with altering the interacting partners of EZH2.(A) *Venn-diagram show the percentage of common/overlapping proteins in control and 30 minutes GSNO (100 µmol/L) exposed EA. hy926 cells as analyzed through orbitrap mass spectrophotometer.* ***(B)*** *Data showing the number of total and unique interacting proteins present in EA. hy926 cells upon exposure to GSNO (100 µmol/L) for 30 minutes.* ***(C)*** *Heat map based visualization of all the uniquely interacting proteins in control and GSNO treated EA. hy926 cells.* ***(D)*** *Heat map based visualization of uniquely interacting proteins in Control and GSNO treated groups with a PEP score ≥5. Values represent the mean ± SD. *p < 0.05, and **p < 0.01 by unpaired t-test for two groups.*

We next performed a close analysis of the interactome data which indicated few interesting association patterns of EZH2 in untreated and GSNO treated conditions. Firstly, as observed through co-immunoprecipitation experiment, EZH2 was found to be associated with histone H3 in untreated cells, however, such association was not detected upon GSNO exposure. Surprisingly, nuclear-to-cytosolic shuttling protein 14-3-3 was found to be associated with EZH2 in untreated conditions while a complete loss of association was observed upon GSNO challenge **(Figure 3.2.2.5 C, D) (Tables 3.2.2.1-3.2.2.2)**. Although, we expected such association with 14-3-3 to be prominent upon GSNO exposure due to EZH2 cytosolic shuttling after S-nitrosylation, however, we observed an opposite correlation. Such data indicated that EZH2 may be using 14-3-3 during natural cytosolic localization while its cytosolic localization upon S-nitrosylation is likely to be driven by other unknown factors. More interestingly, upon GSNO exposure, we detected EZH2 association with many proteins of the endosome/lysosome/proteasome pathway proteins including several Rab family of proteins, HSP70&90 chaperon proteins, cathepsin D lysosomal protease, lysosome-associated membrane glycoprotein 1, proteasome subunit beta type-5/alpha type-4, lysosomal acid ceramidase **(Figure 3.2.2.5 C, D) (Tables 3.2.2.1-3.2.2.2)**. EZH2 was not found to be associated with these proteins in control conditions.

Table 3.2.2.1: List of all unique proteins associated with EZH2 in untreated(control) EA. hy926 cells

S.NO	Description	Exp. q-value: Combined	Sum PEP Score	Coverage [%]	# Peptides	# PSMs	# Unique Peptides
1.	Vitamin D-binding protein	0	12.02	10	3	5	3

2.	Keratin, type I cuticular Ha4	0	7.491	10	5	14	3
3.	Fibronectin	0	5.419	1	1	1	1
4.	Semenogelin-1	0	3.294	7	2	4	2
5.	60S ribosomal protein L23a	0	3.018	13	2	4	2
6.	Heterogeneous nuclear ribonucleoproteins A2/B1	0	2.772	5	2	4	1
7.	60S ribosomal protein L14	0	2.617	6	1	2	1
8.	Lysosomal protective protein	0	2.438	3	1	2	1
9.	60S ribosomal protein L22	0	2.428	10	1	2	1
10.	40S ribosomal protein S15a	0	2.277	18	2	4	2
11.	60S ribosomal protein L8	0	2.186	4	1	2	1
12.	Heterogeneous nuclear ribonucleoprotein R	0	1.904	2	1	2	1
13.	Heterogeneous nuclear ribonucleoprotein Q GN=SYNCRIP PE=1 SV=2	0	1.904	2	1	2	1
14.	60S ribosomal protein L7a	0	1.85	5	1	2	1
15.	Semenogelin-2	0	1.844	4	1	2	1
16.	Putative histone H2B type 2-C	0	1.69	5	1	2	1
17.	Putative histone H2B type 2-D	0	1.69	5	1	2	1
18.	60S ribosomal protein L23	0.004	1.558	6	1	2	1
19.	Probable ATP-dependent RNA helicase DDX17	0.004	1.44	2	1	2	1
20.	Probable ATP-dependent RNA helicase DDX5	0.004	1.44	2	1	2	1
21.	Y-box-binding protein 3 OS=Homo sapiens	0.004	1.38	2	1	2	1
22.	Y-box-binding protein 2	0.004	1.38	2	1	2	1
23.	Y-box-binding protein 1	0.004	1.38	2	1	2	1

24.	60S ribosomal protein L35	0.004	1.338	8	1	2	1
25.	40S ribosomal protein S8	0.004	1.325	5	1	1	1
26.	Histone H3.3	0.004	1.2	5	1	2	1
27.	Histone H3.1t	0.004	1.2	5	1	2	1
28.	Histone H3.3C	0.004	1.2	5	1	2	1
29.	Histone H3.1	0.004	1.2	5	1	2	1
30.	Histone H3.2	0.004	1.2	5	1	2	1
31.	Proteasome subunit beta type-6	0.004	1.196	4	1	2	1
32.	60S ribosomal protein L27	0.004	1.189	7	1	2	1
33.	Olfactomedin-like protein 3 sapiens	0.004	1.18	2	1	2	1
34.	ADP/ATP translocase 3	0.007	1.14	3	1	2	1
35.	ADP/ATP translocase 2	0.007	1.14	3	1	2	1
36.	ADP/ATP translocase 1	0.007	1.14	3	1	2	1
37.	Phosphatidylinositol 4,5-bisphosphate 3-kinase catalytic subunit alpha isoform	0.007	1.08	1	1	1	1
38.	Adenosylhomocysteinase	0.007	1.07	3	1	2	1
39.	60S ribosomal protein L24	0.007	1.066	5	1	2	1
40.	14-3-3 protein epsilon	0.007	1.063	3	1	2	1
41.	Peptidyl-prolyl cis-trans isomerase A	0.01	0.96	5	1	2	1
42.	Myosin regulatory light chain 2, skeletal muscle isoform	0.014	0.937	11	1	2	1
43.	Heterogeneous nuclear ribonucleoprotein H	0.014	0.935	1	1	1	1
44.	Heterogeneous nuclear ribonucleoprotein H2	0.014	0.935	1	1	1	1
45.	Tumor necrosis factor alpha-induced protein 2	0.014	0.924	2	1	2	1
46.	Prostaglandin-H2 D-isomerase	0.013	0.915	4	1	1	1

47.	60S ribosomal protein L21	0.013	0.903	7	1	2	1
48.	Peroxisomal sarcosine oxidase	0.023	0.858	8	1	1	1

Table 3.2.2.2: List of all unique proteins associated with EZH2 in EA. hy926 cells upon GSNO treatment

S.No	Description	Exp. q value :Combined	Sum PEP Score	Coverage [%]	# Peptides	# PSMs	# Unique Peptides
1.	Keratin, type II cytoskeletal 71	0	19.924	11	6	27	2
2.	Cathepsin D	0	19.908	23	9	19	9
3.	Proteasome subunit beta type-5	0	9.822	23	5	11	5
4.	Heat shock protein HSP 90-alpha	0	9.085	8	5	11	2
5.	Gamma-glutamylcyclotransferase	0	8.324	14	2	6	2
6.	Apolipoprotein D	0	6.496	20	4	11	4
7.	Neuroblast differentiation-associated protein AHNAK	0	6.342	4	4	7	4
8.	Acid ceramidase	0	6.119	7	3	6	3
9.	Lysosome-associated membrane glycoprotein 1	0	5.893	6	3	6	3
10.	Annexin A5	0	5.796	8	2	4	2
11.	Carbonic anhydrase 1	0	5.501	11	2	4	2
12.	Fructose-bisphosphate aldolase A	0	5.423	10	3	8	3
13.	Uromodulin	0	5.358	6	4	8	4
14.	Short-chain dehydrogenase/reductase family 9C member 7	0	5.239	9	3	5	3
15.	Kallikrein-7	0	4.912	13	2	6	2
16.	Deleted in malignant brain tumors 1 protein	0	4.4	9	2	3	2
17.	Serotransferrin	0	4.289	4	3	6	3

18.	Gamma-glutamyl hydrolase	0	4.087	6	2	6	2
19.	Bleomycin hydrolase	0	3.78	7	3	6	3
20.	Calmodulin-like protein 5	0	3.776	9	1	1	1
21.	Proteasome subunit alpha type-3	0	3.687	9	2	4	2
22.	Keratin, type I cytoskeletal 18	0	3.348	6	3	10	2
23.	Purine nucleoside phosphorylase	0	3.195	7	2	5	2
24.	Ganglioside GM2 activator	0	3.167	8	2	4	2
25.	Alpha-1-antitrypsin	0	3.144	5	2	4	2
26.	Triosephosphate isomerase	0	2.876	8	2	4	2
27.	Galectin-3	0	2.853	9	2	4	2
28.	Tropomyosin alpha-4 chain	0	2.515	4	1	2	1
29.	Proteasome subunit alpha type-4	0	2.479	8	2	3	2
30.	Histone H2B type 1-A	0	2.166	13	2	4	2
31.	Proteasome subunit alpha type-1	0	2.164	5	1	2	1
32.	40S ribosomal protein S3	0	2.136	9	2	3	2
33.	Carboxypeptidase A4	0	2.052	4	2	4	2
34.	Catenin beta-1	0	2.023	2	2	3	2
35.	Small nuclear ribonucleoprotein Sm D3	0	1.983	8	1	2	1
36.	Glyceraldehyde-3-phosphate dehydrogenase, testis-specific	0	1.974	2	1	5	1
37.	U1 small nuclear ribonucleoprotein 70 kDa	0	1.926	5	2	4	2
38.	Proteasome subunit alpha-type 8	0	1.92	4	1	2	1
39.	Proteasome subunit alpha type-7	0	1.92	4	1	2	1
40.	Immunoglobulin lambda-like polypeptide 5	0	1.765	7	1	2	1
41.	Immunoglobulin lambda constant 6	0	1.765	14	1	2	1
42.	Immunoglobulin lambda constant 1	0	1.765	14	1	2	1

43.	Ras-related protein Rab-10	0	1.729	6	1	2	1
44.	Ras-related protein Rab-1A	0	1.729	5	1	2	1
45.	Ras-related protein Rab-3C	0	1.729	5	1	2	1
46.	Ras-related protein Rab-39A	0	1.729	5	1	2	1
47.	Ras-related protein Rab-3A	0	1.729	5	1	2	1
48.	Ras-related protein Rab-43	0	1.729	5	1	2	1
49.	Ras-related protein Rab-14	0	1.729	5	1	2	1
50.	Ras-related protein Rab-3B	0	1.729	5	1	2	1
51.	Ras-related protein Rab-15	0	1.729	5	1	2	1
52.	Ras-related protein Rab-8A	0	1.729	5	1	2	1
53.	Ras-related protein Rab-6B	0	1.729	5	1	2	1
54.	Ras-related protein Rab-12	0	1.729	5	1	2	1
55.	Ras-related protein Rab-4A	0	1.729	5	1	2	1
56.	Ras-related protein Rab-33B	0	1.729	5	1	2	1
57.	Putative Ras-related protein Rab-1C	0	1.729	5	1	2	1
58.	Ras-related protein Rab-4B	0	1.729	5	1	2	1
59.	Ras-related protein Rab-37	0	1.729	5	1	2	1
60.	Ras-related protein Rab-3D	0	1.729	5	1	2	1
61.	Ras-related protein Rab-1B	0	1.729	5	1	2	1
62.	Ras-related protein Rab-35	0	1.729	5	1	2	1
63.	Ras-related protein Rab-30	0	1.729	5	1	2	1
64.	Ras-related protein Rab-6A	0	1.729	5	1	2	1
65.	Ras-related protein Rab-39B	0	1.729	5	1	2	1
66.	Ras-related protein Rab-8B	0	1.729	5	1	2	1
67.	Immunoglobulin J chain	0	1.662	8	1	2	1
68.	Cytosol aminopeptidase	0	1.621	1	1	2	1

69.	Retinoid-inducible serine carboxypeptidase	0	1.618	2	1	2	1
70.	Protein S100-A6	0	1.604	9	1	2	1
71.	Cystatin-M	0	1.579	7	1	2	1
72.	Serpin B7	0	1.575	3	1	2	1
73.	60S ribosomal protein L36	0	1.541	9	1	2	1
74.	Calpain-1 catalytic subunit	0	1.515	1	1	2	1
75.	Destrin	0	1.447	4	1	2	1
76.	Proteasome subunit beta type-7	0	1.426	3	1	2	1
77.	60S ribosomal protein L13	0	1.39	6	1	2	1
78.	Transmembrane glycoprotein NMB	0	1.364	3	1	2	1
79.	Apolipoprotein A-II	0	1.344	9	1	2	1
80.	Speckle targeted PIP5K1A-regulated poly(A) polymerase	0	1.341	1	1	1	1
81.	Leucine-rich alpha-2-glycoprotein	0	1.322	3	1	2	1
82.	Loricrin	0	1.316	3	1	4	1
83.	Malate dehydrogenase, mitochondrial	0	1.3	3	1	2	1
84.	Translocator protein	0	1.246	5	1	2	1
85.	Testis-specific Y-encoded-like protein 2	0	1.214	1	1	2	1
86.	Heterogeneous nuclear ribonucleoprotein M	0	1.211	2	1	2	1
87.	Proteasome subunit alpha type-5	0.003	1.208	3	1	1	1
88.	Insulin-degrading enzyme	0.006	1.194	1	1	2	1
89.	Very-long-chain enoyl-CoA reductase	0.009	1.174	3	1	2	1
90.	Sesquipedalian-1	0.009	1.156	4	1	1	1
91.	60S ribosomal protein L28	0.009	1.149	5	1	2	1
92.	Histone H2B type 2-E1	0.011	1.113	7	1	2	1
93.	Epiplakin	0.011	1.11	1	1	2	1
94.	Plectin	0.011	1.11	0	1	2	1
95.	STE20-like serine/threonine-protein kinase	0.011	1.106	1	1	4	1
96.	Cytospin-B	0.011	1.106	1	1	4	1
97.	Chromobox protein homolog 6	0.014	1.07	2	1	2	1

98.	Chromobox protein homolog 8	0.014	1.07	2	1	2	1
99.	Rho guanine nucleotide exchange factor 40	0.014	1.065	1	1	2	1
100	Myosin-10	0.014	1.053	1	1	1	1
101	Vinculin	0.014	1.048	1	1	1	1
102	Heterogeneous nuclear ribonucleoprotein A1-like 2	0.014	1.045	4	1	1	1
103	Lamin-B1	0.014	1.043	1	1	2	1
104	Lamin-B2	0.014	1.043	1	1	2	1
105	Heat shock 70 kDa protein 6	0.014	1.032	1	1	2	1
106	Heat shock 70 kDa protein 1B	0.014	1.032	1	1	2	1
107	Heat shock 70 kDa protein 1-like	0.014	1.032	1	1	2	1
108	Toll-interacting protein	0.013	1.025	3	1	2	1
109	Reticulon-4	0.013	1.025	1	1	1	1
110	Ergosterol biosynthetic protein 28 homolog	0.021	1.005	6	1	2	1
111	Histidine--tRNA ligase, cytoplasmic	0.021	1.003	2	1	1	1
112	Stress-70 protein, mitochondrial	0.021	1.003	1	1	3	1
113	Exocyst complex component 4	0.021	0.998	2	1	3	1
114	Cystatin-SA	0.024	0.963	5	1	2	1
115	Leucine-rich repeat-containing protein 15	0.029	0.947	2	1	2	1
116	Tubulin alpha chain-like 3	0.029	0.942	2	1	2	1
117	Tubulin alpha-8 chain	0.029	0.942	2	1	2	1
118	Tubulin alpha-4A chain	0.029	0.942	2	1	2	1
119	Uncharacterized protein CCDC197	0.031	0.914	7	1	1	1
120	Ras-related C3 botulinum toxin substrate 3	0.031	0.903	4	1	2	1
121	Ras-related C3 botulinum toxin substrate 2	0.031	0.903	4	1	2	1
122	Ras-related C3 botulinum toxin substrate 1	0.031	0.903	4	1	2	1
123	Prosaposin	0.031	0.889	2	1	1	1
124	Transcription factor AP-2-delta	0.031	0.886	2	1	1	1

125	40S ribosomal protein S4, X isoform	0.031	0.882	3	1	1	1
126	Serpin B10	0.031	0.867	3	1	1	1
127	H(+)/Cl(-) exchange transporter 3	0.03	0.85	1	1	2	1
128	Fibrinogen gamma chain	0.03	0.841	3	1	2	1

3.2.3 NO caused the degradation of EZH2 primarily through autophagosome-lysosome pathway while inhibition of endogenous NO machinery reversed NO dependent degradation, activity and localization of EZH2

Because we observed association of many endosomal/lysosomal and proteasomal proteins, we therefore questioned the role of lysosomal and proteasomal degradation pathways in S-nitrosylation dependent degradation of EZH2. The role of post-translational modification-dependent regulation of EZH2 protein degradation is least studied. Because we observed EZH2 protein degradation upon NO exposure, we therefore explored the key degradation machinery responsible for S-nitrosylated EZH2. Because ubiquitination of proteins plays a key role in degradation and previous report indicated ubiquitination mediated degradation of EZH2[130], we first assessed the level of EZH2 ubiquitination upon NO exposure and found that S-nitrosylated EZH2 are heavily ubiquitinated upon NO exposure **(Figure 3.2.3.1)**.

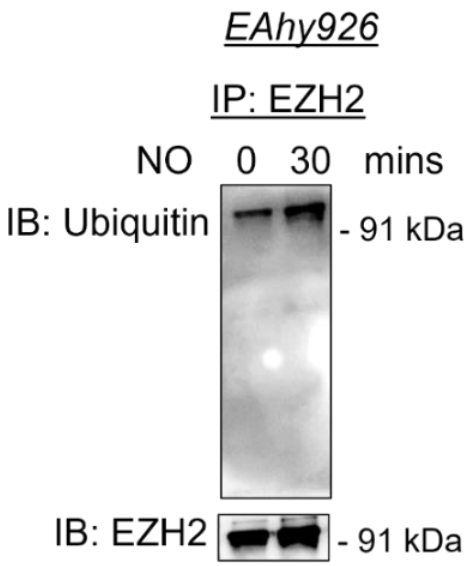

Figure 3.2.3.1 Elevated ubiquitination of EZH2 occurs on exposure to NO in EC to mark its degradation: *EA. hy926 cells exposed to SNP (500 µmol/L) for 30 minutes followed by co-immunoprecipitation to pulldown EZH2.This pulldown samples were then subjected to immunoblotting with ubiquitin antibody to show the presence of ubiquitinated EZH2.*

Cells use lysosomal and proteasomal degradation pathways for protein degradation, we thus used pharmacological inhibitors of proteasomal and autophagosome-lysosome pathway to evaluate their relative contribution towards degradation of S-nitrosylated EZH2. Inhibition of proteasomal pathway using MG132 was unable to reverse the level of EZH2 upon NO exposure **(Figure 3.2.3.2 A)**. In contrast, inhibition of autophagosome-lysosome pathway using bafilomycin A significantly although partially reversed EZH2 degradation upon NO challenge **(Figure 3.2.3.2 B)**.

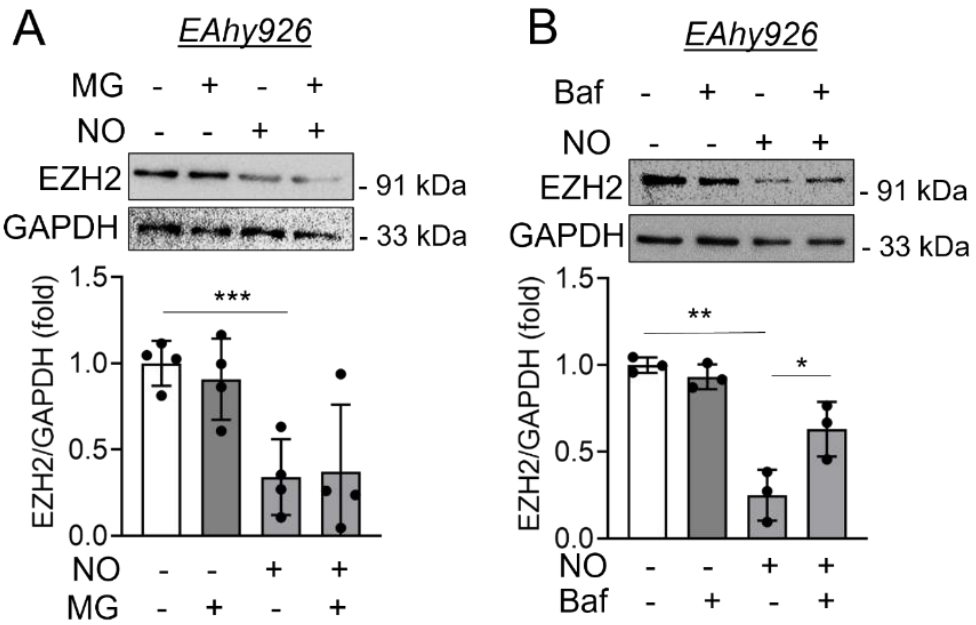

Figure 3.2.3.2 Exposure to NO in EC cause EZH2 degradation primarily through the autophagosome-lysosome pathway. (A) *Immunoblotting analysis of EZH2 in EA. hy926 cells pretreated with MG-132(MG) (1 µmol/L) for 2 hrs followed by exposing to SNP (500 µmol/L) for another 2 hrs. (n = 4)* ***(B)*** *Immunoblotting for EZH2 in cultured EA. hy926 cells pretreated with Bafilomycin A1(Baf) (100 nmol/L) for 2 hours followed by exposing to SNP (500 µmol/L) for additional 2 hrs. (n=4)*

We then inhibited both proteasomal and autophagosome-lysosome pathway to evaluate the effect of such combination inhibition on EZH2 protein level. In so doing, we detected complete reversal of EZH2 protein level upon combination inhibition of proteasomal and autophagosome-lysosomal pathways **(Figure 3.2.3.3 A)**. All these data indicated that degradation of EZH2 upon NO exposure primarily occurs through autophagosome-lysosome pathway, however, an inhibition of the autophagosome-lysosome pathway could likely switch S-nitrosylated EZH2 degradation through proteasomal pathway. Successful inhibition of autophagosome-lysosomal pathway upon bafilomycin A treatment was confirmed through increase in p62 level **(Figure 3.2.3.3 B)**.

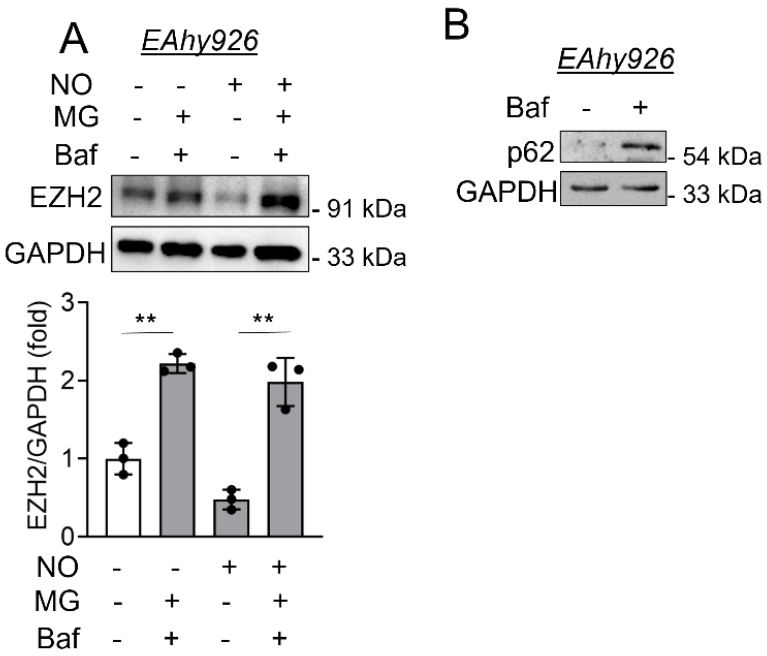

Figure 3.2.3.3 Effect of inhibited proteasomal and autophagosome-lysosome pathway combination on EZH2 degradation (A)*Immunoblotting for EZH2 protein in cultured EA. hy926 cells pretreated with both MG-132 (1 µmol/L) and bafilomycinA1 (100 nmol/L) for 2 hrs followed by exposing to SNP (500 µmol/L) for additional 2 hrs. (n=4)* ***(B)*** *Immunoblotting to show the presence of elevated p62 in EA. hy926 cells upon treatment with bafilomycin A1 (100 nmol/L) to confirm disruption of autophagosome-lysosome pathway. NOS inhibitor treatment reversed NO dependent reduction in EZH2 and H3K27me3 level.*

We next questioned whether inhibition of endogenous NO producing machinery could alter the downstream effect of natural inducers of endogenous NO production machinery in EC such as bradykinin. We exposed the EC with L-NAME, a nonselective inhibitor of all type of NO synthase (NOS) prior to inducing with bradykinin. As observed earlier in our study, bradykinin induction caused reduction in EZH2 level which is completely reversed upon inhibition of NOS with L-NAME **(Figure 3.2.3.4 A)**. We also performed the assay in *ex vivo* rat aorta model which further revealed reversal of EZH2 protein degradation and

protection of H3K27me3 in aortic tissues exposed to L-NAME prior to bradykinin treatment **(Figure 3.2.3.4 B-C)**. We then performed localization analysis of EZH2 in cells exposed to bradykinin alone or in combination with L-NAME. As expected, bradykinin induction caused cytosolic translocation of EZH2 which are also found to be localized with actin cytoskeleton, however, inhibition of NOS family of protein in bradykinin treated EC using L-NAME restricted EZH2 localization to nucleus **(Figure 3.2.3.4 D)**.

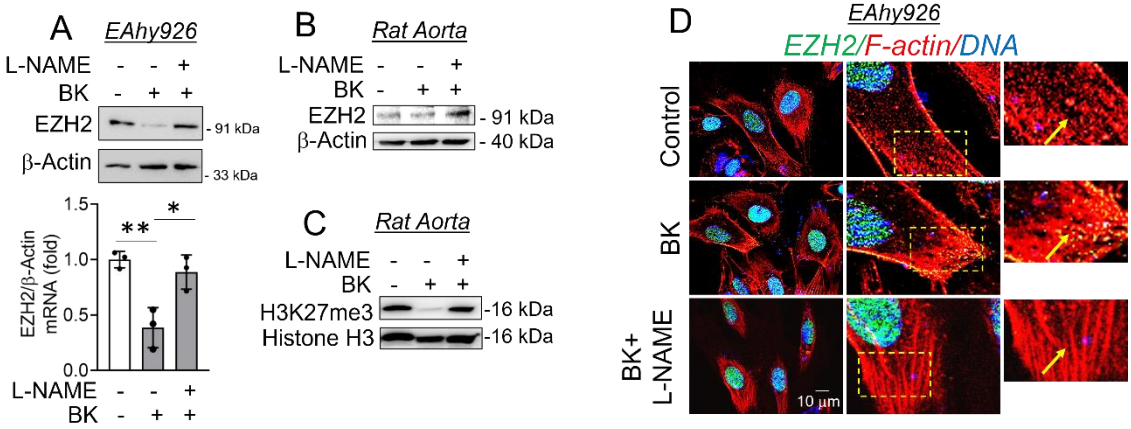

Figure 3.2.3.4 Indigenous NO inducer Bradykinin effects on EC were reversed on pretreatment with L-NAME*. **(A)**Immunoblotting for EZH2 with protein lysate collected from cultured EA. hy926 cells pretreated with L-NAME (1 mmol/L) for 1 hr followed by exposing to bradykinin(BK) (10 µmol/L) for additional 2hrs. (n=3) **(B-C)** Rat aortic rings were pretreated with L-NAME (1 mmol/L) for 1 hr followed by exposing to bradykinin (10 µmol/L) for additional 2 hrs. Immunoblot analysis were carried out for EZH2 **(B)** and H2K27me3 **(C)** in these tissue lysates. (n=3) **(D)** EZH2 (green) immunostaining along with F-actin (Red) staining of EA. hy926 cells after pretreating with L-NAME (1 mmol/L) for 1 hr followed by exposing to bradykinin (10 µmol/L) for additional 2hrs. DAPI staining is shown in blue.(Scale bar: 10 µm) (n=3) Values represent the mean ± SD. *p < 0.05, and **p < 0.01 by unpaired t-test for two groups.*

3.2.4 Protecting the level of EZH2 downstream product H3K27me3 through inhibition of demethylases reversed NO dependent effect on endothelial migration and gene expression changes

EZH2's effect on cellular function is primarily dependent on its regulation of gene expression changes through repressive H3K27me3 mark in the chromatin. Moreover, NO signaling pathway converges to changes in expression of genes associated with endothelial survival, proliferation and migration. We therefore wanted to investigate whether EZH2 dependent catalysis of H3K27me3 play any role in dictating NO driven regulation of endothelial function and gene expression changes. To do so, we took a retrograde approach in which we pre-incubated the cells with GSK-J4, a selective inhibitor of H3K27me3 specific demethylase JMJD3 and UTX. We first confirm that inhibition of JMJD3 and UTX reversed NO dependent reduction in H3K27me3 level **(Figure 3.2.4.1 A)**. We next performed endothelial migration using wound healing assay and observed that NO induced endothelial migration is abrogated upon preserving the level of H3K27me3 through inhibition of demethylase JMJD3 and UTX **(Figure 3.2.4.1 B)**.

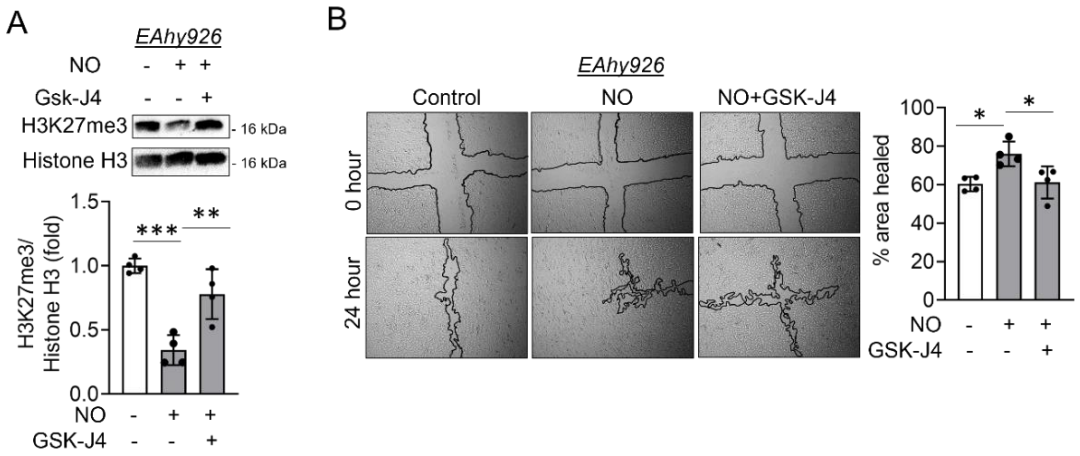

Figure 3.2.4.1 GSK-J4, a demethylase inhibitor protects H3K27me3 level in NO exposed EC and reversed NO-dependent cell migration and gene expression changes. (A) *Immunoblotting for H3K27me3 in EA. hy926 cells pretreated with GSK-J4 (5 µmol/L) for 4 hrs followed by challenging them with SNP (500 µmol/L) for additional 2 hours (n=4).* ***(B)*** *Scratch wound healing assay to show the healing rate of EA. hy926 cells which are pretreated with GSK-J4 (5 µmol/L) for 4 hrs followed by treatment with SNP (500 µmol/L). Healing rate was followed until 24 hrs post-SNP treatment. Images were acquired using bright field microscope adapted with a camera for phase contrast imaging. (n=4).*

In similar experimental settings, we next detected the transcript level expression of NO-responsive genes in EC using qPCR experiment. Based on previously reported data sets, we choose to detect the transcript level of NO responsive genes; VEGFa, TBX20, MMP2, FGF2, KDR, TIE2, TEK, and Angiopoietin-2[131]. Through this analysis, we detected significant increase in expression of VEGFa, TBX20, MMP2, FGF2, and Angiopoietin-2 upon NO exposure **(Figure 3.2.4.2)**. Pretreatment of EC with GSK-J4 prior to NO exposure completely abrogated NO dependent increment in VEGFa, TBX20, MMP2,

FGF2, and Angiopoietin-2 transcript level **(Figure 3.2.4.2)**. Surprisingly, although reported earlier to be responsive to NO in EC, in the present experimental settings, we were unable to record any changes in transcript level of KDR, TIE2, and TEK genes **(Figure 3.2.4.2)**.

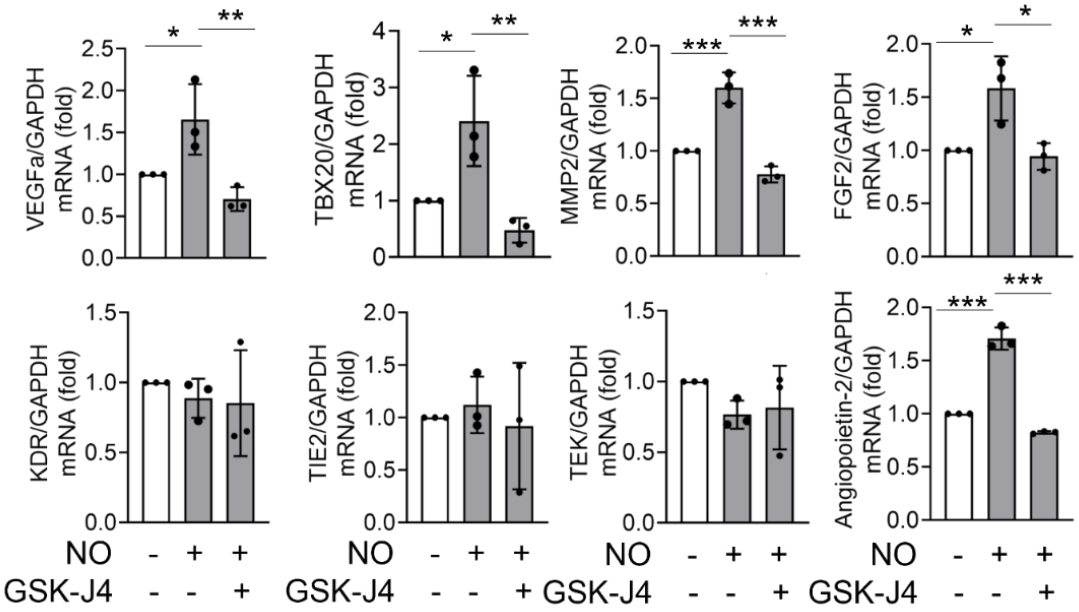

Figure 3.2.4.2 GSK-J4, reverses gene expression changes in NO exposed EC. *RT-qPCR analysis to measure the transcript level expression of VEGFa, TBX20, MMP2, FGF2, KDR, TIE2, TEK, and Angiopoietin in EA. hy926 cells pretreated with GSK-J4 (5 µmol/L) for 4 hrs followed by challenging them with SNP (500 µmol/L) for additional 4 hrs (n=4). Values represent the mean ± SD. *p < 0.05, **p < 0.01, and ***p < 0.001 by unpaired t-test for two groups*.

3.3 DISCUSSION:

A key regulatory pathway of NO-dependent cellular function is through S-nitrosylation of protein which is a reversible post-translational modification. Extensive studies have shown that S-nitrosylation regulates diverse physiological and pathological processes including

angiogenesis, adaptive immunity, diabetes, heart failure, stroke etc. through modulating stability, activity, subcellular localization, conformation change, or protein-protein interaction of target proteins.[132] Although NO signaling alters gene expression changes in vascular endothelium[133], however, the role of NO-dependent S-nitrosylation of proteins in defining the epigenetic landscape of EC is not clearly understood.

PRC2 complex is one of the most abundant and well-studied complexes engaged in gene repression through regulation of chromatin compaction. EZH2 being the catalytic unit of PRC2 complex catalyzes the deposition of H3K27me3 mark that causes chromatin compaction and thereby resulting in the repression of gene expression. Nevertheless, how S-nitrosylation regulate EZH2 protein and thereby the activity of the crucial PRC2 complex was never reported. Herein, for the first time we described that NO caused S nitrosylation of EZH2 protein leading to inhibition of its catalytic activity, disassembly of SUZ12 from PRC2 complex bound EZH2, cytosolic translocation of the protein followed by ubiquitination and degradation through autophagosome-lysosome pathway. Moreover, mass spectrometric analysis revealed S-nitrosylation of EZH2 significantly alters its interactome preferentially allowing association with proteins of the endosome/lysosome/proteasome pathways. We also demonstrated that natural induction of endogenous NO machinery in EC also imparts the exact same effect on EZH2 protein.

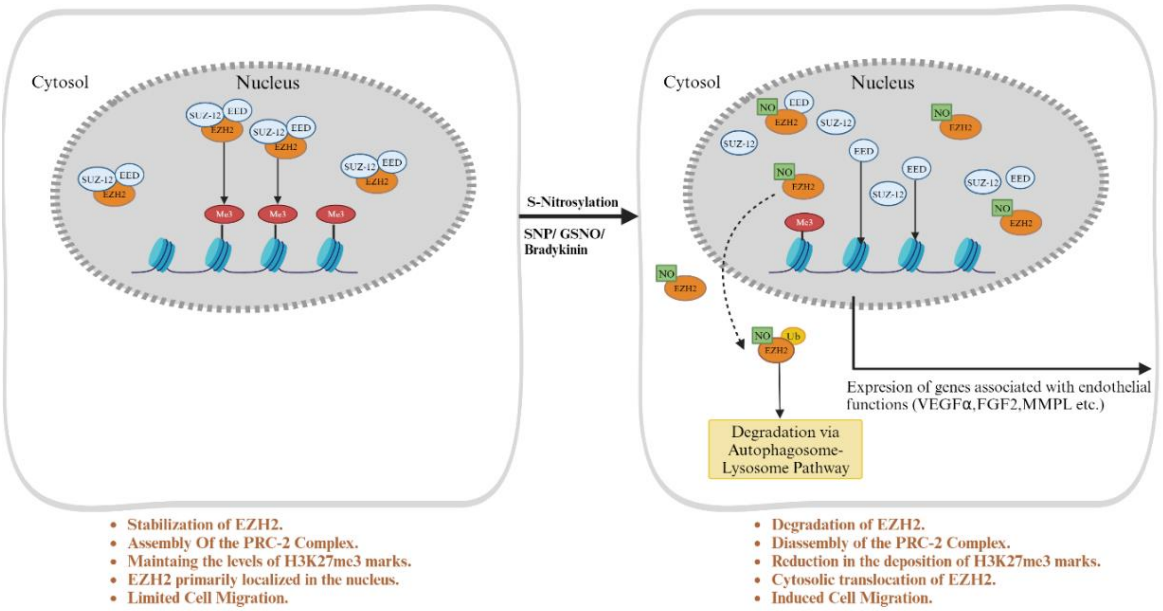

Figure 3.3.1 Schematic depicting the effect of EZH2 S-nitrosylation on its stability, translocation and catalytic activity of PRC2. *PRC2 consists mainly of EZH2, SUZ12, and EED, residing primarily in the nucleus. The major subunit of PRC2 i.e. histone methyltransferase EZH2 localizes primarily in the nucleus and is responsible for deposition and maintenance of the levels of H3K27me3. These cells also have a limited cell migration capacity. On exposure of these cells to NO, S-Nitrosylation of specific cysteine residues on EZH2 occur leading to a decline in their stability which is marked by reduction in EZH2 protein levels along with dissociation of SUZ12 from EZH2 bound PRC2 complex. Upon disassembly, S- Nitrosylated EZH2 translocate from the nucleus to the cytosol where it undergoes ubiquitination followed by its degradation primarily through the autophagosome lysosome pathway. Additionally, there is a significant effect on the catalytic activity of EZH2, which is shown by reduction in the deposition of the H3K27me3 marks on histone H3. NO dependent S-nitrosylation of EZH2 also causes a spike in the migratory activities of EC due to EZH2 recruitment to the F-actin and likely contributing towards remodeling prior to degradation. The schematic diagram was prepared using BioRender (Agreement number: WB26FEOYBU).*

Most importantly, we demonstrated that such S-nitrosylation of EZH2 was responsible for NO-dependent epigenetic regulation of endothelial gene expression and cellular migration (Figure 3.3.1). Post-translational modification of EZH2 protein through phosphorylation at several sites were reported earlier[47,133–135]. Such modifications of EZH2 differentially regulated the localization, function and its association with other proteins of the PRC2 complex. For instance, AMPK phosphorylated EZH2 at T311 to disrupt the interaction between EZH2 and SUZ12 thereby attenuating PRC2-dependent methylation of histone H3 at Lys27 in ovarian and breast cancer. Moreover, such phosphorylation of EZH2 by AMPK caused upregulation of PRC2 target genes, many of which are known tumor suppressors thereby suppressing the growth of tumor cells[47]. During breast cancer metastases, p38-mediated EZH2 phosphorylation at T367 promotes EZH2 cytoplasmic localization and potentiates EZH2 binding to vinculin and other cytoskeletal regulators of cell migration and invasion. Interestingly, ectopic expression of a phospho-deficient T367A-EZH2 mutant is sufficient to inhibit EZH2 cytoplasmic expression, disrupt binding to cytoskeletal regulators, and reduce EZH2-mediated adhesion, migration, invasion, and development of spontaneous metastasis[133]. In the present study, we observed that S nitrosylation of EZH2 in specific at cysteine caused its cytosolic localization, a transient binding to actin cytoskeleton, ubiquitination of EZH2 protein followed by degradation through autophagosome lysosome pathway. A very recent study demonstrated DCAF1 mediated phosphorylation of EZH2 at T367 to augment its nuclear stabilization and enzymatic activity in colon cancer cells. Such DCAF1 mediated EZH2 phosphorylation followed by nuclear localization led to elevated levels of H3K27me3 and altered expression of growth regulatory genes in cancer cells[134]. In contrast, herein we report that S-nitrosylation of cysteine residue of EZH2 caused its cytosolic localization followed by lysosomal degradation. Moreover, S-nitrosylation at cysteine also leads to inactivation of

EZH2's catalytic activity most likely due to early dissociation of SUZ12 protein from PCR2 complex. Although, phosphorylation dependent regulation of EZH2 protein and the PRC2 complex are well documented, however, other post-translational modifications especially NO dependent S-nitrosylation of EZH2 and its regulation of the overall function of this protein has never been reported. Herein, we demonstrated endogenous NO producing machinery of EC as well as external supplementation of NO using donors regulated EZH2 binding with SUZ12, its localization, and protein stability. Such effect of NO on EZH2 contributed towards NO driven gene expression changes and endothelial migration. These are primarily achieved by NO through S-nitrosylation of EZH2 protein at specific cysteine residues.

In EC endogenous eNOS dependent release of NO drives cell survival, migration and growth typically acting through canonical and non-canonical pathways[136,137]. Canonically, NO induces soluble guanyl cyclase (sGC) and in downstream Protein Kinase G to mediate actin remodeling required for cell migration[138,139]. Moreover, NO signaling also promote endothelial gene expression changes associated with endothelial survival and growth[140,141]. Such gene expression changes by NO in EC was thought to be primarily controlled by gene transcription and mRNA translation via iron-responsive elements[142]. Herein, for the first time, we reported that eNOS dependent NO release instigates non canonical pathway through S-nitrosylation of EZH2 protein and its product H3K27me3 thereby controlling the epigenetic regulation of gene expression. This was supported by our data wherein preserving the level of EZH2 catalytic product H3K27me3 through inhibition of the demethylases JMJD3-UTX reversed NO dependent gene expression changes in EC. Moreover, we also observed that regulation of EZH2 by NO was independent of the cell type under study which is also been supported through our data in HEK-293 cells exposed to NO. In parallel to well reported function of NO[143,144] as well as

EZH2[17,18,145] in actin cytoskeleton remodeling, we observed that NO exposure caused transient localization of EZH2 on the actin cytoskeleton most likely prior to its degradation through autophagosome-lysosomal pathway. In addition, preserving the level of H3K27me3 via inhibition of demethylases reversed NO effect on cell migration.

Through the present study, we are unable to establish whether the effect of NO on endothelial migration is mainly driven by its regulation of EZH2 actin cytoskeleton remodeling axis or via regulation of EZH2-H3K27me3-gene expression regulation axis. Nonetheless, NO dependent remodeling of actin cytoskeleton may not alone be driven by canonical sGC-cGMP-PKG-VASP pathway, in addition, regulation of EZH2 via NO may contribute towards its actin remodeling function.

In summary, our study for the first time reported that NO signaling pathway converges to epigenetically regulate gene expression via controlling the stability and catalytic activity of PRC2 complex, in specific the EZH2 component of the complex. This is primarily driven by NO through S nitrosylation of specific cysteine residues of EZH2 which promotes early dissociation of SUZ12 from EZH2-PCR2 complex followed by cytosolic localization of EZH2 and its degradation through autophagosome-lysosome pathways. We also showed that such an effect of NO on EZH2 is cell type independent. Moreover, we also reported that NO driven gene expression changes in EC is primarily dependent on NO regulation of EZH2 and its catalytic product H3K27me3Our findings shed light into a new mechanism of NO mediated regulation of EZH2 and PCR2 complex to regulate gene expression associated with endothelial function.

Chapter 4:
C329 and C700 residues govern S-Nitrosylation dependent regulation of EZH2 protein, PRC2 complex, and catalytic activity

4.1 INTRODUCTION:

PRC2 complex is critical for development and disease pathogenesis. EZH2 being a part of the PRC2 complex is the essential catalytic component that finally drives H3K27me3 formation to cause repression of gene expression. By doing so, EZH2 essentially regulates spatiotemporal gene repression which is a crucial part of the development while disrupting such tight control leads to embryonic lethality or disease pathogenesis[37]. Therefore, understanding the underlining mechanism that governs the EZH2 function independent of its transcriptional regulation is imperative in current juncture. Modulation of EZH2 function through PTMs remains to be elusive even though few studies indicated regulation of EZH2 through phosphorylation and its degradation through ubiquitination. Regulation of EZH2 via other PTMs such as Acetylation, SUMOylation, O-GlcNAcylation is also well reported[48].

Cellular NO signaling, especially in EC, is essential for endothelial survival and migration. NO does so by conventionally regulating both canonical and non-canonical pathways. Through canonical pathways, NO controls the activity of soluble guanylyl cyclase, which in downstream governs the level of cGMP, thereby regulating further downstream signaling. Through the non-canonical pathway, NO works via nitrosylation of different proteins at different residues (majorly through nitrosylation of cysteine, methionine and tyrosine residues), thus determining the function of these proteins[101–103,146].

The complex cellular regulation of S-nitroso thiol (SNO) homeostasis is well managed, and any disruptions in this balance can lead to alterations in the redox state, thereby contributing to a myriad of disease conditions[146]. Despite its significance, the precise role of S-nitrosylated proteins and nitrosative stress metabolites in inflammation, as well as their modulation of inflammatory processes, remains inadequately studied[99,147]. To counteract the pathological effects of NO, the cells activate defense mechanisms,

including cellular denitrosylases such as Thioredoxin (Trx) and S-nitrosoglutathione reductase (GSNOR) systems[78]. These systems have garnered considerable attention as potential novel anti-inflammatory molecules. Still NO is yet to be established as a direct regulator of epigenetic processes even though it is well entrenched that NO treatment alters endothelial gene expression. Certain studies also indicate that through the regulation of the cGMP-Protein kinase G (PKG) axis as well as coordinating nitrosylation of the transcription factor, NO can alter gene expression[103].

In this study, with the help of the In-sillico analysis prediction tools. we have provided the insights into the identification and involvement of specific sites/a.a. residues within key protein EZH2, and offering valuable insights about the functions of those locations/a.a. residues and the impact of those mutations on the EZH2 landscape. This study, aims to delve deeper into the functional consequences of mutation at predicted S-nitrosylation sites of EZH2. Using computational models and bioinformatics tools, we seek the effects of the structural alterations induced by these mutations and their subsequent effects on EZH2 stability and catalytic activity. Additionally, through experimental validation, we aim to provide mechanistic insights into the regulatory mechanisms governing EZH2 activity and its implications in physiological and pathological contexts.

4.2 RESULTS:

4.2.1 S-nitrosylation of EZH2 at cysteine 329 and cysteine 700 is important for its stability and methyltransferase activity respectively

Upon confirming the effect of NO on S-nitrosylation of EZH2 and associated changes in its stability, catalytic activity, PRC2 assembly and translocation, we next focused on

detecting the possible residues of EZH2 that could be S-nitrosylated. To confirm this, we used GPS-SNO (http://sno.biocuckoo.org/) prediction tools as stipulated in methodology section. Such analysis predicted three possible sites at cysteine 260, 329, and 700 of EZH2 protein with score of 3.158, 2.576, and 3.109 respectively which is beyond the set cut off value of 2.443**(Figure 4.2.1.1 A)**. Predicted cysteine residues 260 and 329 lies within the domain II of EZH2 which essentially allows SUZ12 association with EZH2, in contrast, predicted cysteine residue at 700 lies within the catalytic SET domain of EZH2 which is essential for its enzymatic activity.

To further decipher the role of each of these cysteine residues, we generated point mutated constructs of these cysteine by using site-directed mutagenesis kit to convert the codon to code for serine in places of the actual cysteine (TGT/TGC to AGT/AGC) residues **(Figure 4.2.1.1 B)**.

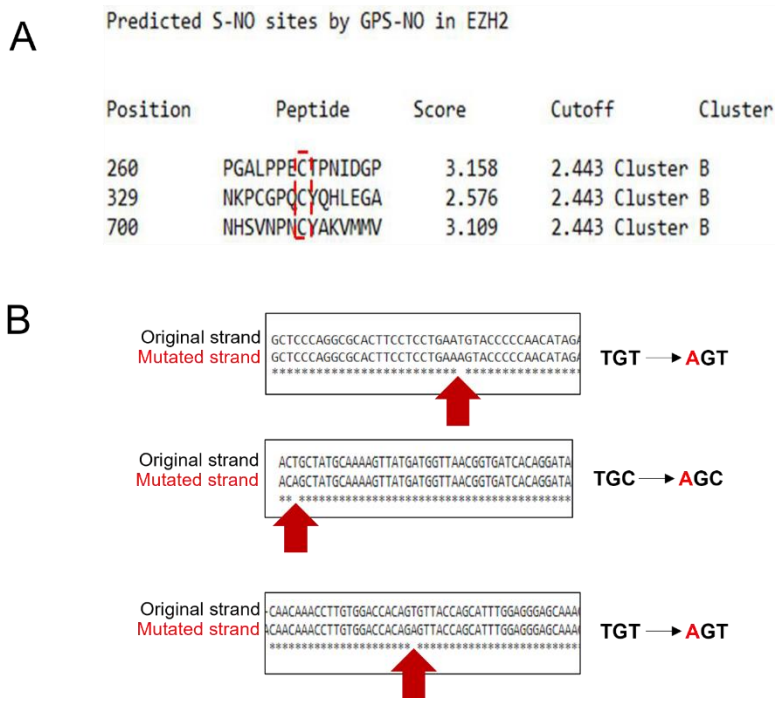

Figure 4.2.1.1 In silico S-nitrosylation prediction analysis and generating point mutants for identified residues using site directed mutagenesis kit. *(A) Using pre-*

validated software, we performed an in-silico analysis to predict possible cysteine residues that could be S-nitrosylated and identified three cysteine residues at position 260, 329 and 700 (out of 34 total cysteine present in EZH2) that were predicted to be S-nitrosylated. (B) Confirming the insertion of point mutations at these three predicted cysteine sites leading to their conversion to serine using Sanger sequencing technique.

Using overexpression of these constructs in HEK-293 cells, we first performed biotin switch assay to assess the S-nitrosylation of these mutated EZH2. Such analysis revealed partial loss of S-nitrosylation of EZH2 for each of the mutants EZH2 C260S, EZH2 C329S, and EZH2 C700S. Interestingly, a complete loss of S-nitrosylation signal was not detected with single mutation indicating multiple cysteine residues were likely to be S-nitrosylated in EZH2 protein upon NO exposure **(Figure 4.2.1.2 A)**.

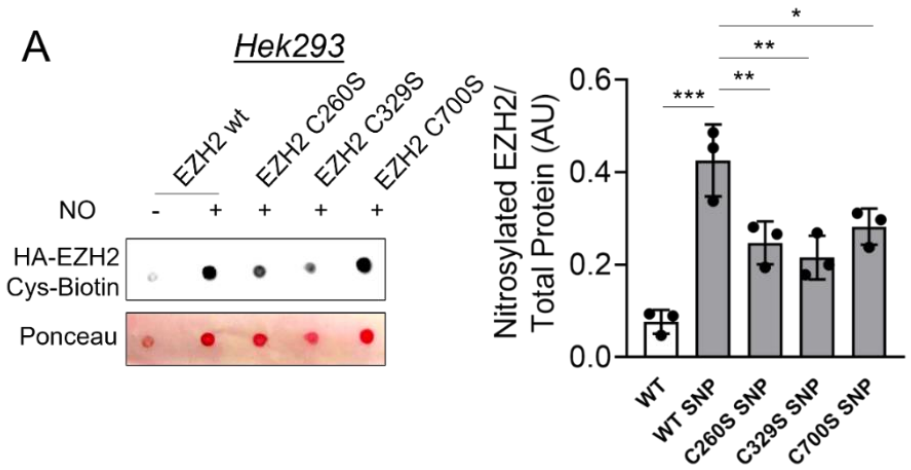

Figure 4.2.1.2 Biotin Switch assay to show the differential effect of NO on the different versions of the point mutated EZH2 (A) *Biotin Switch assay followed by dot-blot and Ponceau staining of HA immunoprecipitated cell lysates of HEK-293 cells overexpressing WT and mutant EZH2 (having point mutations at cysteines 260, 329, and 700) followed by challenging with SNP (500 µmol/L) for 2 hrs to show the levels of S-nitrosylated HA tagged EZH2. (n=3).*

We then analysed the effect of NO exposure on EZH2 protein and its catalytic product H3K27me3 level in cells overexpressed with WT and mutated form of the EZH2 gene. As observed earlier, NO exposure caused significant loss of HA tagged EZH2 protein and H3K27me3 level in cells overexpressed with HA tagged EZH2 WT gene **(Figure 4.2.1.3 A-B)**. A comparable loss of HA tagged EZH2 protein and H3K27me3 level was also detected in cells overexpressed with HA tagged EZH2 C260S mutant gene **(Figure 4.2.1.3 A-B)**. Interestingly, NO exposure did not alter the level of HA tagged EZH2 protein in cells overexpressed with HA tagged EZH2 C329S mutant gene, however, H3K27me3 level in these cells were significantly reduced upon NO exposure **(Figure 4.2.1.3 A-B)**. In contrast, NO significantly diminished the level of HA tagged EZH2 C700S protein in cells overexpressing HA tagged EZH2 C700S mutant, however, surprisingly, H3K27me3 level upon NO challenge remained relatively unaltered in these cells **(Figure 4.2.1.3 A-B)**.

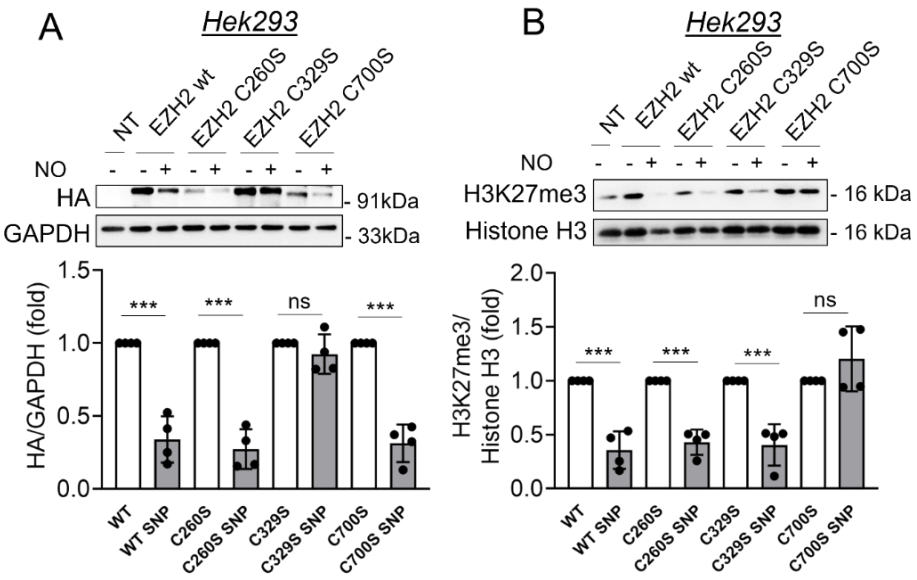

Figure 4.2.1.3 Point mutated EZH2 protein responded differentially to NO in the context of its effects on the stability and catalytic activity of EZH2.

(A-B) *Immunoblotting for HA (EZH2)* ***(A)****and H3K27me3* ***(B)*** *in cell lysates collected from HEK-293 cells containing wild type or mutated versions of EZH2 (C260S, C329S, C700S) and were exposed to SNP (500 µmol/L) for 2 hrs. (n=4)*

We next decided to generate a double mutant form of EZH2 gene where both cysteine residues at location 329 and 700 are mutated to serine thereby generating a double mutant named EZH2 C329S C700S mutant. We then overexpressed this double mutant in HEK-293 cells followed by treating the cells with NO. Double mutated (at cysteine 329 and 700 residues) form of the HA tagged EZH2 was completely insensitive to NO exposure both in context to the level of HA tagged EZH2 C329S C700S protein as well as its product H3K27me3 **(Figure 4.2.1.4)**. In similar settings, cells overexpressing WT EZH2 gene showed significant reduction in both HA tagged EZH2 protein and H3K27me3 level **(Figure 4.2.1.4)**.

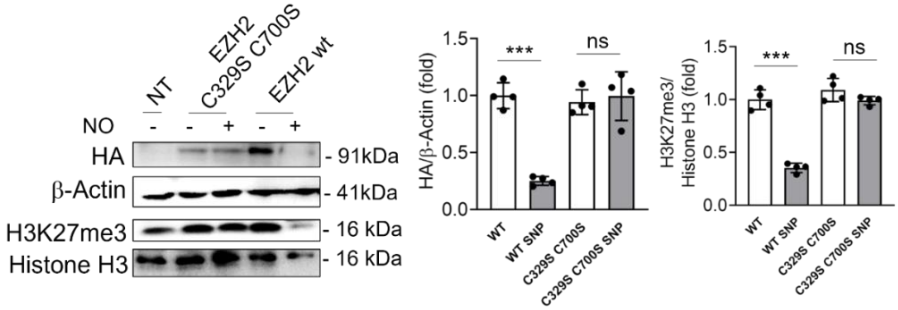

Figure 4.2.1.4 Effect of NO on the stability and catalytic activity on the double mutated version of EZH2 *Immunoblotting experiments to show the levels of HA (EZH2) and H3K27me3 in HEK-293 cells transfected with wild-type and the double mutant version of EZH2(created by inserting point mutations to convert cysteine to serine at positions C329 and C700) and exposed to SNP (500 µmol/L) for 2 hrs. (n=4).*

We next performed immunofluorescence experiment and confocal imaging study to ascertain the effect of these individual and double mutations of EZH2 on NO driven HA tagged EZH2 localization. In so doing, we observed that NO exposure caused significant

cytosolic delocalization of HA tagged EZH2 wt, C260S, and C700S mutated forms of HA tagged EZH2**(Figure 4.2.1.5)**. Interestingly, NO was unable to induce significant cytosolic localization of HA tagged EZH2 C329S and double mutated HA tagged EZH2 C329S C700S protein **(Figure 4.2.1.5)**.

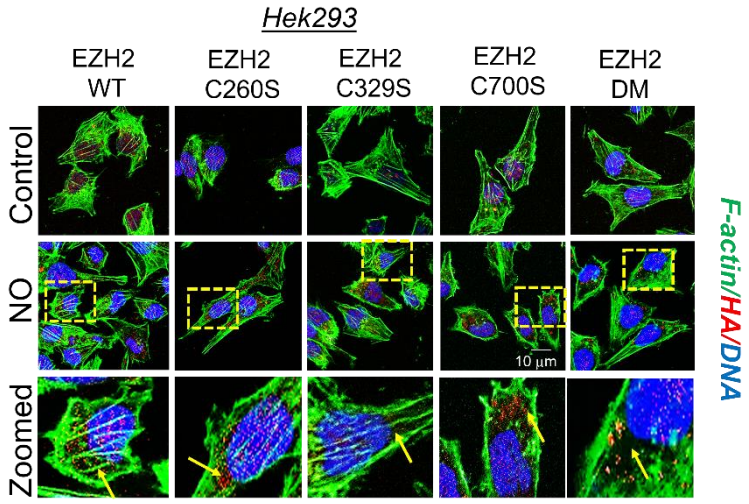

Figure 4.2.1.5 Immunofluorescence to show the effect of NO exposure on the stability and catalytic activity on the point and double mutated versions of EZH2 *Immunostaining for HA (EZH2) (Red) along with F-actin (green) staining in HEK-293 cells to localize HA tagged EZH2 in wild-type and mutated versions, following their exposure to SNP (500 µmol/L) for 2 hrs. DAPI staining is shown in blue (Scale bar: 10 µm) (n=3) Values represent the mean ± SD. ***p < 0.001 by unpaired t-test for two groups.*

4.2.2 S-nitrosylation of EZH2 protein at C329 and C700 causes conformational changes in EZH2-SUZ12 complex leading to loose association of SUZ12 with the SAL domain of EZH2

Upon experimental validation of EZH2's S-nitrosylation and its effect on EZH2-SUZ12 interaction, catalytic activity, localization and EZH2 protein stability, we next employed molecular dynamics analysis to understand the effect of S-nitrosylation on EZH2 interaction with SUZ12 protein. Through alphafold modelling of EZH2-SUZ12, we showed the initial conformations of the EZH2-SUZ12 complex in both the EZH2 WT and EZH2 S-nitrosylated at C324 (originally C329) and C695 (originally C700) residues **(Figure 4.2.2.1 A)** while also clearly visualizing the S-nitrosylation at C324 **(Figure 4.2.2.1 B)** and C695 **(Figure 4.2.2.1 C)**.

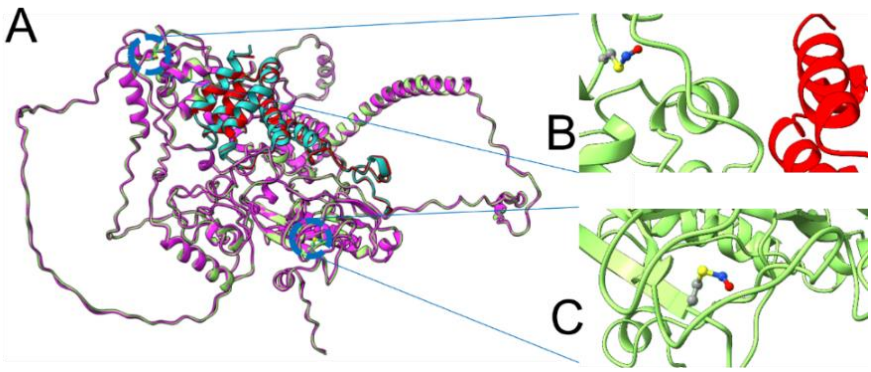

Figure 4.2.2.1 Structural illustration of the initial structural alignment of the wildtype and S-nitrosylated EZH2 protein of the EZH2-SUZ12 complex (A). *The magenta and green color represents the EZH2 chain of both WT and S-nitrosylated version, while the cyan and red color indicates the SUZ12 chain.* ***(B)*** *It also provides a close-up view of S nitrosylation at position C324 of EZH2 in the S-nitrosylated protein and* ***(C)*** *also zooms in on the S-nitrosylation at position C695 of EZH2 in the S-nitrosylated protein.*

The RMSD calculations elucidate the extent to which the conformations of the EZH2 WT and EZH2 S-nitrosylated complexes deviated from their initial states during the course of

MD simulations. In comparison to the WT complex, a sharp rise of RMSD values is observed for S-nitrosylated complex after 100 ns indicating possible change in the overall conformations during the simulations. A system showed larger conformational changes for EZH2 S-nitrosylated than for EZH2 WT complex **(Figure 4.2.2.2 A)**.

Gamblin et al. (2016) reported that residues 112 to 121 within the SAL pack engage with the SET-1 region, serving to stabilize its conformation within the active complex[108]. Importantly for regulation in the human PRC2 complex, the conserved acidic residues 584-588 of SUZ12 reciprocally pack against residues 112-121 of SAL. Consequently, we conducted measurements of the backbone RMSD for both residue ranges, 112-121 of SAL and 584-588 of SUZ12, revealing a significant fluctuation in the RMSD within the SAL region of EZH2 S-nitrosylated with little to negligible RMSD fluctuation for SUZ12 residues ranging from 584-588 **(Figure 4.2.2.2 B-C)**.

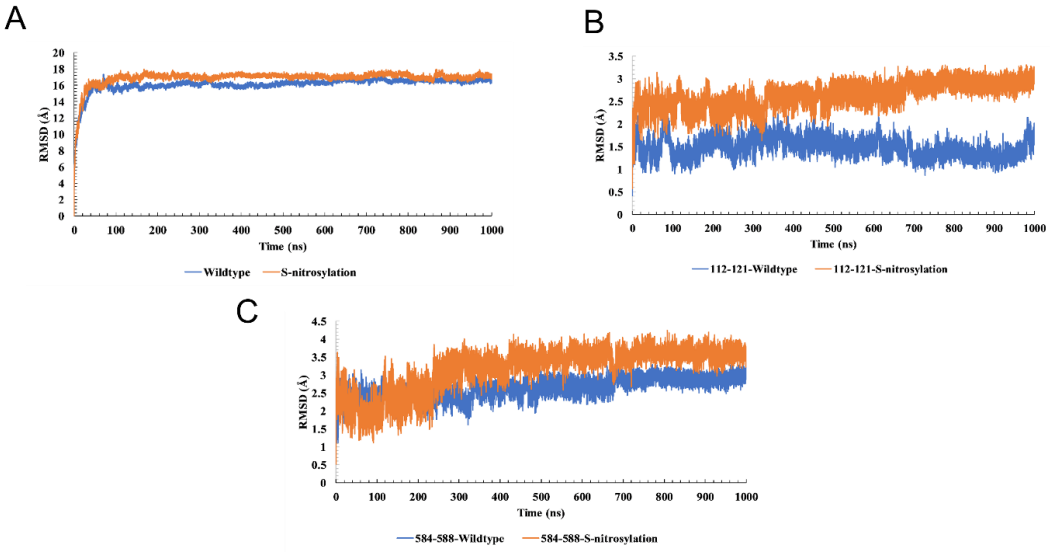

Figure 4.2.2.2 Backbone RMSD calculation for the WT & S-Nitrosylated version of EZH2 (A-D) ***(A)*** *Backbone RMSD of Wildtype and S-nitrosylation, and* ***(B)*** *Backbone RMSD of Wildtype and S-nitrosylation of residue ranges 112-121 of SAL.* ***(C)*** *Backbone RMSD of Wildtype and S-nitrosylation of residue ranges 584-588 of SUZ12.*

Another crucial parameter of MD is root mean square fluctuation (RMSF) to determine the flexibility of protein residues. The RMSF value of both EZH2 WT and EZH2 S-nitrosylated remained relatively stable with a nearly similar trend. **(Figure 4.2.2.3)**.

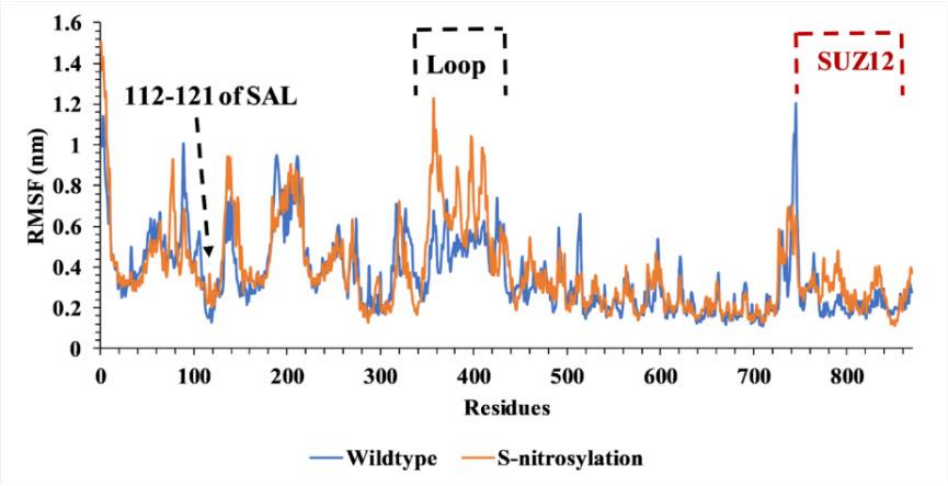

Figure 4.2.2.3 RMSF calculation to determine the protein flexibility for WT and S-nitrosylated EZH2. *MD analysis using root mean square fluctuation (RMSF) to determine the flexibility of protein residues for both WT and S-nitrosylated SAL (region of EZH2) and SUZ-12. The RMSF value of both S-nitrosylated and WT residues remained relatively stable with a nearly similar trend, whereas the residues near the SAL and long loop region (residue 112-121 and 345-421) displayed significant fluctuations.*

Primarily, the residues near the SAL and long loop region (residue 112-121 and 345-421) display significant fluctuations. Apart from these loops and SAL region of EZH2, RMSF analysis shows stable interactions in both the simulated complexes. Subsequently, we visualized the interface hydrogen bond interactions between SAL residues 112-121 and SUZ12 residues 584-588 throughout 1 μs simulation. Interestingly, in the EZH2 WT, we observed the oxygen atom of LEU166 in EZH2 interacting through the hydrogen bond with

LYS587 of SUZ12 and the HE22 atom of GLN117 in EZH2 interacting with the OD2 atom of ASP585 in SUZ12 **(Figure4.2.2.6 A-B)**. These interactions persisted throughout the simulation. In the case of S-nitrosylated mutant, these two hydrogen bond interactions were initially established and maintained up to 300 ns. However, beyond this time point, the interactions were no longer observed.

Hydrogen bonds (H-bonds) are important non-covalent interactions that help stabilize protein-ligand and protein-protein complexes. To better understand the dynamics of these interactions at the interface, we analysed the H-bonds formed between specific residues 112-121 of SAL and 584-588 of SUZ12. This examination allowed us to gain insights into the overall stability and binding strength of the complexes **(Figure4.2.2.4 A)**. During the simulations, we closely observed the formation of H-bonds within a distance of 3.5 Å. Upon conducting the analysis, it was discovered that the specific residues 112-121 of SAL were found to interact with 584-588 of SUZ12 in the EZH2 WT complex. This interaction resulted in an average of 2 hydrogen bonds. Conversely, the S-nitrosylated counterpart exhibited a significantly lower average of 0.35 hydrogen bonds suggesting EZH2 WT complex have stronger interactions than EZH2 S-nitrosylated variant. This observation also aligns with the energy profile **(Figure4.2.2.4 B)**.

A

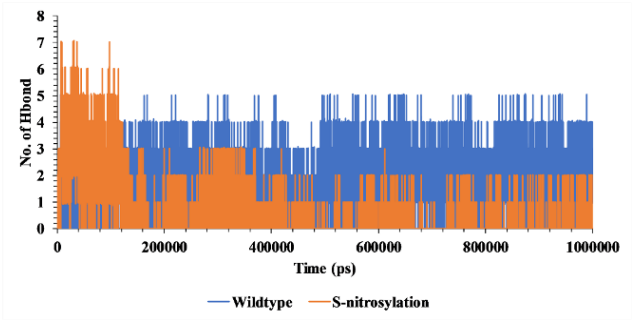

B

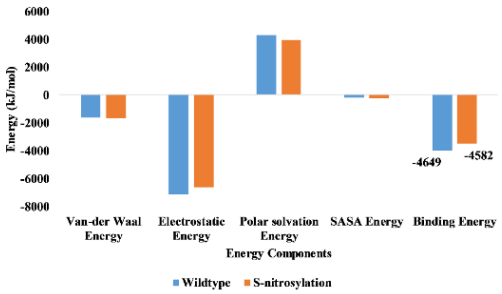

Figure 4.2.2.4 H-bond formation and energy profile calculation for the SAL region of EZH2 and SUZ-12. (A) *H bond contact formed between residues 112-121 of SAL and 584-588 of SUZ12 over the course of 1μs MD simulation.* ***(B)*** *MMPBSA binding free energy.*

We further measured the distance between the oxygen atom of LEU166 in EZH2 and the hydrogen atom of LYS587 in SUZ12, as well as the distance between GLN117 in EZH2 and ASP585 in SUZ12. A sharp increase in the distance between GLN117 and the interacting residue ASP585 after 150 ns in the EZH2 S-nitrosylation complex simulation. **(Figure4.2.2.5)** was observed, that ultimately led to the disruption of the interaction.

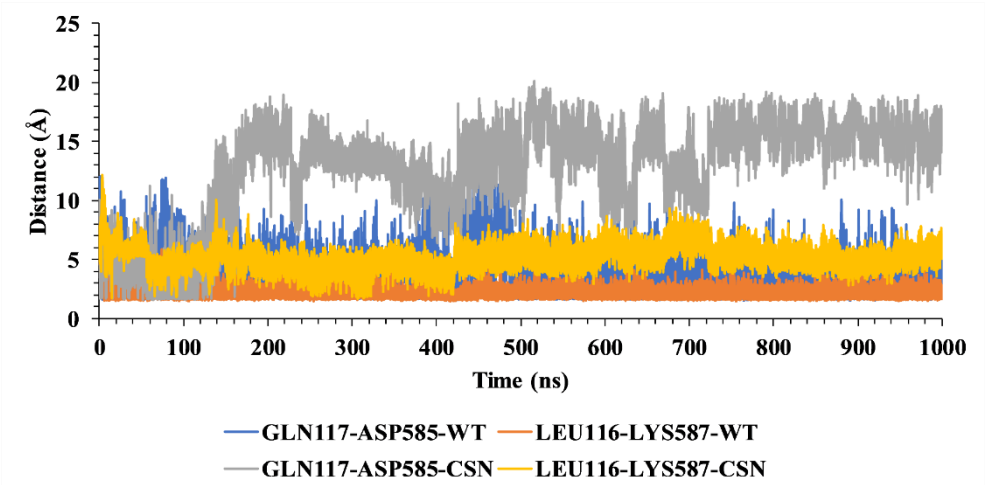

Figure 4.2.2.5 H-bond Distance calculation between specific atoms of EZH2 and SUZ 12 *H bond distance between the oxygen atom of LEU166 in EZH2 with and hydrogen atom of LYS587 in SUZ12, and the HE22 atom of GLN117 in EZH2 with the OD2 atom of ASP585 in SUZ12.*

Such distance between the oxygen atom of LEU166 in EZH2 and the hydrogen atom of LYS587 in SUZ12, as well as the distance between the HE22 atom of GLN117 in EZH2 and its interacting atom OD2 of ASP585 in SUZ12 at 100 ns (after stabilization of the complex upon initial simulation) and at 800 ns, was also presented through the structure analysis **(Figure 4.2.2.6 A-D)**.

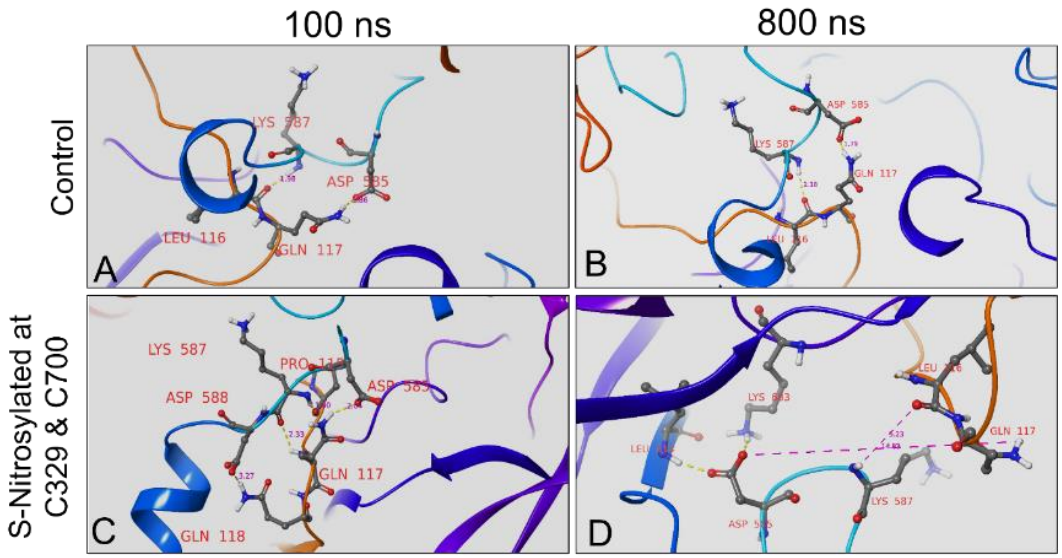

Figure 4.2.2.6. Structural analysis for the WT and S-nitrosylated EZH2 at C324 and C695 through GROMACS 5.1.5 version. (A-D) *Structural illustration of EZH2-SUZ12 complex near the SAL (112-121) domain of EZH2 in both EZH2 WT and EZH2 S-nitrosylated forms at 100 ns and 800 ns of simulation. Structural data reflects the distance between unique residues of EZH2 (LEU116 and GLN117) and SUZ12 (ASP585 and LYS587) to reflect potential for hydrogen bonds which were lost at 800 ns only in EZH2-SUZ12 complex having S-nitrosylated form of EZH2 at C324 and C695.*

To determine the more accurate free energy binding of all complexes, we utilized the MM/PBSA-based method. The binding free energy in this context refers to the total of all non-bonded interaction energies between the EZH2 and SUZ12 during the MD simulation, including van der Walls, electrostatic, polar solvation, and SASA energies. A more negative binding free energy indicates a stronger affinity between the EZH2 and the SUZ12. We calculated the binding free energies using 1μs MD trajectory, revealing that EZH2 WT and EZH2 S-nitrosylation have a binding free energy of -4649.807 ± 454.449 kJ/mol and -4582.981 ± 453.056 kJ/mol, Subsequently, estimation of their contributions to overall ΔΔG_bind=66 kJ/mol indicates that the contributions vary from one system to the

next. On average, the wildtype state tends to have a marginally higher contribution **(Figure 4.2.2.7 A and Table 4.2.2.1)**. Furthermore, the comparison of the binding energy decomposition between selected residue of SAL and SUZ12 in EZH2 WT and EZH2 S-nitrosylated complexes located at the binding interface reveals that the EZH2 WT predominantly contributes to binding in locally stabilizing manner, Conversely, EZH2 S-nitrosylation displays less contribution to binding energy and these effects might be the consequence of introduced nitrosylation at cysteine 324 and 695. **(Figure 4.2.2.7 B-C)**. Overall, these modeling results suggest that S-nitrosylation of the cysteine residues might induce a conformational change in the SAL region which is crucial for the regulation of the PRC2 complex. This conformational change weakens the SUZ12-SAL interaction, ultimately resulting in the destabilization of the SUZ12-EZH2 complex.

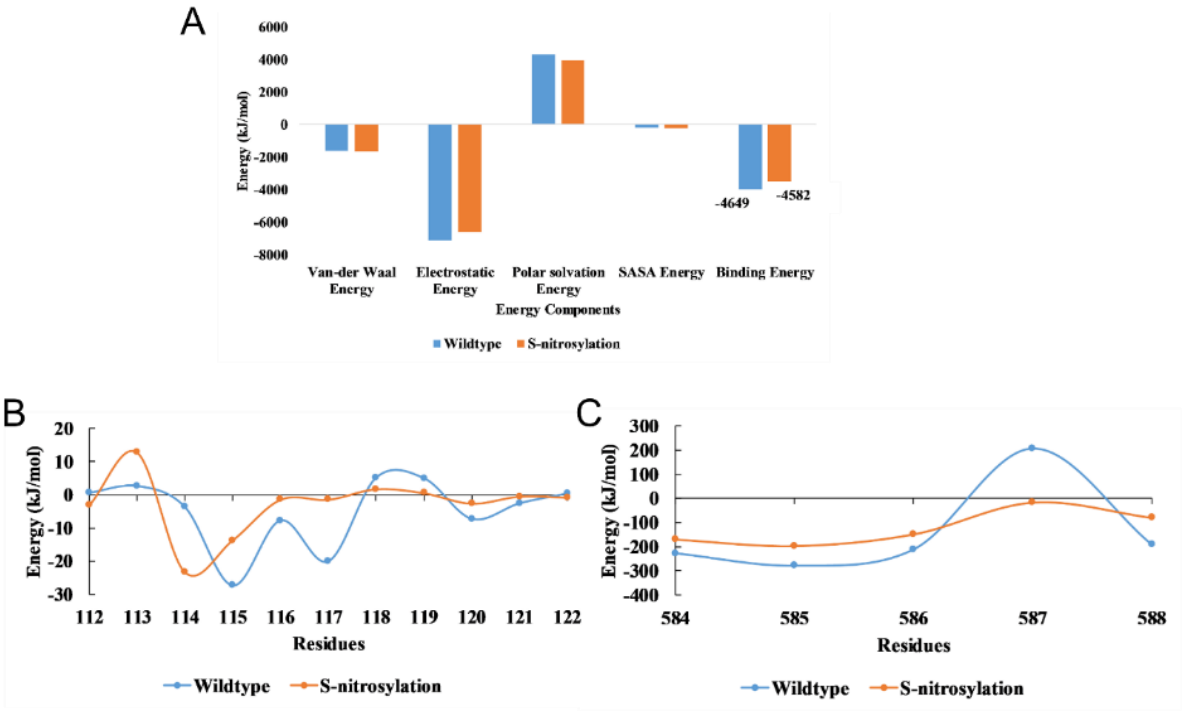

Figure 4.2.2.7 Binding free energy calculation for EZH2 and EZH2-SUZ12 complex ***(A)*** *MMPBSA binding free energy.* ***(B)*** *Binding energy per residue of 112-121 of EZH2,* ***(C)*** *Binding energy per residue of 584-588 of SUZ12*

Compounds	Van-der Waal energy (kJ/mol)	Electrostatic energy (kJ/mol)	Polar solvation energy (kJ/mol)	SASA energy (kJ/mol)	Binding energy (kJ/mol)
Wildtype	-1630 ± 62	-7099 ± 618	4275 ± 332	-196 ± 10	-4649 ± 454
S-nitrosylation	-1657 ± 76	-6642 ± 706	3923 ± 351	-206.485 ± 7	-4583 ± 453

Table 4.2.2.1: Contribution of individual interaction components and binding free energy forthe EZH2-SUZ12 Complex.

4.3 DISCUSSION:

The complex array of post-translational modifications (PTMs) intricately enriches our understanding of protein functions and regulation, adding layers of depth, knowledge and complexity to our understanding. Among these modifications, S-nitrosylation emerged as a pivotal regulator, involving the covalent attachment of a NO moiety to cysteine residues of target proteins. As discussed above in detail, this enzymatic reaction has diverse implications in various diseases and cellular processes as it extends an important role in various cardiovascular diseases and associated disorders. This process also plays an important role in many other disease conditions such as during neurodegenerative disorders like Alzheimer's and Parkison's disease or during cancer, inflammation, immune response, drug resistance, oxidative stress and redox signalling etc. For eg- S-nitrosylation of β-amyloid precursor protein (APP) and tau, protein occurs during Alzheimer's which promotes the cleavage of APP and production of amyloid-beta (Aβ), leading to neuronal dysfunction and neurodegeneration[148]. During Parkison's as well S-

nitrosylation results in enhancing the oligomerization of α-synuclein protein that support neurotoxicity, and contribute to dopaminergic neuron degeneration[149,150]. Altered S-nitrosylation of proteins involved in DNA repair and apoptotic pathways occur conferring resistance to chemotherapy agents[151] leading to drug resistance has also been observed. Another example of S-nityrosylation of proteins leading to diseased pathophysiology including Ras and NF-κB, which regulate pro-inflammatory cytokines and chemokines expression and promote tumor growth and survival in many cancer types[87].

In recent years, the integration of computational tools and experimental approaches has facilitated the identification and characterization of putative S-nitrosylation sites within key proteins, offering invaluable insights into their functional consequences. In the context of epigenetic regulation, the PRC2 stands out as a key player in controlling gene expression involved in cellular differentiation and cell type identity through the methylation of histone H3 lysine 27 (H3K27me3). EZH2, a methyltransferase enzyme which is the main subunit of PRC2, is responsible for catalyzing the addition of methyl groups to histone H3 on lysine residues leading to a repressive chromatin state. The catalytic activity of this PRC2 complex resides in the SET domain of the EZH2. EZH2 orchestrates histone methylation, modulating gene expression patterns pivotal in diverse biological processes, including development, differentiation, and disease pathogenesis.

Dysregulation of EZH2, via overexpression or activating mutations, is associated with various cancers as it results in aberrant histone methylation[39,152]. For e.g.-The increased expression of EZH2 has been recognized as a marker in breast cancer-initiating cells, potentially reflecting its involvement in regulating cellular stemness. Within a subset of lymphomas[153] missense mutations in EZH2 have been identified in recent studies[154]. These mutations, particularly at residues Y641 and A677, have been found to be linked to

upregulation of the tri-methylase activity of EZH2. Consequently, mutant cells retaining at least one wild-type allele exhibit elevated global levels of the H3K27me3 mark[152,155].

The findings of the crystal structure of the SET domain of EZH2 sheds light on the molecular mechanisms underlying its function and dysregulation in various disease conditions such as cancer. The crystal structure confirms the similarity of the SET domain of EZH2 with other SET domain containing methyltransferases. However, the dissimilarity arises among the positioning of certain domains within EZH2.Notably, the I-SET and post-SET domains of EZH2 are found in unconventional positions relative to the core SET domain. This abnormal arrangement results in the incomplete formation of the cofactor binding site and the obstruction to the substrate binding groove[155]. Additionally, a novel CXC domain located at the N-terminal of the SET domain may contribute to this inactive conformation. This further validates the importance of the interactions within the PRC2 complex that influence the conformation of EZH2 and in turn affecting its catalytic state.

While the regulation of EZH2 activity and stability has been extensively studied, the role of S-nitrosylation in modulating EZH2 function remains poorly understood. The strategy of using in silico prediction software to identify potential cysteine residues in the EZH2 protein that could possibly be S-nitrosylation has been employed. For this, we used an online tool that has been published and validated by Xue et al., 2010, and identified the potential S-nitrosylation sites within EZH2. Using this pre-validated software, we performed an *in silico* analysis to predict possible cysteine residues that could be S-nitrosylated and identified three cysteine residues at position 260, 329 and 700 (out of 34 total cysteine present in EZH2) that were predicted to be S-nitrosylated. This prompted us to investigate into the functional implications of S-nitrosylation at these specific sites. Also, the preliminary in-silico analysis along with molecular simulation studies have suggested that mutation at

predicted S-nitrosylation sites of EZH2 may induce structural alterations, thereby modulating its stability and catalytic activity. The comprehensive validation of these predictions through integrated computational and experimental approaches have proven the complex interplay between S-nitrosylation and EZH2 function.

Through a combination of immunoblot and computational modelling experiments, we identified cysteine residues 329 and 700 as critical sites for S-nitrosylation-mediated regulation of EZH2. These findings are consistent with previous reports highlighting the importance of cysteine residues in mediating redox-dependent modifications of proteins[156]. Through site-directed mutagenesis, we specifically identified that S-nitrosylation of Cysteine 329 and Cysteine 700 residues were responsible for EZH2 protein translocation/degradation and catalytic deactivation respectively. Molecular dynamics analysis suggested structural changes in EZH2 protein upon S-nitrosylation causing instability of EZH2-SUZ12 complex.

Our molecular dynamics simulation study provided evidence that upon S-nitrosylation of EZH2 at C329 and C700, caused changes in the structure of EZH2 SAL domain leading to dissociation of SUZ12 binding with EZH2. Furthermore, through site directed mutagenesis of EZH2 at C329 and C700 depicted that S-nitrosylation of C329 is responsible for EZH2 cytosolic translocation and degradation while S-nitrosylation of C700 was primarily responsible for catalytic inactivation of EZH2.

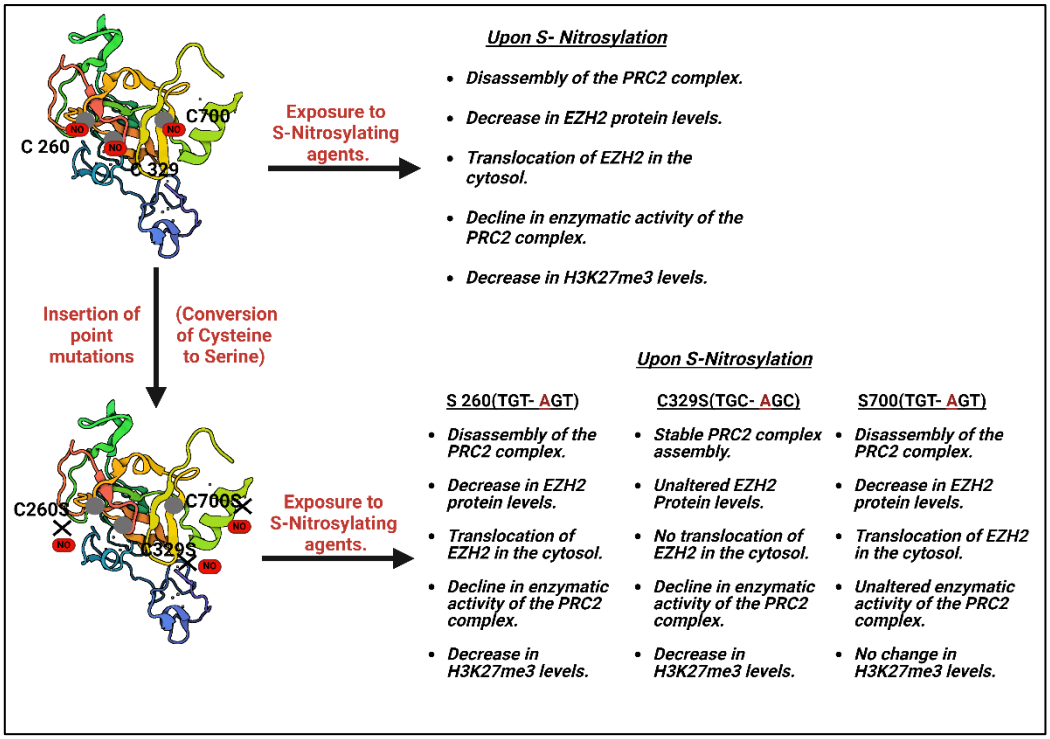

Figure 4.3.1 Schematic depicting the effect of point mutation on cysteine residues of EZH2 converting them to serine, impacting its stability, translocation and catalytic activity upon upon S-nitrosylation. *Upon S-Nitrosylation EZH2 undergoes a decline in its protein levels, disassociation of the SUZ 12 leading to the disassembly of the PRC2 complex along with a decline in H3K27me3 levels which marks a decrease in its methyltransferase activity as well. In-silico prediction analysis revealed 3 cysteine residues on EZH2(position 260,329 & 700) that undergo S-nitrosylation that are mainly involved in maintaining the stability and methyltransferase activity of the PRC2 complex. Upon insertion of point mutations at these residues leading to their conversion to serine depicted the importance of these sites in regulating the PRC2 complex. Cysteine 329 is involved with maintaining the stability of the PRC2 complex and regulating its translocation whereas cysteine 700 is involved with maintenance the catalytic activity of the PRC 2 complex.*

By integrating computational and experimental methodologies, we have successfully identified and verified the specific cysteines responsible for such an effect on the EZH2

landscape. Together our study aims to connect the bridge between experimental assays and molecular dynamics simulations, offering a comprehensive understanding of the regulatory roles of S-nitrosylation on EZH2 function. Ultimately, this understanding of the structural basis of EZH2 dysregulation provides valuable insights and these findings may pave the way for the development of novel therapeutic strategies targeting EZH2-mediated epigenetic dysregulation in various disease settings. Furthermore, elucidating the intricate mechanisms governing PRC2 function opens avenues for exploring novel approaches to modulate chromatin regulation in various cellular processes

Chapter 5:
Conclusion, Limitations and Future Perspectives

5.1 THESIS CONCLUSION

In this study, we have addressed whether S-nitrosylation-mediated post-translational modification on the cysteine residues of histone methyltransferase EZH2 had any impact on its stability, translocation and catalytic activity. We have also identified the specific cysteine residues on EZH2 responsible for maintaing its structural and functional activities and how S-nitrosylation (a PTM) could function as an epigenetic modifier and can regulate the gene expression changes. It has also provided proof on the interplay between NO signaling and epigenetic regulation through the modulation of EZH2 by elucidating the role of S-nitrosylation in regulating EZH2 function, localization, and stability. It has also demonstrated this role on the regulation of endothelial functions such as migration and survival.

With the help of molecular simulations studies and experimental assays, we identified specific cysteine residues (C329 and C700) within EZH2 as critical targets of S-nitrosylation, orchestrating its subcellular localization, catalytic activity, and interaction with other PRC2 components.

In conclusion, these findings highlight the significance of post-translational modifications, particularly S-nitrosylation, in governing EZH2 activity and the dynamics of the PRC2 complex. Moreover, this study also bridges the gap between NO signaling and epigenetic regulation in EC , by shedding light on a previously unexplored aspect of NO-mediated cellular function.

The integration of molecular dynamics simulations with experimental validation, has increased our understanding of the complex regulatory mechanisms governing EZH2 function. Furthermore, the identification of specific cysteine residues as key regulators of EZH2 activity opens avenues for the development of targeted therapeutic strategies aimed at mitigating epigenetic dysregulation in various disease contexts.

This study not only uncovers a novel mechanism of NO-mediated epigenetic regulation but also explains the potential of targeting S-nitrosylation of EZH2 and further emphasizing its therapeutic role in human diseases characterized by aberrant epigenetic alterations, thereby paving the way for innovative treatment strategies in diverse pathological conditions.

5.2 LIMITATIONS

- Although we have focused our experiments on the role of S-nitrosylation in regulating EZH2 stability, localization and function, we are cognizant that this effect may not be a direct consequence of nitrosylation rather a chain of event that possibly modulate other post-translational modification of EZH2 which may be analysed in future studies.
- We have not explored inducible NOS (iNOS) driven NO mediated effect on EZH2 S-nitrosylation and its associated regulation.
- We are still not clear about the mechanism of EZH2's cytosolic translocation upon NO exposure which can be explored in future studies.
- Also, the physiological relevance of this effect of NO on EZH2 and PRC2 complex in the context of the functioning of the blood vessels is yet to be discovered.

5.3 FUTURE PERSPECTIVES

We observed how NO signaling can regulate the epigenetic processes by post-translationally modifying EZH2 and thereby regulating gene expression. This will open up a new area of research on identifying the nitrosylation dependent regulation of epigenetic processes via NO generated through eNOS/iNOS/nNOS in diverse cell types, thereby mediating NO-induced gene expression changes.

Future investigations are needed to elucidate the precise mechanism by which EZH2 translocate into the cytosol upon exposure to NO. Furthermore, exploring the physiological significance of this NO-induced effect on EZH2 in relation to the functionality of blood vessels remains a key area for future research.

This study can also lay the foundation to further explain how NO can mitigate signaling through governing epigenetic processes and understanding the effect of global nitrosylation in governing diverse epigenetic processes and utilizing this knowledge to identify new signalling mechanisms and targets that can be altered for better therapeutic outcomes.

References

1. Bird, A. DNA methylation patterns and epigenetic memory. *Genes Dev* **16**, 6–21 (2002).
2. Kouzarides, T. Chromatin modifications and their function. *Cell* **128**, 693–705 (2007).
3. Esteller, M. Non-coding RNAs in human disease. *Nature Reviews Genetics 2011 12:12* **12**, 861–874 (2011).
4. Deevy, O. & Bracken, A. P. PRC2 functions in development and congenital disorders. *Development* **146**, (2019).
5. Schuettengruber, B. & Cavalli, G. Recruitment of polycomb group complexes and their role in the dynamic regulation of cell fate choice. *Development* **136**, 3531–3542 (2009).
6. Simon, J. A. & Kingston, R. E. Mechanisms of polycomb gene silencing: knowns and unknowns. *Nat Rev Mol Cell Biol* **10**, 697–708 (2009).
7. Eskeland, R. *et al.* Ring1B compacts chromatin structure and represses gene expression independent of histone ubiquitination. *Mol Cell* **38**, 452–464 (2010).
8. Sing, A. *et al.* A vertebrate Polycomb response element governs segmentation of the posterior hindbrain. *Cell* **138**, 885–897 (2009).
9. Schoeftner, S. *et al.* Recruitment of PRC1 function at the initiation of X inactivation independent of PRC2 and silencing. *EMBO J* **25**, 3110–3122 (2006).
10. Margueron, R. & Reinberg, D. The Polycomb complex PRC2 and its mark in life. *Nature 2011 469:7330* **469**, 343–349 (2011).
11. Shaver, S., Casas-Mollano, J. A., Cerny, R. L. & Cerutti, H. Origin of the polycomb repressive complex 2 and gene silencing by an E(z) homolog in the unicellular alga Chlamydomonas. *Epigenetics* **5**, 301–312 (2010).
12. Margueron, R. *et al.* Ezh1 and Ezh2 maintain repressive chromatin through different mechanisms. *Mol Cell* **32**, 503–518 (2008).
13. Chammas, P., Mocavini, I. & Di Croce, L. Engaging chromatin: PRC2 structure meets function. *British Journal of Cancer 2019 122:3* **122**, 315–328 (2019).
14. Shi, Y. *et al.* Structure of the PRC2 complex and application to drug discovery. *Acta Pharmacol Sin* **38**, 963 (2017).
15. Wu, H. *et al.* Structure of the Catalytic Domain of EZH2 Reveals Conformational Plasticity in Cofactor and Substrate Binding Sites and Explains Oncogenic Mutations. *PLoS One* **8**, 83737 (2013).

16. Kasinath, V. *et al.* Structures of human PRC2 with its cofactors AEBP2 and JARID2. *Science* **359**, 940 (2018).

17. Su, I. H. *et al.* Polycomb group protein ezh2 controls actin polymerization and cell signaling. *Cell* **121**, 425–436 (2005).

18. Gunawan, M. *et al.* The methyltransferase Ezh2 controls cell adhesion and migration through direct methylation of the extranuclear regulatory protein talin. *Nat Immunol* **16**, 505–516 (2015).

19. Dobenecker, M. W. *et al.* Signaling function of PRC2 is essential for TCR-driven T cell responses. *J Exp Med* **215**, 1101–1113 (2018).

20. Anwar, T. *et al.* p38-mediated phosphorylation at T367 induces EZH2 cytoplasmic localization to promote breast cancer metastasis. *Nature Communications 2018 9:1* **9**, 1–13 (2018).

21. Varambally, S. *et al.* The polycomb group protein EZH2 is involved in progression of prostate cancer. *Nature* **419**, 624–629 (2002).

22. Bryant, R. J., Winder, S. J., Cross, S. S., Hamdy, F. C. & Cunliffe, V. T. The polycomb group protein EZH2 regulates actin polymerization in human prostate cancer cells. *Prostate* **68**, 255–263 (2008).

23. Wang, J. & Wang, G. G. No Easy Way Out for EZH2: Its Pleiotropic, Noncanonical Effects on Gene Regulation and Cellular Function. *Int J Mol Sci* **21**, 1–16 (2020).

24. Huang, J. *et al.* The noncanonical role of EZH2 in cancer. *Wiley Online LibraryJ Huang, H Gou, J Yao, K Yi, Z Jin, M Matsuoka, T ZhaoCancer science, 2021•Wiley Online Library* **112**, 1376–1382 (2021).

25. Zingg, D., Debbache, J., Schaefer, S., … E. T.-N. & 2015, undefined. The epigenetic modifier EZH2 controls melanoma growth and metastasis through silencing of distinct tumour suppressors. *nature.comD Zingg, J Debbache, SM Schaefer, E Tuncer, SC Frommel, P Cheng, N Arenas-RamirezNature communications, 2015•nature.com*.

26. Tiffen, J., Wilson, S., Gallagher, S. J., Hersey, P. & Filipp, F. V. Somatic Copy Number Amplification and Hyperactivating Somatic Mutations of EZH2 Correlate With DNA Methylation and Drive Epigenetic Silencing of Genes Involved in Tumor Suppression and Immune Responses in Melanoma. *Neoplasia* **18**, 121–132 (2016).

27. Zingg, D., Arenas-Ramirez, N., Haeusel, J., Sommer, L. & Correspondence, B. The histone methyltransferase Ezh2 controls mechanisms of adaptive resistance to tumor immunotherapy. *cell.comD Zingg, N Arenas-Ramirez, D Sahin, RA Rosalia, AT Antunes, J Haeusel, L SommerCell reports, 2017•cell.com* **20**, 854–867 (2017).

28. Yiew, N., Greenway, C., Zarzour, A., … S. A.-J. of B. & 2019, undefined. Enhancer of zeste homolog 2 (EZH2) regulates adipocyte lipid metabolism independent of adipogenic differentiation: role of apolipoprotein E. *ASBMB*.

29. Ahmad, F., Patrick, S., Sheikh, T., … V. S.-J. of & 2017, undefined. Telomerase reverse transcriptase (TERT)-enhancer of zeste homolog 2 (EZH2) network regulates lipid metabolism and DNA damage responses in glioblastoma. *Wiley Online LibraryF Ahmad, S Patrick, T Sheikh, V Sharma, P Pathak, PB Malgulwar, A Kumar, SD JoshiJournal of neurochemistry, 2017•Wiley Online Library* **143**, 671–683 (2017).

30. Siamwala, J. H. *et al.* Nitric Oxide Reverses the Position of the Heart during Embryonic Development. *Int J Mol Sci* **20**, (2019).

31. Yan, K. S. *et al.* EZH2 in Cancer Progression and Potential Application in Cancer Therapy: A Friend or Foe? *Int J Mol Sci* **18**, (2017).

32. Gan, L. *et al.* Epigenetic regulation of cancer progression by EZH2: From biological insights to therapeutic potential. *Biomark Res* **6**, 1–10 (2018).

33. Majumder, S. *et al.* Shifts in podocyte histone H3K27me3 regulate mouse and human glomerular disease. *J Clin Invest* **128**, 483–499 (2018).

34. Siddiqi, F. S. *et al.* The Histone Methyltransferase Enzyme Enhancer of Zeste Homolog 2 Protects against Podocyte Oxidative Stress and Renal Injury in Diabetes. *J Am Soc Nephrol* **27**, 2021–2034 (2016).

35. Chen, Y. H., Hung, M. C. & Li, L. Y. EZH2: a pivotal regulator in controlling cell differentiation. *Am J Transl Res* **4**, 364 (2012).

36. Li, T., Yu, C. & Zhuang, S. Histone Methyltransferase EZH2: A Potential Therapeutic Target for Kidney Diseases. *Front Physiol* **12**, 640700 (2021).

37. Tan, J. Z., Yan, Y., Wang, X. X., Jiang, Y. & Xu, H. E. EZH2: biology, disease, and structure-based drug discovery. *Acta Pharmacologica Sinica 2014 35:2* **35**, 161–174 (2013).

38. Takawa, M. *et al.* Validation of the histone methyltransferase EZH2 as a therapeutic target for various types of human cancer and as a prognostic marker. *Cancer Sci* **102**, 1298–1305 (2011).

39. Simon, J. A. & Lange, C. A. Roles of the EZH2 histone methyltransferase in cancer epigenetics. *Mutat Res* **647**, 21–29 (2008).

40. Kuser-Abali, G. *et al.* The cytosolic role of EZH2-IMPDH2 complex in melanoma progression and metastasis via GTP regulation. *bioRxiv* 2021.11.02.467024 (2021) doi:10.1101/2021.11.02.467024.

41. Bachmann, I. M. *et al.* EZH2 expression is associated with high proliferation rate and aggressive tumor subgroups in cutaneous melanoma and cancers of the endometrium, prostate. *academia.eduIM Bachmann, OJ Halvorsen, K Collett, IM Stefansson, O Straume, SA HaukaasJ Clin Oncol, 2006•academia.edu* **24**, 268–273 (2006).

42. Simon, C. *et al.* A key role for EZH2 and associated genes in mouse and human adult T-cell acute leukemia. *Genes Dev* **26**, 651 (2012).

43. Ntziachristos, P. *et al.* Genetic inactivation of the polycomb repressive complex 2 in T cell acute lymphoblastic leukemia. *Nat Med* **18**, 296–301 (2012).

44. Zhang, J. *et al.* The genetic basis of early T-cell precursor acute lymphoblastic leukaemia. *Nature* **481**, 157–163 (2012).

45. Sashida, G. *et al.* Ezh2 loss promotes development of myelodysplastic syndrome but attenuates its predisposition to leukaemic transformation. *Nat Commun* **5**, (2014).

46. Cha, T. L. *et al.* Akt-mediated phosphorylation of EZH2 suppresses methylation of lysine 27 in histone H3. *Science* **310**, 306–310 (2005).

47. Wan, L. *et al.* Phosphorylation of EZH2 by AMPK Suppresses PRC2 Methyltransferase Activity and Oncogenic Function. *Mol Cell* **69**, 279 (2018).

48. Li, Z. *et al.* Post-translational modifications of EZH2 in cancer. *Cell & Bioscience 2020 10:1* **10**, 1–13 (2020).

49. Kaneko, S. *et al.* Phosphorylation of the PRC2 component Ezh2 is cell cycle-regulated and up-regulates its binding to ncRNA. *Genes Dev* **24**, 2615 (2010).

50. Wei, Y. *et al.* CDK1-dependent phosphorylation of EZH2 suppresses methylation of H3K27 and promotes osteogenic differentiation of human mesenchymal stem cells. *Nat Cell Biol* **13**, 87 (2011).

51. Popovic, D., Vucic, D. & Dikic, I. Ubiquitination in disease pathogenesis and treatment. *Nature Medicine 2014 20:11* **20**, 1242–1253 (2014).

52. Zhou, M. J., Chen, F. Z. & Chen, H. C. Ubiquitination involved enzymes and cancer. *Medical Oncology* **31**, 1–7 (2014).

53. Consalvi, S., Brancaccio, A., Dall'agnese, A., Puri, P. L. & Palacios, D. Praja1 E3 ubiquitin ligase promotes skeletal myogenesis through degradation of EZH2 upon p38α activation. *Nature Communications 2017 8:1* **8**, 1–11 (2017).

54. Shen, Z. *et al.* Downregulation of Ezh2 methyltransferase by FOXP3: New insight of FOXP3 into chromatin remodeling? *Biochimica et Biophysica Acta (BBA) - Molecular Cell Research* **1833**, 2190–2200 (2013).

55. Yu, Y. L. *et al.* Smurf2-mediated degradation of EZH2 enhances neuron differentiation and improves functional recovery after ischaemic stroke. *EMBO Mol Med* **5**, 531 (2013).

56. Gallo, L. H., Ko, J. & Donoghue, D. J. The importance of regulatory ubiquitination in cancer and metastasis. *Cell Cycle* **16**, 634–648 (2017).

57. Wang, X. *et al.* A covalently bound inhibitor triggers EZH2 degradation through CHIP-mediated ubiquitination. *EMBO J* **36**, 1243–1260 (2017).

58. Sun, C. *et al.* Diverse roles of C-terminal Hsp70-interacting protein (CHIP) in tumorigenesis. *J Cancer Res Clin Oncol* **140**, 189–197 (2014).

59. Zhang, P. *et al.* ZRANB1 Is an EZH2 Deubiquitinase and a Potential Therapeutic Target in Breast Cancer. *Cell Rep* **23**, 823–837 (2018).

60. Lee, J. E., Park, C. M. & Kim, J. H. USP7 deubiquitinates and stabilizes EZH2 in prostate cancer cells. *Genet Mol Biol* **43**, e20190338 (2020).

61. Li, B. *et al.* MELK mediates the stability of EZH2 through site-specific phosphorylation in extranodal natural killer/T-cell lymphoma. *Blood* **134**, 2046–2058 (2019).

62. Guo, Y. *et al.* Regulation of EZH2 protein stability: new mechanisms, roles in tumorigenesis, and roads to the clinic. *EBioMedicine* **100**, 104972 (2024).

63. Wan, J. *et al.* PCAF-primed EZH2 acetylation regulates its stability and promotes lung adenocarcinoma progression. *Nucleic Acids Res* **43**, 3591–3604 (2015).

64. Riising, E. M., Boggio, R., Chiocca, S., Helin, K. & Pasini, D. The Polycomb Repressive Complex 2 Is a Potential Target of SUMO Modifications. *PLoS One* **3**, e2704 (2008).

65. Du, L., Chen, Y. & Rosen, S. Abstract 1279: SUMOylation upregulates EZH2 expression by modifying transcriptional factor E2F1. *Cancer Res* **80**, 1279–1279 (2020).

66. Du, L., Fakih, M. G., Rosen, S. T. & Chen, Y. SUMOylation of E2F1 Regulates Expression of EZH2. *Cancer Res* **80**, 4212–4223 (2020).

67. Zeng, Y. *et al.* Regulation of EZH2 by SMYD2-Mediated Lysine Methylation Is Implicated in Tumorigenesis. *Cell Rep* **29**, 1482-1498.e4 (2019).

68. Yuan, H. *et al.* SETD2 restricts prostate cancer metastasis by integrating EZH2 and AMPK signaling pathways. *cell.comH Yuan, Y Han, X Wang, N Li, Q Liu, Y Yin, H Wang, L Pan, L Li, K Song, T Qiu, Q PanCancer cell, 2020•cell.com*.

69. Li, Z. *et al.* Methylation of EZH2 by PRMT1 regulates its stability and promotes breast cancer metastasis. *Cell Death Differ* **27**, 3226–3242 (2020).

70. Chu, C. S. *et al.* O-GlcNAcylation regulates EZH2 protein stability and function. *Proc Natl Acad Sci U S A* **111**, 1355–1360 (2014).

71. Lo, P. W. *et al.* O-GlcNAcylation regulates the stability and enzymatic activity of the histone methyltransferase EZH2. *Proc Natl Acad Sci U S A* **115**, 7302–7307 (2018).

72. Tuteja, N., Chandra, M., Tuteja, R. & Misra, M. K. Nitric Oxide as a Unique Bioactive Signaling Messenger in Physiology and Pathophysiology. *J Biomed Biotechnol* **2004**, 227 (2004).

73. Stamler, J. S. Redox signaling: nitrosylation and related target interactions of nitric oxide. *Cell* **78**, 931–936 (1994).

74. Yan, Q. The Yin-Yang Dynamics in Cancer Pharmacogenomics and Personalized Medicine. *Methods in Molecular Biology* **2547**, 141–163 (2022).

75. Luiking, Y. C., Engelen, M. P. K. J. & Deutz, N. E. P. REGULATION OF NITRIC OXIDE PRODUCTION IN HEALTH AND DISEASE. *Curr Opin Clin Nutr Metab Care* **13**, 97 (2010).

76. Kelm, M. Nitric oxide metabolism and breakdown. *Biochimica et Biophysica Acta (BBA) - Bioenergetics* **1411**, 273–289 (1999).

77. Paradise, W. A. *et al.* Nitric Oxide: Perspectives and Emerging Studies of a Well Known Cytotoxin. *Int J Mol Sci* **11**, 2715 (2010).

78. Benhar, M., Forrester, M. T. & Stamler, J. S. Protein denitrosylation: enzymatic mechanisms and cellular functions. *Nat Rev Mol Cell Biol* **10**, 721–732 (2009).

79. Welch, G. & Loscalzo, J. Nitric oxide and the cardiovascular system. *J Card Surg* **9**, 361–371 (1994).

80. Ng, Q. S. *et al.* Effect of nitric-oxide synthesis on tumour blood volume and vascular activity: a phase I study. *Lancet Oncol* **8**, 111–118 (2007).

81. Hayashi, T. *et al.* Nitric oxide and endothelial cellular senescence. *Pharmacol Ther* **120**, 333–339 (2008).

82. Spinetti, G., Kraenkel, N., Emanueli, C. & Madeddu, P. Diabetes and vessel wall remodelling: from mechanistic insights to regenerative therapies. *Cardiovasc Res* **78**, 265 (2008).

83. Chen, J. *et al.* Endothelial Nitric Oxide Synthase Regulates Brain-Derived Neurotrophic Factor Expression and Neurogenesis after Stroke in Mice. *The Journal of Neuroscience* **25**, 2366 (2005).

84. Džoljić, E., Grabatinić, I. & Kostić, V. Why is nitric oxide important for our brain? *Funct Neurol* **30**, 159 (2015).

85. Moncada, S. & Erusalimsky, J. D. Does nitric oxide modulate mitochondrial energy generation and apoptosis? *Nat Rev Mol Cell Biol* **3**, 214–220 (2002).

86. Moncada, S. & Higgs, E. A. The discovery of nitric oxide and its role in vascular biology. *Br J Pharmacol* **147**, S193 (2006).

87. Seth, D. & Stamler, J. S. The SNO-proteome: Causation and Classifications. *Curr Opin Chem Biol* **15**, 129 (2011).

88. Foster, M. W., McMahon, T. J. & Stamler, J. S. S-nitrosylation in health and disease. *Trends Mol Med* **9**, 160–168 (2003).

89. Loscalzo, J. & Welch, G. Nitric oxide and its role in the cardiovascular system. *Prog Cardiovasc Dis* **38**, 87–104 (1995).

90. Liu, V. W. T. & Huang, P. L. Cardiovascular roles of nitric oxide: A review of insights from nitric oxide synthase gene disrupted mice. *Cardiovasc Res* **77**, 19–29 (2008).

91. Ridnour, L. A. *et al.* The chemistry of nitrosative stress induced by nitric oxide and reactive nitrogen oxide species. Putting perspective on stressful biological situations. *Biol Chem* **385**, 1–10 (2004).

92. Roy, R., Wilcox, J., Webb, A. J. & O'Gallagher, K. Dysfunctional and Dysregulated Nitric Oxide Synthases in Cardiovascular Disease: Mechanisms and Therapeutic Potential. *International Journal of Molecular Sciences 2023, Vol. 24, Page 15200* **24**, 15200 (2023).

93. Levine, A. B., Punihaole, D. & Levine, T. B. Characterization of the Role of Nitric Oxide and Its Clinical Applications. *Cardiology* **122**, 55–68 (2012).

94. Chatterji, A., Banerjee, D., Billiar, T. R. & Sengupta, R. Understanding the role of S-nitrosylation/nitrosative stress in inflammation and the role of cellular denitrosylases in inflammation modulation: Implications in health and diseases. *Free Radic Biol Med* **172**, 604–621 (2021).

95. Hu, Y., Xiang, J., Su, L. & Tang, X. The regulation of nitric oxide in tumor progression and therapy. *https://doi.org/10.1177/0300060520905985* **48**, (2020).

96. Khan, F. H. *et al.* The Role of Nitric Oxide in Cancer: Master Regulator or NOt? *Int J Mol Sci* **21**, 1–30 (2020).

97. Xu, W., Liu, L. Z., Loizidou, M., Ahmed, M. & Charles, I. G. The role of nitric oxide in cancer. *Cell Research 2002 12:5* **12**, 311–320 (2002).

98. Toh, Y. *et al.* Alcohol drinking, cigarette smoking, and the development of squamous cell carcinoma of the esophagus: Molecular mechanisms of carcinogenesis. *Int J Clin Oncol* **15**, 135–144 (2010).

99. Luiking, Y. C., Engelen, M. P. K. J. & Deutz, N. E. P. REGULATION OF NITRIC OXIDE PRODUCTION IN HEALTH AND DISEASE. *Curr Opin Clin Nutr Metab Care* **13**, 97 (2010).

100. Derbyshire, E. R. & Marletta, M. A. Structure and regulation of soluble guanylate cyclase. *Annu Rev Biochem* **81**, 533–559 (2012).

101. Luo, S. *et al.* Roles of Protein S-Nitrosylation in Endothelial Homeostasis and Dysfunction. *https://home.liebertpub.com/ars* **40**, 186–205 (2024).

102. Koning, T. *et al.* S-Nitrosylation in endothelial cells contributes to tumor cell adhesion and extravasation during breast cancer metastasis. *Biol Res* **56**, (2023).

103. Pilz, R. B. & Casteel, D. E. Regulation of Gene Expression by Cyclic GMP. *Circ Res* **93**, 1034–1046 (2003).

104. Mintz, J. *et al.* Current Advances of Nitric Oxide in Cancer and Anticancer Therapeutics. *Vaccines (Basel)* **9**, 1–39 (2021).

105. Gupta, K. J. *et al.* Regulating the regulator: nitric oxide control of post-translational modifications. *New Phytologist* **227**, 1319–1325 (2020).

106. Gould, N., Doulias, P. T., Tenopoulou, M., Raju, K. & Ischiropoulos, H. Regulation of protein function and signaling by reversible cysteine S-nitrosylation. *J Biol Chem* **288**, 26473–26479 (2013).

107. Xue, Y. *et al.* GPS-SNO: computational prediction of protein S-nitrosylation sites with a modified GPS algorithm. *PLoS One* **5**, (2010).

108. Justin, N. *et al.* Structural basis of oncogenic histone H3K27M inhibition of human polycomb repressive complex 2. *Nature Communications 2016 7:1* **7**, 1–11 (2016).

109. AlphaFold Protein Structure Database. https://alphafold.ebi.ac.uk/.

110. Schrödinger Release 2022-2: Protein Preparation Wizard; Epik, Schrödinger, LLC, New York, NY, 2016; Impact, Schrödinger, LLC, New York, NY, 2016; Prime, Schrödinger, LLC, New York, NY, 2019.

111. Margreitter, C., Petrov, D. & Zagrovic, B. Vienna-PTM web server: a toolkit for MD simulations of protein post-translational modifications. *Nucleic Acids Res* **41**, (2013).

112. Harvey, M. J. & De Fabritiis, G. An Implementation of the Smooth Particle Mesh Ewald Method on GPU Hardware. *J Chem Theory Comput* **5**, 2371–2377 (2009).

113. Ryckaert, J. P., Ciccotti, G. & Berendsen, H. J. C. Numerical integration of the cartesian equations of motion of a system with constraints: molecular dynamics of n-alkanes. *J Comput Phys* **23**, 327–341 (1977).

114. The PyMOL Molecular Graphics System, Version 1.8 Schrödinger, LLC. https://www.sciepub.com/reference/159710.

115. Humphrey, W., Dalke, A. & Schulten, K. VMD: Visual molecular dynamics. *J Mol Graph* **14**, 33–38 (1996).

116. Kumari, R., Kumar, R. & Lynn, A. g_mmpbsa--a GROMACS tool for high-throughput MM-PBSA calculations. *J Chem Inf Model* **54**, 1951–1962 (2014).

117. Van Der Spoel, D. *et al.* GROMACS: Fast, flexible, and free. *J Comput Chem* **26**, 1701–1718 (2005).

118. Tripathi, S. M., Akash, S., Rahman, M. A. & Sundriyal, S. Identification of synthetically tractable MERS-CoV main protease inhibitors using structure-based virtual screening and molecular dynamics potential of mean force (PMF) calculations. *J Biomol Struct Dyn* (2023) doi:10.1080/07391102.2023.2283780.

119. Tan, J. Z., Yan, Y., Wang, X. X., Jiang, Y. & Xu, H. E. EZH2: Biology, disease, and structure-based drug discovery. *Acta Pharmacologica Sinica* vol. 35 161–174 Preprint at https://doi.org/10.1038/aps.2013.161 (2014).

120. Kuzmichev, A., Nishioka, K., Erdjument-Bromage, H., Tempst, P. & Reinberg, D. Histone methyltransferase activity associated with a human multiprotein complex containing the Enhancer of Zeste protein. *Genes Dev* **16**, 2893–2905 (2002).

121. Schlesinger, Y. *et al.* Polycomb-mediated methylation on Lys27 of histone H3 pre-marks genes for de novo methylation in cancer. *Nat Genet* **39**, 232–236 (2007).

122. Cao, R. *et al.* Role of histone H3 lysine 27 methylation in Polycomb-group silencing. *Science* **298**, 1039–1043 (2002).

123. Lee, S. H. *et al.* The role of EZH1 and EZH2 in development and cancer. *BMB Rep* **55**, 595–601 (2022).

124. Chen, Y. H., Hung, M. C. & Li, L. Y. EZH2: a pivotal regulator in controlling cell differentiation. *Am J Transl Res* **4**, 364 (2012).

125. Ghobashi, A. H. *et al.* Activation of AKT induces EZH2-mediated β-catenin trimethylation in colorectal cancer. *iScience* **26**, 107630 (2023).

126. Riising, E. M., Boggio, R., Chiocca, S., Helin, K. & Pasini, D. The Polycomb Repressive Complex 2 Is a Potential Target of SUMO Modifications. *PLoS One* **3**, e2704 (2008).

127. Li, Z. *et al.* Methylation of EZH2 by PRMT1 regulates its stability and promotes breast cancer metastasis. *Cell Death & Differentiation 2020 27:12* **27**, 3226–3242 (2020).

128. Gottimukkala, K. P. *et al.* Regulation of SATB1 during thymocyte development by TCR signaling. *Mol Immunol* **77**, 34 (2016).

129. Hemish, J., Nakaya, N., Mittal, V. & Enikolopov, G. Nitric oxide activates diverse signaling pathways to regulate gene expression. *J Biol Chem* **278**, 42321–42329 (2003).

130. Yu, Y. L. *et al.* Smurf2-mediated degradation of EZH2 enhances neuron differentiation and improves functional recovery after ischaemic stroke. *EMBO Mol Med* **5**, 531–547 (2013).

131. Matrone, G. *et al.* Nuclear S-nitrosylation impacts tissue regeneration in zebrafish. *Nat Commun* **12**, (2021).

132. Foster, M. W., Hess, D. T. & Stamler, J. S. Protein S-nitrosylation in health and disease: a current perspective. *Trends Mol Med* **15**, 391–404 (2009).

133. Anwar, T. *et al.* p38-mediated phosphorylation at T367 induces EZH2 cytoplasmic localization to promote breast cancer metastasis. *Nat Commun* **9**, (2018).

134. Ghate, N. B. *et al.* Phosphorylation and stabilization of EZH2 by DCAF1/VprBP trigger aberrant gene silencing in colon cancer. *Nat Commun* **14**, (2023).

135. Yan, J. *et al.* EZH2 phosphorylation by JAK3 mediates a switch to noncanonical function in natural killer/T-cell lymphoma. *Blood* **128**, 948–958 (2016).

136. Kapil, V. *et al.* The Noncanonical Pathway for In Vivo Nitric Oxide Generation: The Nitrate-Nitrite-Nitric Oxide Pathway. *Pharmacol Rev* **72**, 692–766 (2020).

137. Tejero, J., Shiva, S. & Gladwin, M. T. Sources of Vascular Nitric Oxide and Reactive Oxygen Species and Their Regulation. *Physiol Rev* **99**, 311–379 (2019).

138. Francis, S. H., Busch, J. L. & Corbin, J. D. cGMP-dependent protein kinases and cGMP phosphodiesterases in nitric oxide and cGMP action. *Pharmacol Rev* **62**, 525–563 (2010).

139. Gobeil, F. *et al.* Nitric oxide signaling via nuclearized endothelial nitric-oxide synthase modulates expression of the immediate early genes iNOS and mPGES-1. *J Biol Chem* **281**, 16058–16067 (2006).

140. Parenti, A. *et al.* Nitric oxide is an upstream signal of vascular endothelial growth factor-induced extracellular signal-regulated kinase1/2 activation in postcapillary endothelium. *J Biol Chem* **273**, 4220–4226 (1998).

141. Cooke, J. P. & Losordo, D. W. Nitric oxide and angiogenesis. *Circulation* **105**, 2133–2135 (2002).

142. Förstermann, U. *et al.* Nitric oxide synthase isozymes characterization, purification, molecular cloning, and functions. *Hypertension* (1994) doi:10.1161/01.HYP.23.6.1121.

143. Yu, J. *et al.* Endothelial nitric oxide synthase is critical for ischemic remodeling, mural cell recruitment, and blood flow reserve. *Proc Natl Acad Sci U S A* **102**, 10999–11004 (2005).

144. Morales-Ruiz, M. *et al.* Vascular endothelial growth factor-stimulated actin reorganization and migration of endothelial cells is regulated via the serine/threonine kinase Akt. *Circ Res* **86**, 892–896 (2000).

145. Titelbaum, M. *et al.* Ezh2 harnesses the intranuclear actin cytoskeleton to remodel chromatin in differentiating Th cells. *iScience* **24**, (2021).

146. Gupta, K. J. *et al.* Regulating the regulator: nitric oxide control of post-translational modifications. *New Phytologist* **227**, 1319–1325 (2020).

147. Förstermann, U. & Münzel, T. Endothelial Nitric Oxide Synthase in Vascular Disease. *Circulation* **113**, 1708–1714 (2006).

148. Sultana, R. & Butterfield, D. A. Role of oxidative stress in the progression of Alzheimer's disease. *J Alzheimers Dis* **19**, 341–353 (2010).

149. Wilkaniec, A. *et al.* Extracellular Alpha-Synuclein Oligomers Induce Parkin S-Nitrosylation: Relevance to Sporadic Parkinson's Disease Etiopathology. *Mol Neurobiol* **56**, 125–140 (2019).

150. Uehara, T. *et al.* S-nitrosylated protein-disulphide isomerase links protein misfolding to neurodegeneration. *Nature* **441**, 513–517 (2006).

151. Jaffrey, S. R. & Snyder, S. H. The biotin switch method for the detection of S-nitrosylated proteins. *Sci STKE* **2001**, (2001).

152. Chase, A. & Cross, N. C. P. Aberrations of EZH2 in cancer. *Clin Cancer Res* **17**, 2613–2618 (2011).

153. Sneeringer, C. J. *et al.* Coordinated activities of wild-type plus mutant EZH2 drive tumor-associated hypertrimethylation of lysine 27 on histone H3 (H3K27) in human B-cell lymphomas. *Proc Natl Acad Sci U S A* **107**, 20980–20985 (2010).

154. McCabe, M. T. *et al.* Mutation of A677 in histone methyltransferase EZH2 in human B-cell lymphoma promotes hypertrimethylation of histone H3 on lysine 27 (H3K27). *Proc Natl Acad Sci U S A* **109**, 2989–2994 (2012).

155. Wu, H. *et al.* Structure of the Catalytic Domain of EZH2 Reveals Conformational Plasticity in Cofactor and Substrate Binding Sites and Explains Oncogenic Mutations. *PLoS One* **8**, 83737 (2013).

156. Marino, S. M. & Gladyshev, V. N. Structural analysis of cysteine S-nitrosylation: a modified acid-based motif and the emerging role of trans-nitrosylation. *J Mol Biol* **395**, 844–859 (2010).

Appendix A1: List of publications

From Thesis:

Sakhuja A, Katakia YT, Tripathi SM, Bhattacharyya R, Thakkar NP, Ramakrishnan SK, Chakraborty S, Thakar S, Sundriyal S, Chowdhury S, Majumder S. S-nitrosylation of EZH2 at C329 and C700 interplay with PRC2 complex assembly, methyltransferase activity, and EZH2 stability to regulate endothelial functions. (under revision in Nature communications) (Pre-print available on bioRxiv, doi: https://doi.org/10.1101/2024.02.06.579117)

Other Publications:

1. Pandya-Thakkar N, Pereira BMV, Katakia YT, Ramakrishnan SK, Thakar S, **Sakhuja A**, Rajeev G, S Soorya, Thieme K, Majumder S. Elevated H3K4me3 through MLL2-WDR82 upon hyperglycemia causes Jagged ligand dependent Notch activation to interplay with differentiation state of endothelial cells. Frontiers in Cell and Developmental Biology, 2022 22;10:839109.

2. Katakia YT, Pandya-Thakkar N, Thakar S**, Sakhuja A**, Goyal R, Sharma H, Dave R, Mandloi A, Basu S, Nigam I, Kuncharam BVR, Chowdhury S, Majumder S. Dynamic alterations of H3K4me3 and H3K27me3 at ADAM17 and Jagged-1 gene promoters cause inflammatory switch of endothelial cells. Journal of Cellular Physiology, 2022;237(1):992-1012.

Appendix A2: List of conferences

1) Poster Presentation – 92nd ANNUAL MEETING OF THE SOCIETY OF BIOLOGICAL CHEMISTS (INDIA), BITS PILANI, K.K. Birla Goa Campus, 18-20 December,2023.

Title: S-Nitrosylation of Enhancer of Zeste Homolog-2 disrupts Polycomb Repressive Complex 2 to interplay with catalysis of H3K27me3

Ashima Sakhuja*, Ritobrata Bhattacharya, Yash T Katakia, Srinjoy Chakraborty, S Ramakrishnan, Niyati Pandya Thakkar, Sumukh Thakar, Syamantak Majumder

2) Won 3rd Prize in Poster presentation – Regional Young Investigators' Meeting (RYIM), Birla Institute of Technology & Science, 18-20 January,2024.

Title: Studying the post-translational regulation of Enhancer of Zeste Homolog-2 on its function as Histone Methyltransferase of the Polycomb repressive complex

Ashima Sakhuja*, Ritobrata Bhattacharya, Yash T Katakia, Srinjoy Chakraborty, S Ramakrishnan, Niyati Pandya Thakkar, Sumukh Thakar, Syamantak Majumder

3) **Abstract accepted at the – Gordon Research Conference - Endothelial Cell Phenotypes in Health and Disease, Rey Don Jaime Grand Hotel in Castelldefels, Barcelona, Spain**

Title: Studying the post-translational regulation of Enhancer of Zeste Homolog-2 on its function as Histone Methyltransferase of the Polycomb repressive complex

Ashima Sakhuja*, Ritobrata Bhattacharya, Yash T Katakia, Srinjoy Chakraborty, S Ramakrishnan, Niyati Pandya Thakkar, Sumukh Thakar, Syamantak Majumder

Appendix A3: List of biographies

Brief biography of supervisor

Dr. Syamantak Majumder received his PhD from Anna University, Chennai, India (2007-2011) in field of Cell and Vascular Biology and moved to University of Rochester, Rochester, NY, USA as a Post Doctoral Fellow (2011-2014) followed by another Post Doctoral Training at St Michael's Hospital, University of Toronto, Toronto, ON, Canada (2014-2017). Dr. Majumder has more than 17 years of experience in the field of vascular biology including diabetic complications. Dr. Majumder has authored 57 (5 as corresponding author and 20 as the first author) published research articles, reviews, editorials and book chapters including 49 research articles in peer-reviewed journals with a Google Scholar h-index of 27, about 2174 Citations and i-10 index of 44. His team is trying to identify and target the epigenetic mechanisms driving endothelial inflammation (J Cell Physiol. 2021, IF 6.6; Communication Biology 2022, IF 6.6) during diabetes (Cells 2021, IF 7.7; Frontiers in Cell and Developmental Biology, IF 6.1) that lead to cardiovascular and kidney diseases. He is currently supervising seven PhD students. Dr. Majumder's work has been funded by multiple grants from DST, SERB, DBT, ICMR and DRDO including high value projects as PI or Co-PI such as DBT BUILDER and DST-PURSE.

Brief biography of Co-supervisor

Prof. Shibasish Chowdhury obtained a master's degree in physical chemistry from Calcutta University. Then, he shifted to biophysics and obtained a Ph.D. degree from Molecular Biophysics Unit (MBU) at the Indian Institute of Science, Bangalore on "Computer modelling studies on G-rich unusual DNA structure". Subsequently, entered into the protein folding field and worked as a postdoctoral research fellow in the Department of Chemistry and Biochemistry, University of Delaware, the USA. Currently, Prof. Chowdhury is working as a Professor in the Department of Biological Sciences, Birla Institute of Technology and Science, Pilani. His major area of interest lies in elucidating complex relationships among sequence-structure-function and analysis of bio-molecular structures using model building and computational techniques. His group is involved in decoding inherent molecular signals within miRNA, which plays a crucial role in the specificity of target binding and gene silencing. He is involved in analyzing the molecular basis of different biological processes like drug resistance, molecular recognition, and evolution.

Brief biography of the candidate

Ms. Ashima Sakhuja graduated with a Bachelor degree in Zoology from Gargi College, University of Delhi in 2016. She later graduated with Masters in Zoology from Panjab University, Chandigarh in 2018. She qualified CSIR NET JRF in December 2018 and GATE in 2019. She then joined BITS Pilani for her PhD in 2019 under supervision of Prof. Syamantak Majumder. She has published 2 research articles in peer reviewed journals. Alongside research, she has also been involved in teaching and has taken courses for first degree students in BITS Pilani, Pilani Campus.